REDUCTION OF VANADIUM TRICHLORIDE BY METAL ALKYLS: SYNTHETIC, SPECTRAL AND X-RAY CRYSTAL STUDIES

Prasanna Chandrasekhar

A Thesis

in

The Department

of

Chemistry

Presented in Partial Fulfillment of the Requirements
for the degree of Master of Science at
Concordia University
Montréal, Québec, Canada

November, 1980

ABSTRACT

REDUCTION OF VANADIUM TRICHLORIDE BY METAL ALKYLS: SYNTHETIC, SPECTRAL AND X-RAY CRYSTAL STUDIES

Prasanna Chandrasekhar

This work presents results of a study of the reactions of VCl_3 with $ZnEt_2$ and $AlEt_3$ and with $ZnCl_2$, in the solvents THF(Tetrahydrofuran) and CH_3CN, these solvents being chosen to give a fair representation of the range of solvent media available- the former being fairly weakly coordinating and the latter being strongly coordinating with Pi-acceptor properties. X-ray diffraction studies of two of the products are presented.

The successfully isolated crystalline compounds have the formulations $VCl_2{:}2THF$ (A) (from $ZnCl_2$ in THF), $V(THF)_4ZnCl_4$ (B) (from $ZnEt_2$ in THF), $V(NCCH_3)_6ZnCl_4$ ("VEZN", C) (from $ZnEt_2$ in CH_3CN) and $Cl_2(THF)_3VOV(THF)_3Cl_2$ ("TVA", D) (from $AlEt_3$ in THF).

X-ray Diffraction studies of the structure of C showed it to consist of an ion pair, V^{II} octahedrally coordinated by CH_3CN (peculiarly nonlinear) and Zn tetrahedrally coordinated by Cl. Study of the structure of D revealed an entity isolated in crystalline form for the first time, two octahedrally coordinated V^{III} atoms connected by an O-bridge, chlorines in the molecule being in trans positions, across the V atoms. A new technique for the mounting of extremely air-sensitive crystals was developed.

UV-Visible spectral studies of all the reaction mixtures and of D dissolved in a range of solvents were also conducted. They reveal an extremely intense absorption at ca. 487 nm, ascribed to the VOV^{4+} species. IR spectra of the successfully isolated crystals as nujol mulls to a range of ca. 300 cm^{-1} are also presented.

Abstract, cont.

A gas-chromatographic search for dissolved product gases when THF was used as solvent revealed the presence of ethane, ethylene and butane. On the basis of their relative amounts, it was postulated that alkylation of the VCl_3 proceeds more to completion with $ZnEt_2$ than with $AlEt_3$, where the increased amounts of ethylene and butane observed may be explained by a premature elimination of the ethyl groups from the Al metal. This is the fundamental theoretical finding of this thesis.

TABLE OF CONTENTS

TABLE OF CONTENTS, cont.

LIST OF TABLES AND FIGURES

LIST OF TABLES AND FIGURES, cont.

PRELIMINARY NOTE

Since the names TVA and VEZN are used so extensively in this thesis as abbreviations for the compounds whose crystal structures were determined, and so much of that which is discussed assumes a knowledge of these structures, it has been thought useful to illustrate these structures here initially. VEZN is $V^{II}(NCHCH_3)_6ZnCl_4$, two ions- CH_3CN octahedrally coordinated to V^{II} and Cl tetrahedrally coordinated to Zn. These ions are shown in Figs. 1A and 1B. TVA is $(THF)_3Cl_2V^{III}\text{-}O\text{-}V^{III}Cl_2(THF)_3$. The vanadium atoms are octahedrally coordinated, each to two chlorines (which are trans), three THFs and the bridging oxygen. The structure is shown in Fig. 2.

Please also note that reference numbers are in brackets and not superscripted.

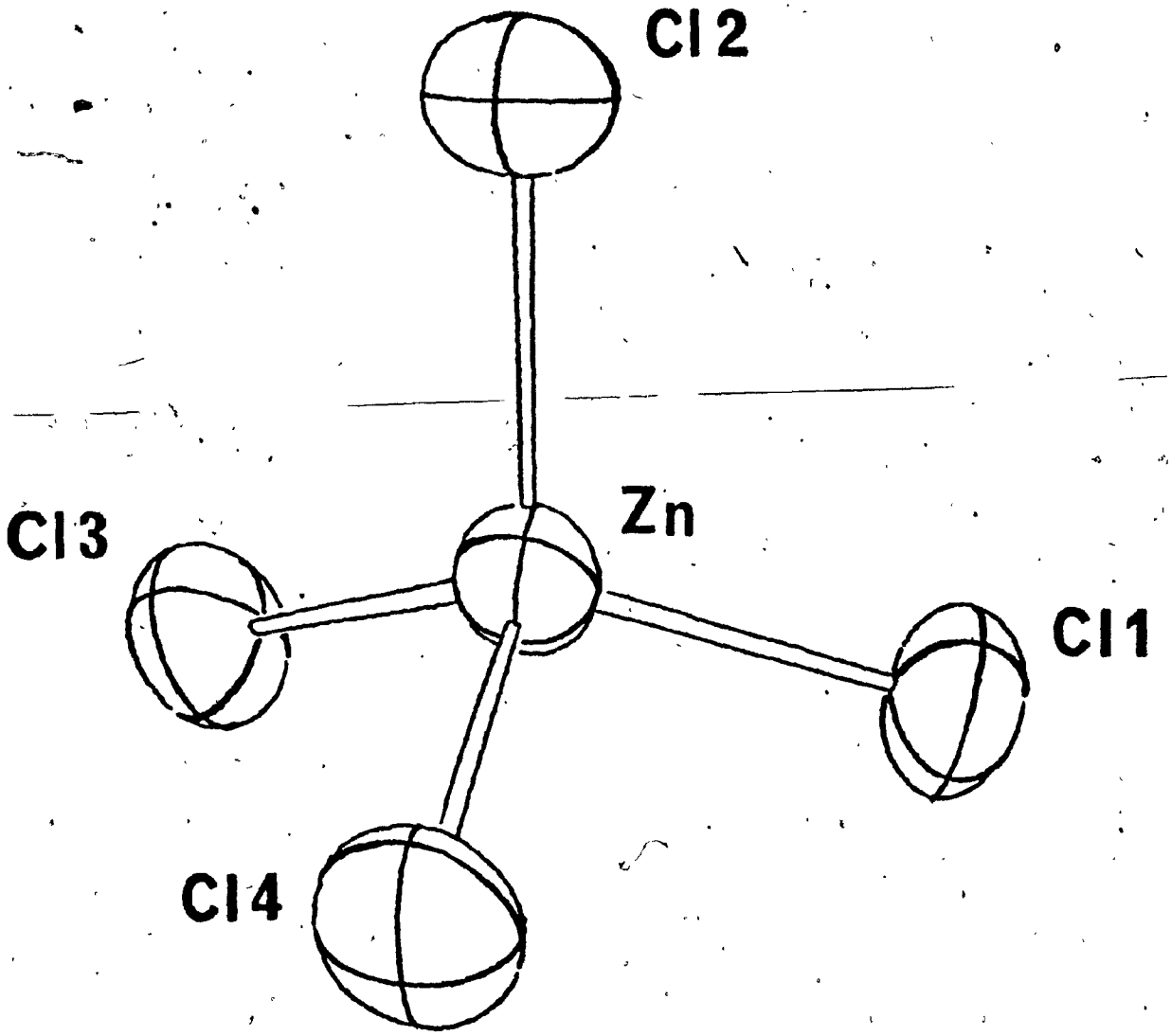

Fig. 1A: ORTEP diagram of $ZnCl_4^{2-}$ in VEZN

$$ZnCl_4^{2-}$$

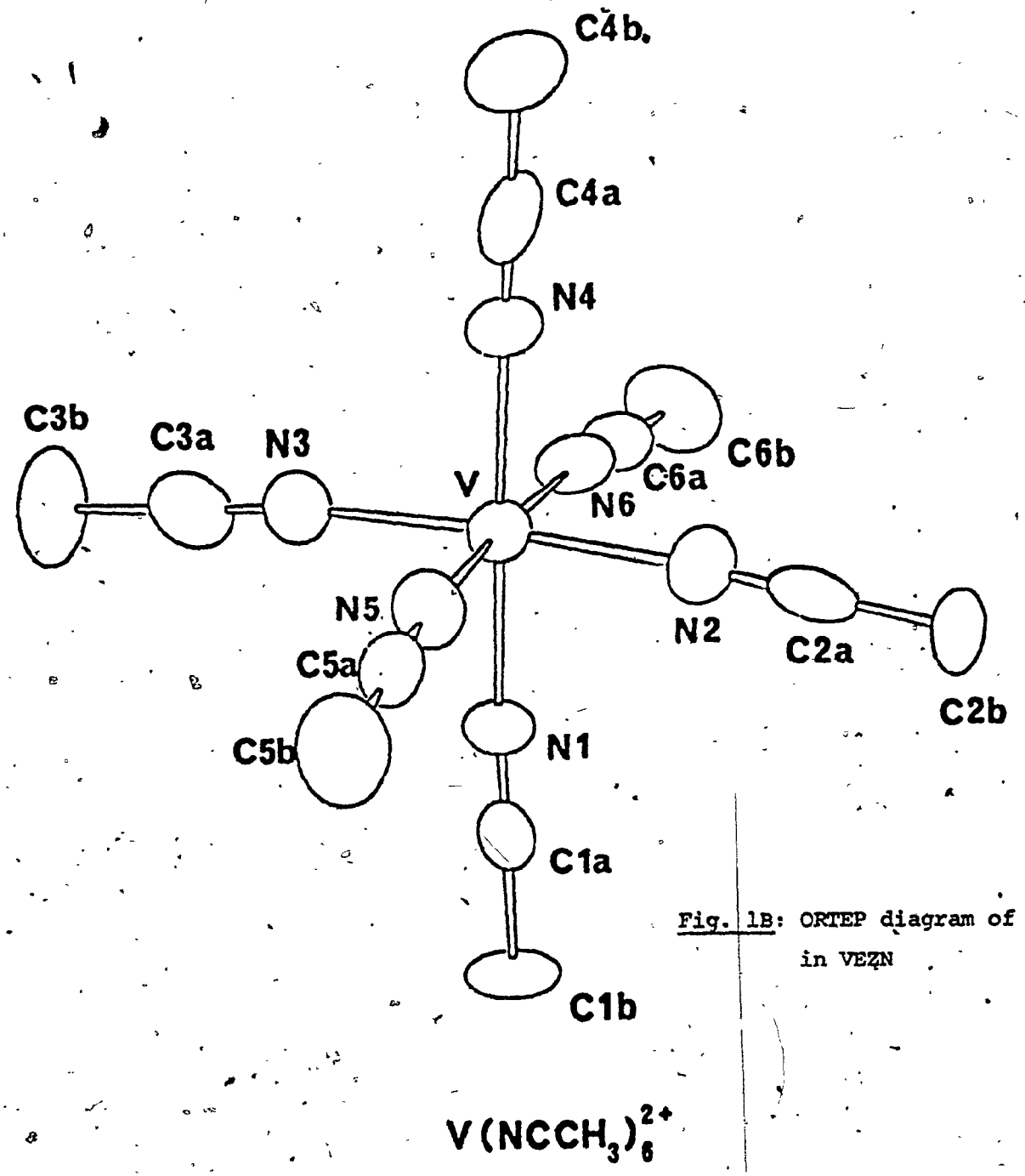

Fig. 1B: ORTEP diagram of $V(NCCH_3)_6$ in VEZN

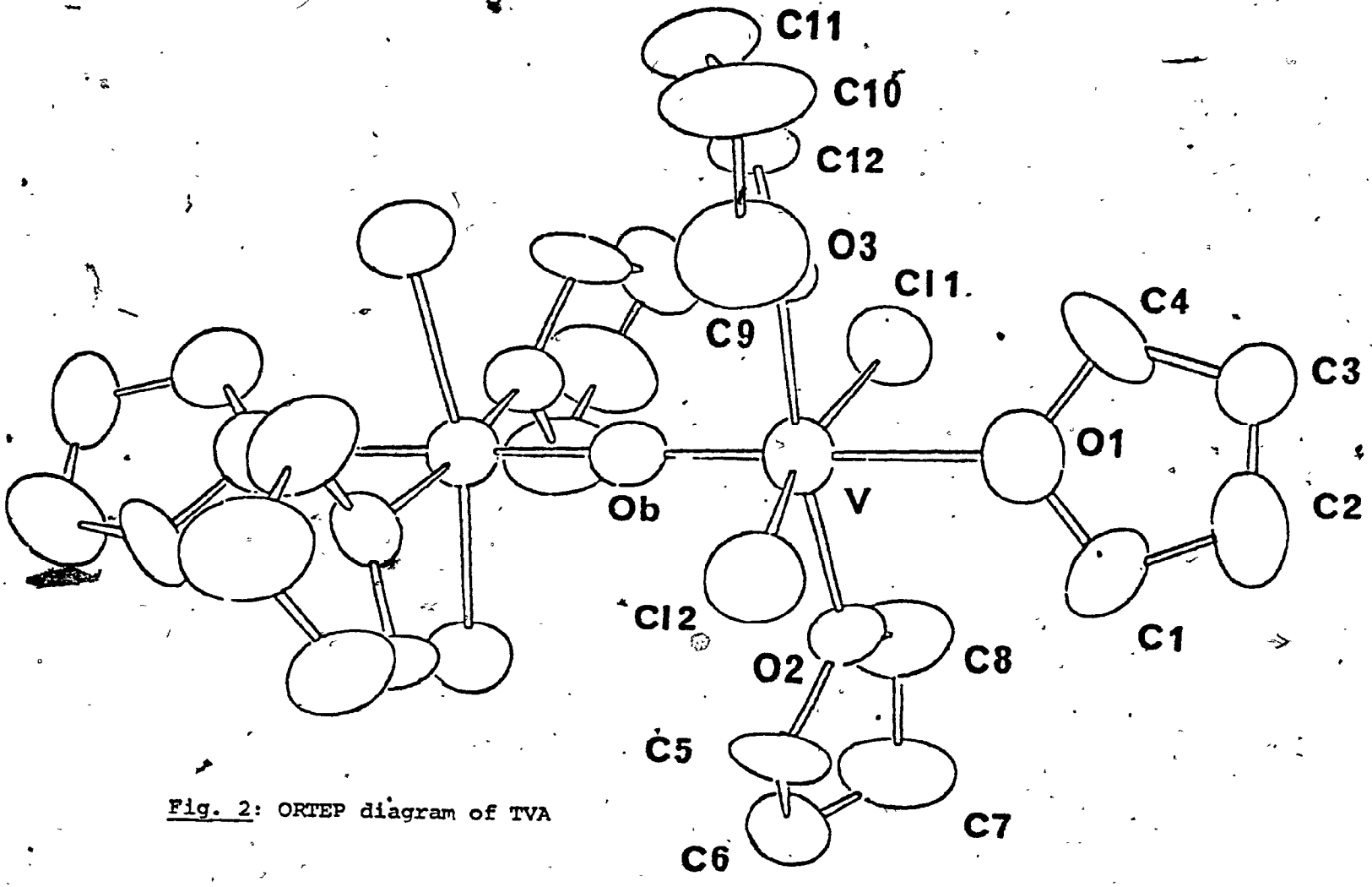

Fig. 2: ORTEP diagram of TVA

$(thf)_3(Cl)_2VOV(Cl)_2(thf)_3$

AIMS AND OBJECTIVES

A first objective of this work has been to achieve a quick and simple method of synthesis of an isolable V^{II} derivative, coordinated to easily diplaceable ligands, that may be easily dissolved in a variety of organic solvents (an achievment which will facilitate the study of the complexing abilities of V(II) with various ligands). It may be mentioned here that this objective has been successfully achieved.

The reaction systems studied in this work are implicated in Ziegler-Natta polymerization catalysis, and are fairly typical except for the fact that in Ziegler-Natta catalysis typically solvents of almost no coordinative capability, such as hexane, are employed, whereas in the present work THF and CH_3CN have been employed. Although the mechanisms involved in reactions of this type have been extensively, and one might say exhaustively studied over a number of years, not much is known about them and about the nature of the catalytically active species present. A secondary objective of this work has therefore been to obtain a better understanding of such systems, and especially to attempt to isolate possibly catalytically active species.

As a tertiary objective, this work has attempted to contribute to a better understanding of the type of bonding that vanadium is most likely to involve itself in in an oxidation state such as +2, especially since previous attempts at studies of V(II) systems have been scarce for various reasons, primarily its extreme sensitivity to air.

SECTION I

GENERAL INTRODUCTION

In this section a discussion of the bonding characteristics of vanadium is presented along with an account of the mechanisms involved in the organometallic reactions of vanadium. Illustrative complex compounds of V(II) are mentioned and a brief background of Ziegler-Natta catalysis is presented.

A:

It is pertinent to commence at this stage with a discussion of the nature of bonding involved in complexes of the type under study in this work. One of the peculiarities of vanadium, due in part to its placement in the periodic table, is the formation of complexes with fewer electrons than required for stability according to the conventional 16 and 18 electron rules [1]. Thus in octahedral coordination, V(III) complexes usually contain 14 electrons assignable to the metal, and V(II) complexes have 15 (as is the case with the isoelectronic Cr(III)). Because of this property, V(II) complexes tend to be mostly 6-coordinate, when a maximum complement of electrons is made available to them. Thus some of the most common V(II) complexes such as $VCl_2(py)_4$ (py=pyridine) [2], as well as some of the earliest discovered, e.g. $Li_4(V(C_6H_5)_6)$ [3], and the more recent ones, (e.g. $V(pyrazole)_4Cl_2$ [4] and $K_4V(SCN)_6$ [5]) fall into this category. V(II) has been known to be other than 6-coordinate (e.g. VL_4^{2+}, L= triphenyl phosphine oxide, dimethyl sulfoxide among others [6] and $V(DMP)^{2+}$, DMP= dimethyl 1,10 phenanthroline [7a, 7b], but self-evidently, this has been so only with extremely bulky or extremely electronegative ligands, and the complexes have been unstable in the extreme [8]. V(II) is a d^3 system, and in the conventional high-spin 6-coordinate (O_h) case, it possesses one electron in each of the nonbonding T_{2g} orbitals. "Facile thermal promotion of these high energy electrons to antibonding levels" [9] can lead easily to bond cleavage and/or oxidation. Oxidation may be either a one-electron process or a two-electron process [10]. The sensitivity to air of the V(II) ion is well known [11], and it may be said that this an oxygen-sensitivity more than it is a moisture sensitivity (cf. thus $V(H_2O)_4Cl_2$, $V(ClO_4)_2 \cdot 6H_2O$ [12] and some of the experimental side-observations in the present work). (One might mention here, in the context of the discussion on nonconformity to the 16

and 18 electron rules, the prime example of stability amongst V complexes, $V(CO)_6^-$, which after all is an 18 electron system). Because of the presence of three symmetrically placed nonbonding electrons, V(II) complexes are stabilized by ligands with Pi-acceptor properties, due to M to L backdonation, according to the bonding model first proposed by Chatt and Duncanson [13]. Such complexes are thus usually fairly kinetically inert [6]. Most V(II) complexes have a magnetic moment near the spin-only value of μ_{eff}= 3.89 B.M., indicating the presence of unpaired electrons; some complexes however have moments that are lower, due to the presence of bridging or polymeric species [14].

B:

For a better ultimate understanding of the reactions conducted during the course of this work, we must briefly consider what is known about the mechanistic aspects of these reactions to the present time. Reactions of the type conducted here, i.e. between a transition metal halide and metal alkyls such as Zn or Al Alkyls and involving the liberation of gaseous hydrocarbon products, can proceed in two general ways. In both cases, due to the Lewis acid nature of the metal (here Zn or Al, hereinafter referred to as the "main-group metal") in the metal alkyl, a preliminary bridging coordination of the halide to the metal is thought to take place, e.g.

$$TiCl_4 + Al(Et)_2Et \longrightarrow TiCl_3 \cdot\cdot Cl \cdot\cdot Al(Et)_2Et \quad \text{(Eq. I-1)}$$

[15]

As will be further discussed later, it is a fundamental postulate of this thesis that at higher temperatures (above circa 40-50°C), the alkyl groups are eliminated as hydrocarbons from the main-group metal itself (through various processes described later), whereas

at lower temperatures a substantial alkylation of the transition metal may take place, with any subsequent elimination of alkyl groups occuring from the transition metal (see for comparison the discussion in ref. [16]). The first (higher temperature) mechanism requires a higher activation energy, which is consistent with the probable free radical nature of the process. The latter (lower temperature) mechanism requires a lower activation energy, which is consistent with known facts about concerted organometallic reactions. These two mechanisms are of course not mutually exclusive. Data obtained by other workers supports the conclusions of the foregoing discussion, as will be shown later.

Since all reactions described in the present work were conducted at low temperature, they can be assumed to have mainly followed the low-temperature pathway, involving preliminary metathetical (exchange) alkylation of the vanadium. It is therefore pertinent to discuss the stability of any V-alkyl bonds produced and the available modes of cleavage of such bonds at this stage. For some time now, the earlier notion that Pi-acceptor ligands coordinated to the transition metal (hereinafter abbreviated as TM) were necessary to stabilize TM-carbon bonds [17] has been dispelled [9], [18]. It is now believed that the role of Pi-acceptor ligands is to bind more firmly so that coordination to the TM occurs in such a way that sites are unavailable for concerted reactions- reactions involving more than one coordination site- to take place.

Cleavage of TM-carbon bonds is now believed to take place in four possible ways [18]: involving reductive (1,1) elimination; involving 1,2 and 1,n eliminations; involving β-elimination of the metal and H from the ligand; and finally, involving dinuclear elimination.

Reductive elimination, e.g.

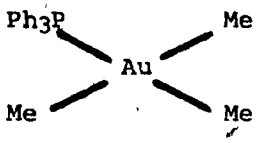

$\longrightarrow$ $(Ph_3P)AuMe + C_2H_6\uparrow$ (Eq. I-2) [19]

is frequently preceded by an oxidative-addition reaction.

1,2 and 1,n eliminations, e.g.

$TiMe_4 \longrightarrow (Me_2Ti{=}CH_2) + CH_4\uparrow$ (Eq. I-3) [20], [21]

are the least common.

β-elimination, represented schematically as

$M\text{-}CH_2\text{-}CH_2 \longrightarrow M\text{-}H + CH_2{=}CHR$ (Eq. I-4)

produces an alkene. If the group X in $M\text{-}CH_2\text{-}CHXR$ is electron-withdrawing, e.g. Cl, this reaction is inhibited. Where a β-hydrogen is unavailable it does not of course take place; thus such groups as $SiMe_3$ [22] and neopentyl [23] have been employed to prevent it. A good example of this elimination is:

$Bu_3PCuCH_2CD_2Et \longrightarrow Bu_3PCuD + CH_2{=}CDEt$ (Eq. I-5) [24]

Dinuclear elimination may involve the formation of metal-metal bonds and/or metal-alkyl bridges. Examples are:

$2(Ph_3P)AuMe \longrightarrow 2Ph_3P + 2Au + C_2H_6\uparrow$ (Eq. I-6) [19]

and the following:

$$Bu_3PCuD + Bu_3PCuCH_2CD_2Et \downarrow$$

$$2Bu_3P + 2Cu + CH_2DCD_2Et \qquad \text{(Eq. I-7)}$$

[24]

Earlier (see for instance refs. [25] and [26]) a free radical mechanism had been generally proposed and agreed upon for the reduction of TM halides by metal alkyls, videlicet

$$TiCl_4 + \frac{1}{n} MR_n \longrightarrow \frac{1}{n}MCl_n + TiCl_3 + R^{\cdot} \qquad \text{(Eq. I-8)}.$$

This mechanism has however been consistently discounted by experimental evidence [16, 27], such as the nonobervance of products of free radical-solvent reactions when solvents prone to such reactions were used. When other modes of reaction are inhibited, however, free-radical pathways do account for some portion of the products observed [15]. The most common of these is H-abstraction from the solvent, especially for hydrocarbon solvents.

C:

Because V(II) chemistry has not been much investigated (for recent advances see, for instance, refs. [28] and [29]), predictions as to the nature of bonding V(II) is most likely to involve itself in are still speculative. It can however be assumed that since V(II) is a d^3 system- a TM in a low oxidation state- it will be stabilized by Pi-acceptor ligands. There are however many bizarre examples of stability that stand out, such as (note absence of Pi-acceptor ligands) Ph_2V [30], Et_2V (from VCl_3 and $AlCl_3$ in ethyl benzene) [31] and $Li_4(VPh_6)$ (from VCl_3:3THF and PhLi) [3]. (Compare also the V(IV) and V(V) compounds $(PhCH_2)_4V$ and $(Me_3SiCH_2)_3VO$ [33,34,35].

Complexes of V(II) with Pi-acceptor ligands have been observed to be thermally more inert and usually insoluble [4,34,36-39]. Halogen atoms are usually strongly coordinating and substantial p_n-d_n interaction may be assumed to occur. Some illustrative examples of such V(II) complexes [3,4,36-39] are:

VL_4X_2 (L= pyrazole, imidazole, N-methyl imidazole, X= halogen)

VA_4X_2 (A= pyridine, β- and γ- picoline, X= halogen)

$V(en)_3X_2$ (X= halogen)

$V(dien)_2X_2$ (X= halogen)

$V(amq)_2Cl_2:2H_2O$ (amq= 8-aminoquinoline)

$VL_3X_2:nH_2O$ (X= halogen, L= 1,10 phenanthroline and 2,2 bipyridyl)

D:

An introduction to this work will be incomplete without a mention of Ziegler-Natta catalysis (for a good review, see ref. [40]). In 1955, K. Ziegler and G. Natta independently* discovered that triethyl aluminum, when added to titanium chlorides in hydrocarbon solvents, served as an extremely efficient catalyst for the polymerization of olefins [41,42,43,44]. Moreover, the polymerization

* though there is some evidence, as with all discoveries, of prior work: a few patents appear to have been taken out on similar systems prior to their discovery.

was conducted at low temperatures and atmospheric pressure, and the polymers obtained had a highly stereoregular character, being either isotactic or syndiotactic. Since then it has been observed that virtually any TM compound, when reacted with a metal alkyl having moderate acid character, such as the Al or Zn alkyls, will serve as a polymerization catalyst for olefins. Soluble compounds such as $Ti(Cp)_2Cl_2$ [45] furnish homogeneous catalysts that are not as stereospecific as the heterogeneous catalysts obtained from insoluble compounds like the halides. The specificity of the catalyst toward a particular type of olefin is analogous to the coordinative ability of the olefin to the TM in question.

The mechanism of Ziegler-Natta catalysis has been the subject of some dispute, and innumerable mechanisms have been proposed. The prediction of a definite mechanism has been hampered by the dearth of catalytically active material capable of being difinitely characterized, e.g. by X-ray diffraction studies. Most mechanisms predict preliminary coordination of the monomer to the TM. For the subsequent steps involving polymer growth, some predict such growth on the main-group metal (e.g. Al) (cf., in this regard, the insertion of $CH_2=CH_2$ into the Al-Et bond in $AlEt_3$ upto a chain length of ca. 100 ([46,47]). A free-radical mechanism involving an unpaired electron on the Al has also been proposed for the polymer growth step [15]. Most mechanisms however predict such growth on the TM. It is also uniformly understood that the TM is reduced to a low oxidation state, and the purpose of a hydrocarbon solvent is to display minimum coordinative capability so that sites are available on the TM for coordination by the monomer.

Among the Ziegler-Natta systems using vanadium compounds with Al alkyls* that are of note and of interest to this work are: $VOCl_3$-Al-

*Such systems have been used to polymerize monomers as far ranging as (isoprene + 1-pentene), (allylsilane + styrene), (butadiene + butene + propene) and vinyl ethers ([48]).

Et_3 [49], where the lowest valence state of V detected is (II) (when excess $AlEt_3$ was used); VCl_3-$AlEt_3$ in n-heptane [50], where the mechanism postulated is that of monomer coordination and chain propagation on the V-atom; and VCl_3:3THF/$(isoBu)_3Al$ in n-hexane for ethylene polymerization [51]. In brief, one may safely say that all the reaction systems studied in this work would be expected to be active if hydrocarbon solvents were substituted for the solvents presently used and if they were prepared in situ.

SECTION II

PRIOR ART

In this section an account of prior synthetic and structural work on V(II) is given. Prior work on oxidation processes capable of leading to the VOV^{4+} species is also discussed. Finally, earlier art on reduction of TM chlorides by metal alkyls is discussed.

A:

First studies on production of organometallic compounds of vanadium in low oxidation states were attempted with $VOCl_3$ and Grignard reagents [52,53,54], but the properties of the products obtained were not clearly known. Among the more recent attempts, Ph_2V [30], Li_4Ph_6V [3], Et_2V [31] and $(Me_3SiCH_2)_3VO$ [55,56] have already been mentioned. $VSO_4:7H_2O$ [57] as well as cyano complexes of V(II) were known before. Seifert and Gerstenberg [11] obtained the first synthetically useful V(II) compounds by electrolytic reduction of solutions of V_2O_5 in nonoxidizing acids. The reduction was accomplished at a Hg cathode in the presence of HCl and with the exclusion of oxygen. Compounds obtained are given in table II-A. In the absence of a strongly acidic solution, all of the above compounds were observed to be oxidized to V(III) either by molecular oxygen or by H_2O.

Methods for the production of V(II) in line with the above- i.e. involving electrolytic reduction of higher-valent vanadium in acidic media- are one of the two common methods used in arriving at V(II) complexes that are synthetically workable for coordination with other ligands. The other method employed is a reduction, also in acidic medium, with zinc dust [14, 58]. Most other synthetic methods for the production of V(II) complexes involve VCl_2 as the starting material and have been cumbersome and time-consuming; for example, the production of $VCl_2(py)_4$ (py= pyridine) is only accomplished by heating VCl_2 with (py) for several days [2,60].

Reduction of VCl_3 in methanol solutions [61,62] containing halogen acids at Hg cathodes was used by Seifert and Auel [14, 58] to obtain a variety of V(II) complexes, the adducts $VX_2:nCH_3OH$, X= Cl, Br, I, n= 2,4 (and 6 with Br). The salts $VX_2:4H_2O$, obtained

TABLE II-A

PRIOR ART ON V(II): (after Seifert & Gerstenberg (*11))

(Abbreviations: s=soluble i= insoluble d= decomposes)

Compound	Properties	Solubility
$VCl_2:4H_2O$	air, moist. sens., oxdzd, above 120°C by H_2O of crystzn.	s. C_2H_5OH, dark blue. i. ether, acetone.
$RbVCl_3:6H_2O$ (also *58)	red violet, d. to $RbVCl_3$ 120°C	i. organics
$NH_4VCl_3:6H_2O$	red violet	i. organics
$VBr_2:6H_2O$	viol. needles, d. to $VBr_2:2H_2O$ (80°C)	d.s. alcohol (brown) d.s. acetone i. ether
$VI_2:4H_2O$	d. 120°C	s. alcohol (violet) d.s. acetone (r.-brown)
$VF_2:4H_2O$		
$V(ClO_4)_2:6H_2O$	unstable, oxdzd. to VO^{2+}	s alcohol, d.s. acetone
$V(C_2O_4):2H_2O$	d. 170°C	i. organics
$V(NH_4)PO_4:6H_2O$	d.	i. organics

others: V(II) carbonate and V(II) acetate, uncharacterized.

subsequently, had magnetic moments near μ_{eff}= 3.80 B.M. corresponding to the spin-only value of V(II), indicating an octahedral, nonpolymeric structure, whereas the magnetic moments of the :$2H_2O$ adducts indicated a polymeric, halogen-bridged structure. Incidentally, VCl_2:(2,4)MeOH, along with the VCl_2:$4H_2O$ described earlier, has been found very versatile in synthesis, and has been used by many workers as a route to the other V(II) complexes. Thus Seifert and Auel [14] used VCl_2:2MeOH again to obtain the complexes

VCl_2:2THF VCl_2:4HCN VCl_2:4(py)

VCl_2:2(dioxan) VCl_2:2DMF VCl_2:4MeCN

(DMF= dimethyl formamide) (Scheme III-1)

The quadri-adducts were all blue-violet compounds (something that incidentally seems to be characteristic of unbridged hexacoordinated V(II) as also seen in the present work) and the di-adducts were all green; all compounds were air- and moisture-sensitive. The magnetic moments of the quadri-adducts (ca. 3.8 B.M. μ_{eff}) indicated unbridged octahedral coordination; a trans-chloro structure was indicated by X-ray powder diffraction photographs which revealed the compounds to be isostructural with $NiCl_2$:4(py), of known crystal structure [63].

V(II) halides were used as a route to a number of complexes with ammine ligands, mentioned earlier, of the general formula $VX_2L_{(2,4)}$ [64]. Khamar and coworkers [36,37] used a reaction of the hydrated V halides in ethanolic solution to obtain a number of pyridine and picoline complexes (also mentioned earlier) of the general formula VL_4X_2, with indicated trans-configuration for the halogens.

Among the more recent complexes isolated, $K_4V(NCS)_6$:EtOH was

obtianed with $VSO_4:6H_2O$ as starting material in a nonacidic aqueous ethanol solution. The imidazole, pyrazole and N-methyl imidazole complexes (VL_4X_2, briefly mentioned earlier [4]), were obtained in ethanolic solution starting with the hydrated V(II) halides which were dehydratedin vacuo prior to use, as well as from $VCl_2:2MeOH$ as starting material [37].

Also starting with the anhydrous V(II) halides, a number of macrocyclic complexes of V(II) were obtained using acetonitrile and DMF solvents [38]. These bore the general formula VLX_2 (X= halg.); the ligand is illustrated below:

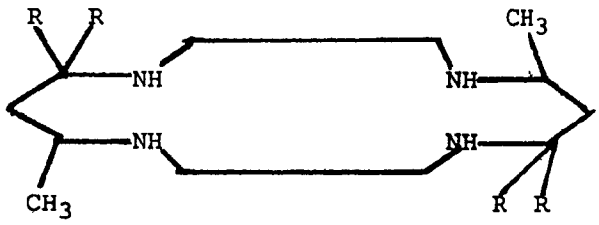

A) R= H, L= meso 5,12 dimethyl 1,4,8,11 tetrazacyclotetradecane

B) R= Me, L= meso, 5,7,10,12,14 hexamethyl 1,4,8,11 tetrazacyclotetradecane.

(Scheme II-2)

Some poly(1-pyrazolyl) borate complexes of V(II), whose crystal structures were subsequently determined [64], were also synthesized starting with the anhydrous (i.e. dehydrated) halides and using ethanol solutions.

B:

One of the most peculiar and interesting results achieved during the course of this work has been the isolation in crystalline form of a V(III)-O-V(III) species. It is relevant at this stage to trace what has been known hitherto about the existence and production of this and similar species. In a kinetic study of the reaction of V(II) and V(IV) (as their perchlorates in 0.5 M $HClO_4$), Newton and Baker ([65a,65b]) found evidence for the existence of a hydrolytic dimer, VOV^{4+}, with an extremely strong and charactersitic absorption band at 425 nm. The overall reaction, $V^{2+} + VO^{2+} + 2H^+ \longrightarrow 2V^{3+} + H_2O$, was shown to proceed through two possible pathways, one a direct one involving an outer-sphere activated complex (responsible for about 35% of the products) and one involving the intermediate VOV^{4+} in the following manner: $VO^{2+} + V^{2+} \longrightarrow VOV^{4+}$ (mode of its production); $VOV^{4+} + 2H^+ \longrightarrow 2V^{3+} + H_2O$ (mode of its destruction); The mode of production was believed to be more rapid than the mode of destruction at the hydrogen ion concentrations used, so that the species was observable by its spectrum, but its concentration at any time was believed to be very small, suggesting a very high extinction for its absorption band. The same species was observed on increasing the pH of the V(III) solution to 2.7. Swinehart [10] observed the species when studies of the oxidation of V(II) by O_2 and H_2O_2 were being conducted, also in the presence of appr. 1 M $HClO_4$. A $Cr-O-Cr^{4+}$ species was observed by Ardon and Plane [67] when $Cr(ClO_4)_2$ was oxidized by molecular oxygen. This was also observed when the oxidation was performed with 2-electron acceptors like Tl^{3+}, ClO_3^-, HClO and $Cr_2O_7^{2-}$, but not with one-electron acceptors like Fe^{3+}, Cu^{2+}, Cl_2 or Br_2.

It is interesting to note that in $HClO_4$, in which medium all these reactions were conducted, the rate of oxidation of V(II) to V(III)

has been shown to be the slowest. Thus it may be speculated that this feature gives VOV^{4+} sufficient time to form, before V^{2+} is consumed by other oxidation pathways. (This property was found in tests of the rate of oxidation of V(II) by air in various media [68]).

In an earlier study, Gandeboeuf et al. [69] observed a species with an identical strong absorption band at ca. 425 nm. This study was in an approximately 1 M $HClO_4$ solution at low pH. This band was presumed by these authors to be due to $V(OH)^{+}_{2}$, and a species observed at a higher pH was thought to be $V_2(OH)^{3+}_{3}$; as will be shown later, these assignments should be reversed. In the presence of perchlorate, an entity given the structure

$$\left[V_2(OH)_2(CH_3COO)_3 \right]^{+} \qquad \text{(Scheme II-3)}$$

was observed, also with a strong absorption near 425 nm; this assignment appears to be more accurate.

In the context of this discussion a final point is worth mentioning. Bridging seems to occur quite commonly in V compounds. Linear V-O-V bridges exist in many compounds, as will be shown later, and even a V(II)-N=N-V(II) entity has been observed [70].

C:

We now come to some prior work of considerable significance towards this thesis: work conducted on the alkylation of TM halides.

Reaction of Zn or Al alkyls with early-TM halides such as those of Ti or V leads primarily to reduction of the metal- to lower valence states or to the atomic state- , halogenation of the Zn or Al, and

the production of hydrocarbon gases- with ethyl as alkyl, butane, ethane and ethylene are produced along with some ethyl chloride. In dealing with the mechanism of these reactions at low termperature, one must preclude free radicals, except when other reaction pathways are blocked, as the experimental evidence is against them [15,16,27], e.g. the inability to isolate products of reactions of Me· with ether [71]. A general scheme, developed for such reactions by Prince and Weiss [27] is:

$$AlEt + \frac{1}{n}MX_n \longrightarrow \frac{1}{n}M^\circ + AlX + \frac{1}{2}C_2H_4 + \frac{1}{2}C_2H_6 \quad (\text{or } \frac{1}{2}C_4H_{10})$$

$$AlR + \frac{2}{n}MX_n \longrightarrow \frac{2}{n}M^\circ + AlX + RX$$

(Scheme II-4)

Here M° represents the completely reduced TM, but in general it may represent one reduced to a lower oxidation state.

Another point worth noting is that hydrogen abstraction can be accomplished from the solvent, but it can also be accomplished in other ways, e.g. from an adjacent alkyl group, as postulated by Eden & Feilchenfeld [15]:

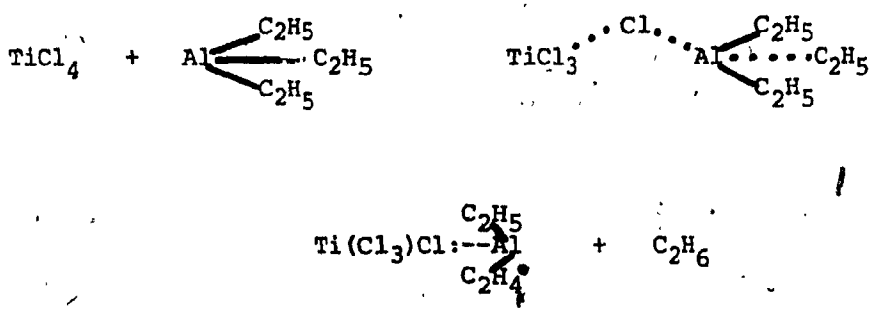

(Scheme II-5)

The most likely process for H-abstraction is from the metal hydride formed during the process of β-elimination. Thus Prince and Weiss [27] found that when an Al alkyl hydride was used in place of the metal alkyl, a 40-fold excess of ethane over ethylene was produced. In all these reactions of Al ethyls with metal halides, ethane was produced much in excess of ethylene, whereas they would be expected, according to Scheme II-4, to be produced in equal quantities, and the discrepancy may be attributed to H-abstraction.

A representative table of gases evolved in such reactions, from ref. [27], is given in tables II-B and II-C. These data have no small bearing on the present work, and have been useful in formulating hypotheses in regard to the prediction of mechanisms of reaction from the relative amounts of hydrocarbon gases evolved. (See G.C. section and section on Conclusions of the Work).

Eden and Feilchenfeld [15] observed that the ratio of butane to ethane increases markedly when less $AlEt_3$ is used (Table II-D). One might attribute this to the fact that with excess $AlEt_3$, ethyl groups are more likely to be eliminated from the Al early in the reaction (through various processes of H-abstraction) whereas with greater quantities of TM present the process of dinuclear elimination leading to butane is more prominent.

The role of the solvent is relatively minor as far as the effect on ratios of gases evolved goes. Only in unsaturated solvents, where extensive alkylation (of the solvent) and polymerization occur, and in halogen solvents, where the solvent takes part in the reaction, is this pronounced.

TABLE II-B

EVOLVED GASES FROM OXIDATION OF $AlEt_3$ WITH METAL CHLORIDES

(after Prince & Weiss (*27))

Halide & Molar Ratio to $AlEt_3$	Percentage composition of gases				
	C_2H_4	C_2H_6	C_4H_{10}	OTHER	% recovery ethyl groups
$CoCl_2$ (2.7)	30	69	1.0	C_4H_8	98
$CoBr_2$ (1.5)	35	60	5.0	-	103
CuCl (1.2)	39.5	58.5	2.0	C_2H_5Cl	72
$CuCl_2$ (0.93)	33	58	9.0	C_2H_5Cl	73
$NiCl_2$ (2.2)	24	75	1.0	C_3	93
$FeCl_3$ (2.0)	39	60.5	0.2	C_3H_8(0.3)	102
AgCl (1.7)	15	62	23	C_2H_5Cl	77

TABLE II-C

EFFECT OF ALKYL GROUP ON OXIDATION OF $AlEt_3$ BY $CoCl_2$

(Abbrvns. for solvent: E= ether, MC= Me-cyclohexane)

(after Prince & Weiss (*27))

Alkyl, (solvent), molar ratio to $AlEt_3$	Evolved gas composition (%age)					
	CH_4	C_2H_4	C_2H_6	iso-C_4H_8	iso-C_4H_{10}	n-C_4H_{10}
Me_3Al, (E), 0.5	84.5		14			0.6
Me_3AlEt_3Al, (E), 0.95	62	13	24			
$(isoC_4H_9)_3Al$, (MC), 2.0	46	4	6.5	18.5	24.5	
$KAl(Et)_3Cl$, (MC), 2.3	32.5	66				1.4

TABLE II-D-1

EFFECT OF Al/$TiCl_x$ RATIO ON GASES EVOLVED IN THEIR REACTION

(Solvent: CCl_4)

(after Eden & Feilchenfeld (*15))

Reaction, (molar ratio)	C_2H_6	butanes	ethyl chloride
	(figures are %ages)		
$AlEt_3/TiCl_4$ (2:1)	84	9	7
$AlEt_3/TiCl_3$ (0.9:1)	99	traces	traces
$AlEt_2Br/TiCl_4$ (2:1)	99	1	0

TABLE II-D-2

BUTANE/ETHANE RATIO AS FUNCTION OF $AlEt_3/TiCl_4$ RATIO

Ratio Al/Ti:	9.1	3.1	0.97	0.84	0.22	0.13
Ratio Butane/Ethane:	0.05	0.0	0.15	0.14	0.28	0.28

D:

Jacob et al. [16] did an extensive study of the reaction of $ZnMe_2$ and $ZnEt_2$ with VCl_4 at low temperature. Their results are summarized in Table II-E. It will be noted that because of the lower temperature of reaction as compared to that in earlier work by Prince and Weiss [27] and Eden and Feilchenfeld [15], a substantial portion of products having V-alkyl bonds (including V-ethyl bonds which are prone to the process of β-elimination) was isolated, something which has no small bearing on the present work (where no such V-alkyl bonds were isolated, presumably due to the effects of the coordinating solvents used as will be discussed later). The extent of alkylation of the V generally depended on the ratio of the Zn alkyl to V used, and the interaction of the solvent with or heating of the products containing V-alkyl bonds usually led to the cleavage of these bonds and consequent reduction of the metal.

TABLE II-E

REACTIONS OF VCl_4 WITH Zn ALKYLS

(after Jacob et al. [16])

VCl_4 + $ZnMe_2$ in hexane, -50°C

a) With V/Zn molar ratio 2:1, $2VCl_3$:MeZnCl:$0.5ZnMe_2$ (μ_{eff}= 2.69 B.M., implying V(III)) and MeCl are produced. Above crystalline product gives methane and a little ethane with acid, giving V^{3+} solution. With THF, it gives a VCl_3(THF) solution and a $2VCl_3$:$ZnCl_2$:8THF ppt..

b) With molar ratio V/Zn 1:1, gives $2MeVCl_2$:MeZnCl:$ZnCl_2$ (or $2VCl_3$:MeZnCl:$ZnMe_2$), μ_{eff}= 2.95B.M. (implying V(III)). Hydrolysis of this gives methane, a little ethane and V^{3+}. Gives dark violet soln. with ether (yielding $2MeVCl_2$:$ZnCl_2$:2(ether) and a ppt. of $3MeVCl_2ZnCl_2$(ether)). With THF, gives methane and greeen $2VCl_2$:$ZnCl_2$6THF, which gives V(II) with mineral acid.

c) With V/Zn molar ratio 2:3, MeCl is produced initially. With more $ZnMe_2$ added, large quantities of methane and ethane, along with VCl_2:1.5MeZnCl and MeVCl:0.5MeZnCl:$ZnCl_2$ are produced.

VCl_4 + $ZnEt_2$ in n-pentane, -10°C

With V/Zn molar ratio 1:1, a mixture of $ZnCl_2$, EtZnCl and violet, air-sensitive $EtVCl_2$ is produced. This decomposes at room temp. to give ethane, ethylene and butane. With ether, it gives $EtVCl_2$:0.5(ether). Treatment with ether for 50 hrs gives VCl_2(0.7(ether)), which with THF gives VCl_2:2THF.

TABLE II-E, cont.

VCl_4 + diallyl zinc

No reaction at low temperature. At room temperature, gives allyl chloride, propene and V(III) with ether solvent.

VCl_4 + dibenzyl zinc

Gives $PhCH_2VCl_3$, which decomposes to give toluene and dibenzyl.

VCl_4 + $ZnEt_2$ in ether

With V/Zn molar ratio 2:3 and at -20°C, gives a deep violet solution, which yields finally $VCl_2:ZnEt_2O(Et)_2$.

SECTION III

EXPERIMENTAL PROCEDURES

A: CRYSTALLOGRAPHIC

It is not proposed here to give a detailed discussion of the theory and practice of the technique of X-ray crystal structure determination. A brief outline of the procedures followed in the present work only is presented. Considerable basic knowledge of X-ray diffraction techniques will be assumed on the part of the reader. Details of the crystal mounting are given in the sections on each individual structure, VEZN and TVA, since they differed for the two structures.

1- Space Group Determination

The space group was determined from an analysis of the diffraction spots on the Weissenberg and Buerger (precession) photographs.

Oscillation photographs were taken with a variation of ± 10° at two approximately perpendicular settings of the crystal axis for purposes of alignment. These were taken on a Weissenberg camera supplied by the Charles Supper Co, (Natick, Massachussetts) as were the subsequent Weissenberg photographs. The second upper level was the highest level measured in the Weissenberg photographs for both crystals. On the basis of the layer line patterns on the Weisenberg 0-level, two reciprocal axes were chosen and precession photographs taken for these axes on a precession camera (also supplied by the Charles Supper Co.). Both cameras used a fine-focus Mo X-ray tube as a source; this was powered at 40 kV and 20 mA by a Picker Nuclear X-ray Generator and Control (Model 809B). Kodak "No-Screen" film was used for the work. The Mo radiation was filtered with Zr foil to yield a K_α wavelength of 0.7107 Å.

The coupling of the Weissenberg camera was such that 1 mm of lateral distance on the 0-level photographs corresponded to a 2° rotation of the crystal. For the precession camera, the reciprocal cell spacing d*, the corresponding spacing on the film y_n, and the

wavelength of the radiation were related by the equation:

$$d^* = \frac{y_n}{60.0\,\text{Å}} \qquad \text{(Eq. III-A-1)}$$

where 60.0 represents the film- crystal distance for the 0-level zones in mm.

2- Intensity Data Collection

An automated 4-circle diffractometer (Picker Nuclear) was used for the intensity data collection. For control , this was interfaced to a PDP 8/s minicomputer in the case of VEZN and to a PDP 8/a minicomputer in the case of TVA. Power for the Mo X-ray tube was provided by a Picker Nuclear Constant Potential Diffraction Generator (model 6238E) (stable to within 0.19 kV and 0.02% mA) set at 40 kV and 20 mA. The takeoff angle for the direct beam was 3.0°. Monochromation was accomplished by a graphite crystal (reflection from the 002 face). Wavelength was taken as 0.7107 Å for the K_α radiation. A 1 mm diameter pinhole collimator was used to direct the radiation at the sample crystal, which was held at a 14.0 cm distance from the point of monochromation. A receiving aperture equipped with adjustable vertical (Top/Bottom, T/B) and horizontal (Right/Left, R/L) slits was located 23.0 cm from the crystal and 2.0 cm from a NaI-TlI scintillation counter. The aperture was also equipped with Ni-foil attenuators calibrated to reduction factors of 2.781, 7.959 and 38.190 to attenuate reflections having intensity of count less than 10,000 cps.

The detector was operated at 1,000 volts (5.60 helipot setting). A

pulse-height analyzer was used to receive 100% of the K_α intensity.

The 0-level Weissenberg was used as a guide for alignment of the crystal on the diffractometer and indexing of the reflections. A strong reflection of low 2θ value on one of the axis lines was chosen. The ω & χ angles on the diffractometer were set at 0, and 2θ set for the reflection chosen. Φ was then set to correspond to $-\Phi$ on the Weissenberg, and the reflection centered manually, with the help of the R/L and T/B shutters. The information obtained thus was used to center (again using the T/B and R/L shutters) a higher reflection on the axis. The axis was scanned to confirm the intensity pattern observed on the Weissenberg, and finally the exact angles were set and recorded for a high-angle reflection. The same procedure was repeated for the other axis represented on the Weissenberg.

In the case of VEZN, the two reflections were finally centered using the PDP 8/s minicomputer run with a program supplied by the Picker Nuclear Co. The two centered reflections, together with the unit cell parameters obtained from the photographs, were used to located the third axis. 12 reflections of high intensity and 2θ angle and covering evenly the reciprocal lattice were chosen and centered using the centering program. Values for ω, χ, and Φ at $\pm 2\theta$ (for reflections hkl and $\bar{h}\bar{k}\bar{l}$) were obtained and these values averaged. The angular parameters so obtained were used in a least squares refinement of the cell parameters. Refined output values were used to calculate an orientation matrix to be used for the data collection on the diffractometer. (The data collection programs were supplied by the Picker Nuclear Co.).

In the case of TVA, the centering- and the rest of the data collection procedure as well- was accomplished in a similar manner to that given above with the help of a data collection package program

developed at the National Research Council of Canada, Ottawa [72].

The θ-2θ scanning method was used to record the integrated intensities of the reflections. The space group symmetry (determined from the photographs to be $P\bar{1}$ for VEZN and C2/c for TVA) was used to instruct the computer to appropriately reduce the proportion of the limiting sphere to be measured and to ignore systematically absent reflections. A maximum and minimum value of 2θ were specified. The scan width was $2.0° + 0.692\tan\theta$. The scan rate was 2°/min in 2θ. The backgrounds were measured for 20 secs. in the case of VEZN and for 0.1 times the scan time for TVA.

For VEZN the output of the intensity data was on puched paper tape, to be transferred (with the use of a Hewlett-Packard 2114A computer) to magnetic tape for data processing. For TVA the output was directly recorded on one of the disks of the PDP 8/a minicomputer but was also available as printout.

A set of three reflections of fairly high intensity were chosen as standards and measured at intervals of 50 reflections. Constancy in their intensity through the data collection process indicated all was well.

3- Data Reduction

Computing was done on a C.D.C. 6400 computer for VEZN and on the PDP 8/a minicomputer for TVA.

For VEZN, reduction of the data to yield a list of structure factors for the reflections was accomplished with the help of a locally written program called PREP. The input consisted among other things

of the raw intensity data, the cell parameters and tables for each atom giving the mean atomic scattering factors at intervals of 0,05 $\mathring{A}^{-1}$ in $\sin\theta / \lambda$, (calculated on the basis of the computations of Ibers and others [73]).

For TVA the data reduction was done using similar programs contained in the N.R.C. package.

After application of the attenuator factors, if necessary, and scaling of the intensities of the reflections, in accordance with the variation of intensity of the strongest of the three standard reflections, the intensity I of each reflection was computed according to the equation

$$I = N - (B_1 + B_2) \times \frac{t_s}{t_b} \qquad \text{(Eq. IIIA-2)}$$

where N is the count recorded for each reflection, B_1 and B_2 the background counts on either side of the reflection, t_s the reflection scan time and t_b the total background scan time. A standard deviation for the intensities, given by the formula

$$\sigma(I) = \left[N + \frac{B_1 + B_2}{2} \left[\frac{t_s}{t_b}\right]^2 + (c \cdot N)^2 \right]^{\frac{1}{2}} \qquad \text{(Eq. IIIA-3)}$$

where the symbols have the meanings given above and c was 0.02 for VEZN and 0.00 for TVA, was calculated.

Reflections of intensity I less than $3\sigma(I)$ were treated as rejects and along with the systematically absent reflections were omitted from the structure solutions.

The intensities were used to compute the relative structure factors,

F_{rel}, using the equation

$$F_{rel}(hkl) = \left[\frac{I(hkl)}{Lp}\right]^{\frac{1}{2}} \qquad \text{(Eq. IIIA-4)}$$

(Lp) represents the usual combined correction factor for the polarization of the X-rays and for the specific geometry of the method of collection, and in our case was given by

$$Lp = \frac{(\cos^2 2\theta_m + \cos^2 2\theta_s)}{\sin 2\theta_s(\cos^2 2\theta_m - 1)} \qquad \text{(Eq. IIIA-5)}$$

where θ_s and θ_m represent the diffraction angles at the crystal and monochromator respectively. The F_{rel}'s were used to obtain the Absolute Structure Factors (F_{abs}) and the scale factor F_{rel}/F_{abs} according to the usual method, first outlined by Wilson [74]. The rate of change of F_{rel}, called sigma (the first derivative of Eq. IIIA-4) was also part of the output in the programs (for each reflection).

4- Structure Solution

The structure solution was accomplished in both cases from an initial identification of the positions of the heavy atoms by the Patterson method [75], [76]. These positions were then used as a phase-basis to obtain the Difference-Fourier plot from which additional atoms could be identified, the procedure being thus repeated, with intervals of refinement of the atomic parameters obtained, until all atoms had been identified.

The structure factor F_{hkl} represents the resultant of the waves scattered by the individual atoms in the unit cell. It is a vector

quantity, and its amplitude and phase are determined by the scattering powers of the atoms and by their relative positions (determining the phase, $\delta = 2\pi(hx + ky + lz)$, for each reflection, where x, y and z are the fractional coordinates of the atoms. The scattering powers of the atoms also depend on their thermal vibrations. The structure factor is thus represented by

$$F^{\circ}_{hkl} = (A^2_{hkl} + B^2_{hkl})^{\frac{1}{2}}$$

$$\text{where } A_{hkl} = \sum_j f_j \cos\delta \quad \& \quad B_{hkl} = \sum_j f_j \sin\delta$$

(Eq. IIIA-6)

the f_j's being the scattering factors for the j'th atom of fractional coordinates (x_j, y_j, z_j) and the δ the phase, $2\pi(hx + ky + lz)$.

In exponential form, F_{hkl} is given by

$$\sum_j f_j \, e^{2\pi i(hx_j + ky_j + lz_j)} \qquad \text{(Eq. IIIA-7)}$$

Considering thermal vibrations of the atoms also, the scattering factor must be corrected using an exponential term,

$$e^{-B\left[\frac{\sin^2\theta}{\lambda^2}\right]} \qquad \text{(Eq. IIIA-8)}$$

where B, the "isotropic" thermal parameter, is related to the mean square amplitude of vibration, $\overline{\mu^2}$, by $B = 8\pi^2\overline{\mu^2}$, the atoms being assumed to vibrate isotropically. If a more refined analysis is to be presented, the atoms must be assumed to vibrate anisotropically, each direction having associated with it a thermal parameter.

The complete structure factor then is Eq. III-A-7 multiplied by the term

$$e^{-(h^2\beta_{11} + k^2\beta_{22} + l^2\beta_{33} + 2hk\beta_{12} + 2hl\beta_{13} + 2kl\beta_{23})}$$

(Eq. IIIA-9)

where the β's are the "anisotropic thermal parameters" whose geometric qualities are related to those of an ellipsoid; the atoms are thus termed thermally vibrating ellipsoids or "thermal ellipsoids". When the anisotropic thermal parameter U, representing directly the mean square amplitude of atomic vibration in $\mathring{A}^2$, is used, the exponential factor above (Eq. IIIA-9) becomes

$$e^{-2\pi^2\left[U_{11}h^2a^{*2} + U_{22}k^2b^{*2} + U_{33}l^2c^{*2} + 2U_{12}hka^*b^* + 2U_{13}hla^*c^* + 2U_{23}klb^*c^*\right]}$$

(Eq. IIIA-10)

where the bracketed term is being multiplied by $2\pi^2$. The use of the U terms is to preferred over the B's and β's. In the case of TVA, U's were exclusively used, whereas in the case of VEZN output in the form of β's was finally converted to U output.

For structure solution by Patterson methods, the square of the structure factor is used in the computation of a density map by the equation

$$\rho(xyz) = \frac{1}{V} \sum_h \sum_k \sum_l (F_{hkl}^2) \cos 2\pi(hx + ky + lz)$$

(Eq. IIIA-11)

V being the volume factor. The peaks represent interatomic vectors for the atoms in the unit cell; for N atoms there are of course N^2 peaks, N being from each atom to itself and thus located as one big peak at the same "origin", leaving N^2-N peaks to be dealt with. To eliminate the diffuse nature of the peaks, the atoms were treated as point scatterers, and a "sharpened" Patterson function, calculated using the modified coefficient

$$F_{hkl}^2 \text{ (sharp)} = \frac{\left[0.1667 + \left[\frac{\sin\theta}{\lambda}\right]^2\right] (F_{obs}hkl)^2}{\left[\sum_{j=1}^{n} f_{oj}\right]^2 e^{-B\left[\frac{\sin\theta}{\lambda}\right]^2}}$$

(where f_{oj} = mean scattering factor for atom j)

(Eq. IIIA-12)

Elimination of the "origin peak" was carried out by using the method outlined by Patterson [76] where the quantity $\sum_{i=1}^{n} f_i^2$ is subtracted from the usual coefficients used.

In the difference-Fourier, in place of the F_{hkl} coefficients used in the calculation of the electron density (the Fourier transform of the structure factors), according to

$$(xyz) = \frac{1}{V} \sum_h \sum_k \sum_l F_{hkl} e^{-2\pi i(hx + ky + lz)} \qquad \text{(Eq. IIIA-13)}$$

an electron-density-difference map, based on the coefficients $(F_{obs}-F_{cal})$ was plotted. In such a map positive peaks will appear where there should be atoms and none are placed, holes will appear where the calculated electron density is basically correct, and ne-

gative peaks will appear (when not suppressed) where too much electron density has been assigned (implying a wrongly placed atom).

Atomic parameters obtained from either of the two methods, the Patterson or the Difference Fourier, were refined using the conventional least-squares method, where the function being minimized (for instance by full-matrix methods when the number of variables is less than ca. 70 as for VEZN, and by block diagonal matrix methods where there are more than ca. 70 variables as in the case of TVA) is:

$$D \equiv \sum_{hkl} w_{hkl} \left(|F_{obs}| - kF_{cal} \right)^2$$

(Eq. IIIA-14)

Here the weight equals $1/\sigma^2$ (the "sigma" value calculated in the initial data reduction) and k is the scale factor for F_{cal}.

To test the degree of correctness of the structure at any stage of the solution, the "R factor" (also known as the residual, reliability or discrepancy index) was calculated.

In its unweighted and weighted forms it is given by:

$$\underline{\text{unweighted}} \quad R = \frac{\sum_{hkl} \left| |F_{obs}|_{hkl} - |F_{cal}|_{hkl} \right|}{\sum_{hkl} |F_{obs}|_{hkl}}$$

(Eq. IIIA-15)

$$\text{weighted } R = \left[\frac{\sum_{hkl} w_{hkl} \left(|F_{obs}|_{hkl} - |F_{cal}|_{hkl} \right)^2}{\sum_{hkl} w_{hkl} \left(|F_{obs}|_{hkl} \right)^2} \right]^{\frac{1}{2}}$$

$$(\text{where } w_{hkl} = 1/\sigma^2)$$

(Eq. IIIA-16)

For TVA, all computer programs used for the above-described processes as well as for the calculation of the geometry of the final crystal structure were contained in the N.R.C package. For VEZN, a modified version of a program called SFLS [77] was used for the least-squares and structure factor calculations and a program called FORDAP [78] was used for the Patterson, Fourier and Difference Fourier calculations, while UTILITY [79] was used to obtain geometric parameters such as bond lengths and bond angles. This latter program first converted each fractional atomic coordinate into an orthogonal one, and also computed standard deviations; for a bond length the standard deviation is:

$$\sigma_l = \left[(\sigma_{x_1}^2 + \sigma_{x_2}^2) \frac{\Delta x}{l}^2 + (\sigma_{y_1}^2 + \sigma_{y_2}^2) \frac{\Delta y}{l}^2 + (\sigma_{z_1}^2 + \sigma_{z_2}^2) \frac{\Delta z}{l}^2 \right]$$

(Eq. IIIA-17)

where σ_{x_1} and σ_{x_2} are (as examples) the estimated standard deviations in the x parameters of atoms 1 and 2 respectively; l is the bond length.

Corrections for anomalous dispersion were not thought necessary. For VEZN, for instance, rough calculations showed that reduction in intensity due to absorption would be as little as 5% in certain directions.

The final structural models obtained were drawn with the help of the program ORTEP [80] and using the HP2114A computer interfaced to a COMPLOT x-y plotter.

Further individual details for the solutions of the structures of VEZN and TVA are given in the appropriate sections (see later).

SECTION III

EXPERIMENTAL PROCEDURES

B: SYNTHETIC

A description of the analytical (spectral and G.C.) techniques used is given in the appropriate sections.

A table giving a list of chemicals used and suppliers is given in Appendix A.

Most of the synthetic work was conducted on a dry-N_2-cum-high-vacuum line (Fig. IIIB-1) using "Schlenk" apparatus (essentially glassware capable of withstanding high vacuum and with a side-arm fitted with a stopcock for N_2 inlet and outlet).

Work of extreme sensitivity or work that was cumbersome was conducted in a dry box supplied by the Kewanee Sci. and Eng. Co. (Lubbock, Texas). The atmosphere of the dry box was tested for air- and moisture sensitivity and content routinely with $ZnEt_2$, which fumes visibly with the slightest trace. This practice was found to be quite appropriate for checking the validity (with regard to spoilage by entry of air or moisture) of any reactions conducted. N_2 on the dry-N_2-cum-high-vacuum line (hereinafter referred to simply as "the line") was dried by passing through P_2O_5. It was also periodically tested for moisture content with $ZnEt_2$ contained in a test Schlenk tube. A separate high-vacuum line was used for distillation of solvents.

Solvents

CH_3CN was dried by stirring with and then refluxing over P_2O_5 repeatedly until the P_2O_5 was observed not to turn yellowish from its original white. The solvent was then distilled twice on the high-vacuum line and stored in the dry box.

THF was distilled over Na under an atmosphere of dry N_2. Benzophe-

Fig. III-B-L (overleaf)

Inert-gas-cum-high-vacuum line, of the type used in this work. Not to scale. Only two hookups shown, one with Schlenk tube attached.

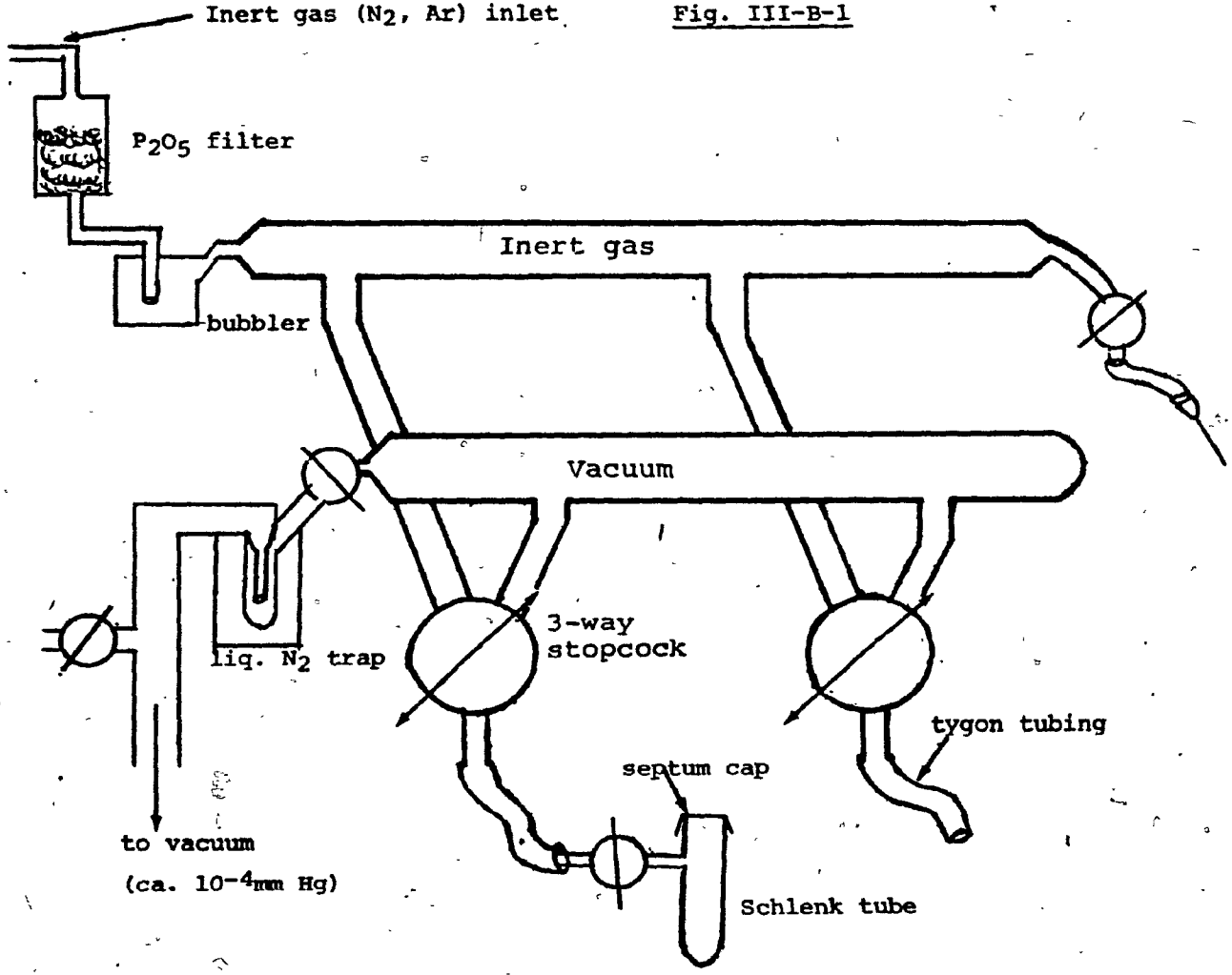
Inert gas (N_2, Ar) inlet
P_2O_5 filter
Inert gas
bubbler
Vacuum
3-way
stopcock
liq. N_2 trap
tygon tubing
septum cap
to vacuum
(ca. 10^{-4}mm Hg)
Schlenk tube

Fig. III-B-1

none was added (appr. 1 g to 500 ml solvent) in the final stages to test for dryness. When dry the solvent turns blue due to the formation of a Na-benzophenone complex. It was then distilled two times under high-vacuum and stored in the dry box.

Diethyl ether, used to wash precipitates, was distilled over Na and finally under high vacuum and stored in the dry box.

DMF, CH_2Cl_2 and $Cl_2CH\text{-}CHCl_2$ were distilled over P_2O_5 prior to vacuum distillation and storage in the dry box.

All solvents were tested with crystals of TVA (see later) for oxygen- and moisture- content. When dry and oxygen-free, the crystals dissolved giving an intense violet coloration. When the solvents went "sour", no such coloration was observed. CH_3CN was found to be the most difficult to dry, and THF was found to go "sour" with a few days keeping in the dry box, perhaps due to the formation of peroxides (though oxygen was presumably excluded) or other decomposition products, or impurities.

Reactants

Solutions of VCl_3 in THF and CH_3CN were prepared to an identical concentration of 0.1 m (10^{-1} mM/ml) by stirring the solid VCl_3 overnight with the solvent (under N_2 on the line) at 50-60°C. Solutions were filtered before use. The CH_3CN solution was green and the THF solution was orange-brown.

$AlEt_3$ was used as supplied by the manufacturer after a single vacuum distillation only. The synthesis of $ZnEt_2$ is described later separately. Spectra of the distilled samples of $AlEt_3$ and $ZnEt_2$ showed no traces of ethylene or of other impurities capable of interfering in any reactions.

The $ZnCl_2$ used was first leached with HCl to remove any Zn dust possibly present, and then dried at 80°c under high vacuum overnight before use. Solutions of $ZnCl_2$ in THF and CH_3CN were saturated solutions, of only approximately known concentration.

Other measurements

Density measurements for VEZN were made in the dry box in a mixture of EtI and benzene solvents by the flotation method.

Elemental analyses were performed by Galbraith Laboratories (Knoxville, Tennessee).

The procedures for the G.C., I.R. and U.V.-Vis. spectral measurements are described in the appropriate sections (see later).

Preparation of $ZnEt_2$

$ZnEt_2$ was prepared from EtI-EtBr and Zn dust (used as a Zn-Cu couple) according to the following procedure, modified from an earlier method ([80b]).

The following materials were required:

Cu oxalate	3.24 g	Zn dust	27.7 g
EtI	16.6 g	EtBr	11.5 g

The procedure is delineated below.

a) Preparation of Zn-Cu couple

The well-powdered Cu oxalate and the Zn dust were mixed well and

heated over a low free flame with continuous shaking until the first traces of a rust color appeared in lumps and the bluish traces of Cu oxalate were completely gone. Heating was then continued for another five minutes. A slow flow of dry N_2 was maintained over the reaction during the heating (total heating time, approximately 50 minutes). The reactants were cooled to room temperature while maintaning the N_2 flow.

b) Preparation of $ZnEt_2$

The EtI and EtBr were mixed well and loaded onto a dropping funnel, flushed previously with N_2. The funnel was attached to a 3-necked flask. The EtI-EtBr mixture was added to the Zn-Cu couple dropwise with constant stirring under a very slow stream of dry N_2, while the temperature was maintained at 50-55°C with an oil bath. The reaction started suddenly, as indicated by the appearance of white fumes (probably of $ZnEt_2$). After the addition of the EtI-EtBr mixture, the temperature was maintained at 50-55°C for appr. 2 hours. The reaction flask was then allowed to cool and finally all stopcocks were closed. The flask was left as such overnight and the product distilled the next day.

c) Distillation of product

Distillation of product was conducted under vacuum. While connecting up the apparatus for this procedure, a flow of N_2 was maintained over the product to prevent contact with air. The product was distilled off at ca. 110°C and collected under liquid N_2 (ca. -196°C). The distillation required approximately 3 hours. After bringing the distillate to room temperature it was taken to the high vacuum line for a final distillation; the first ca. 10% of this distillate was discarded to remove any EtI and EtBr prossibly present in the product (though there should not have been any since a large excess

of Zn used). The $ZnEt_2$ distillate was taken into the dry box for storage in an opaque container (because it was found to be light- sensitive).

$ZnEt_2$ vehemently attacks grease and diffuses through rubber septa and so is a problem to store in sealed container. Boiling point 118°C at 760 mm Hg. Density 1.8625_4^{18}.

SECTION IV

SYNTHESES CONDUCTED

All reactions were conducted at low temperatrue (-50° to -30°C). A slush bath of $CHCl_3$-CCl_4 made by adding liq. N_2 to these solvents was used. The following procedure for the preparation of TVA is illustrative; procedures for other products are given following it.

A: $(THF)_3Cl_2VOVCl_2(THF)_3$ ("TVA")

$AlEt_3$ + VCl_3 (1:1 molar ratio) in THF

Synthesis

5 drops of $AlEt_3$ were added to a previously weighed (evacuated) 25 ml Schlenk tube in the dry box. The tube was evacuated on the line while cooling under liq. N_2, brought to room temperature, and weighed again to determine the amount of $AlEt_3$ taken. 10 ml THF was then added to it in the dry box; the tube was then cooled in the slush bath on the line. A septum cap was put on the tube mouth in place of its ground-glass stopper. The required volume (for a 1:1 molar ratio) (appr. 5 ml) of prepared-and-cooled VCl_3/THF solution (0.1 M, see earlier section on preparation of reactants) was extracted with a syringe and slowly added, through the septum cap, to the $AlEt_3$ (kept at ca. -50°C) while stirring. The solution was initially brown but turned intense violet on warming to appr. -30°C. After addition, the septum cap was removed and the stopper replaced on the tube mouth; the solution in the tube was reduced to appr. 1/3 its original volume by distillation on the line. The tube was then left at ca. -20°C for a few days, when pure crystals of TVA precipitated. The mother liquor was separated by decantation from the crystals; it could then be used for the futher precipitation of crystals after reduction in volume. Nota bene: Variation of the V/Al molar ratio did not lead

to a different product; TVA, along with the excess reactant, was precipitated.

Stability and Preservation

Except in the case of the soluble TVA, all crystals were washed in the solvent of their original precipitation. TVA was washed with ether and dried in vacuo when required for elemental analysis. These ether-washed crystals were not found suitable for crystallographic analysis: they crumbled on touch and displayed in many cases a powder diffraction pattern; from previous experience [81] solvent loss from and consequent degeneration of the crystal lattice appeared to be the cause.

Solutions and free crystals of TVA appeared to be air-sensitive in the extreme (probably not that moisture- sensitive: see later sections, and earlier discussion of V(II)). Under optimum conditions in the dry box, the naked crystals (i.e. those not covered by the mother liquor or anything else) lost crystallinity in approximately 10 minutes. The unexposed crystals were translucent violet, but they became opaque within a few minutes of exposure, even in the dry box, indicating surface decomposition. Mounting the crystals for crystallographic analysis was thus found to be a problem, and is described in a later section. The mother liquor, and the crystals when kept therein, were stable at room temperature for at least 3 months (longest trial). The solutions of the crystals in THF were stable for a few days only. Decomposition was indicated by a decrease in or loss of the characteristic intense violet coloration, with concurrent decrease in intensity of or disappearance of an intense characteristic absorption band (at *ca.* 487 nm).

For preservation, the crystals, with a little covering mother liquor, were immersed in nujol. For elemental analysis, they were washed with ether (as noted earlier), dried ca. 5 minutes in vacuo, and sealed under vacuum in small ampoules after being loaded into these in the dry box.

Solubility

TVA was found to be extremely soluble in the following solvents, giving identically an intense violet coloration in all of them: in THF (as above); in CH_3CN; in CH_2Cl_2; in $CH_2Cl_2CH_2Cl$; and in DMF. Insoluble in diethyl ether (with which it was washed, as noted earlier), benzene, hexane, toluene and similar hydrocarbons. Soluble with decomposition in CH_3OH and acetone. Solutions in CH_3CN were fairly stable, and those in DMF extremely so.

Recrystallization

For crystallographic analysis, a large batch of crystals washed with ether were recrystallized thus: they were redissolved in a small quantity of THF; after reduction in volume by evaporation on the vacuum line, the solution was kept at ca. -20°C for 2 days, when an excellent crop of crystals was obtained. Further concentration of the mother liquor yielded a number of crystal batches. Crystals were used without further washing.

Composition

The elemental analysis for TVA is given in Table IV-A. Its differs from that corresponding to the formula determined by the X-ray study, and corresponds to a loss of solvent from the molecule and approximates to only 4 THF molecules per formula unit (versus 6 for TVA).

TABLE IV-A

ELEMENTAL ANALYSIS FOR TVA, $(THF)_3Cl_2VOVCl_2(THF)_3$

$V_2Cl_4C_{24}H_{48}O_7$, Molecular Weight 692.34 g

	Calculated for above formula (weight %)	Found (weight %)	
V	14.72	16.35	
Cl	26.48	23.89	
C	41.64	33.47	
H	6.99	5.80	
O	16.18	20.49	(by difference)

B: $V(THF)_4ZnCl_4$ ("TVEZ")

$ZnEt_2$ + VCl_3 (1:1 molar ratio) in THF

5 drops $ZnEt_2$ were weighed into a Schlenk tube; 5 ml THF were added followed by the addition of the required volume of a pre-cooled VCl_3/THF solution (0.1 M) at ca. -40°C with constant stirring under N_2 atmosphere (on the line). The solution immediately turned intense violet. It was reduced slightly in volume and preserved for 3 days at ca. -20°C, when purple-black crystals were obtained, found to be insoluble in THF, with which they were subsequently washed, then dried. The elemental analysis is given in table IV-B.

TABLE IV-B

ELEMENTAL ANALYSIS FOR $V(THF)_4ZnCl_4$ ("TVEZ")

$VZnCl_4C_{16}H_{32}O_4$ Molecular weight 546.55 g

	Calculated for above formula (weight %)	Found	
Zn	11.96	10.50	
V	9.32	8.39	
Cl	25.95	27.94	
C	35.16	35.09	
H	5.9	6.04	
O	11.7	12.04	(by difference)

C: $V(THF)_2Cl_2$

$ZnCl_2$ + VCl_3 in THF

Synthesis

A saturated solution of $ZnCl_2$ in THF was prepared by stirring excess $ZnCl_2$ with THF overnight at ca. 60°C. The solution (colorless) was filtered before use. 5 ml of pre-cooled 0.1 M VCl_3/THF were added to 1 ml of the $ZnCl_2$ solution with stirring at ca. -50°C under N_2. The solution obtained had a green coloration (resembling VCl_3/CH_3CN). On keeping for 2 days at ca. -20°C, long green needles were precipitated. These were found to be insoluble in THF, with which they were washed. They were dried and sealed under vacuum for analysis. The analysis (table IV-C) indicates the formula VCl_2:2THF. Seifert and Auel [59] obtained an identically appearing substance, also of formula VCl_2:2THF, in which the structure was shown to be polymeric - octahedral V(II) ions sharing chlorines with successive neighbors. The habit of our crystals (long needles) points to a polymeric structure. As for the coloration of the reaction mixture, it will be noted that the octahedral nonpolymer, VCl_2:$4H_2O$ and the polymeric VCl_2:$2H_2O$ give different colorations (blue and green) in aqueous solution, owing to a slight shift in absorption bands [86] (see also the next section on U.V.-Vis. spectra); the VCl_2:2THF solution therefeore does not necessarily have to be violet.

Discussion

Employment of $ZnCl_2$ was attempted as an "inorganic analog" of previous reactions with $ZnEt_2$, to see if a V-$ZnCl_2$ adduct or possibly a

$ZnCl_4^{2-}$ ion could be isolated. How precisely $ZnCl_2$ could reduce V(III) to V(II), as occured in the reaction, remains a puzzle. The possibility that Zn dust (an impurity usually present in Zn halides) could be the cause was presumably eliminated by leaching the $ZnCl_2$ with HCl prior to use. Other impurities may however have been present. A Zn/Zn^{2+} catalyzed disproportionation of the general type

$$V^{3+} + Zn^{2+} \longrightarrow V^{4+} \text{ or } V^{5+} + Zn^{\circ}$$

$$Zn^{\circ} + V^{3+} \longrightarrow V^{2+} + Zn^{2+}$$

has been suggested [81]. VCl_2:2THF is isolated because it is the least soluble component. $ZnCl_2$ may however not be as "innocent" an agent as it appears to be; in the context of this it is worth noting the polymerization of acrylonitrile and ethyl methacrylate observed in the presence of $ZnCl_2$ in DMF solution by Mostaafa and Mokhtar [81b], as well as numerous other catalysis reactions of $ZnCl_2$ [81b and references therein].

TABLE IV-C

ELEMENTAL ANALYSIS OF $VCl_2 \cdot 2THF$

$VCl_2C_8H_{15}O_2$ Molecular weight 266.06 g

	Calculated for above formula (weight %)	Found
V	19.15	14.36
Cl	26.65	25.09
C	36.12	31.03
H	6.06	5.91
O	12.03	23.58 (by difference)
Zn	0.0	0.03

D: VCl_3 + $AlEt_3$ (1:1 molar ratio) in CH_3CN

The reaction procedure in this case was identical to that given in part A for TVA, except that CH_3CN was used as the solvent. On mixing the reactants at ca. -50°C and warming to ca. -42°C, the usual intense violet coloration was obtained, but this soon turned to a greyish coloration (identically so in more than 6 attempts). No crystalline products were obtainable from the solution. Attempts to preserve the original coloration by keeping at -50°C failed.

E: $V(NCCH_3)_6ZnCl_4$ ("VEZN")

VCl_3 + $ZnEt_2$ (1:1 molar ratio) in CH_3CN

A procedure identical to that given in part B was followed, except that CH_3CN was used as solvent in place of THF, and a reaction temperature of ca. -35°C instead of ca. -50°C was used. An intense violet coloration immediately obtained on mixing of the reactants. The solution was kept, without reduction in volume, at ca. -20°C. Greenish black crystals were precipitated within a few hours. These were found to be insoluble in CH_3CN and were washed with this solvent, dried and sealed under vacuum for elemental analysis as well as crystal structure determination. The analysis is given in table IV-E. Nota bene: Variation in the V/Zn ratio did not lead to a different product; VEZN was obtained along with the precipitated excess reactant.

TABLE IV-D

ELEMENTAL ANALYSIS FOR $V(NCCH_3)_6ZnCl_4$ (VEZN)

$VZnCl_4C_{12}H_{18}N_6$ Molecular weight 504.44 g

	Calculated for above formula (weight %)	Found
V	10.1	6.55
Zn	12.96	10.65
Cl	28.11	28.55
C	28.57	27.85
H	3.6	3.92
N	16.66	16.10
O	0.0	6.41 (by difference)

F: VCl_3 + $ZnCl_2$ in CH_3CN

The procedure followed for this reaction was identical to that given in part C, except that CH_3CN was used as solvent in place of THF, and a reaction temperature of ca. -40°C was used. The $ZnCl_2/CH_3CN$ solution was colorless. On mixing with the VCl_3/CH_3CN solution, the green coloration of the latter was retained. No crystalline products were isolable from the reaction mixture other than excess $ZnCl_2$ (precipitated).

SECTION V

U.V.-VIS. SPECTRAL RESULTS

Experimental

U.V.-Vis. spectra were measured on a Pye-Unicam SP8-100 spectrophotometer (double beam; deuterium lamp U.V., tungsten halide lamp Visible) in "Hellma" quartz cells of 1 cm thickness. The wavelength range was 750-190 nm, except in a very few cases, where the range was 850-190 nm. An ordinate scale maximum of Absorbance 2.0 was employed. The cells had provision for sealing of the contents (necessary due to the air-sensitive nature of the samples) - a ground-glass opening with teflon stopcock (greased when sealing). The samples were loaded into the cells in the dry box and spectra were taken within 2-3 minutes of the loading. All dilutions were conducted with dried solvents in the dry box. Numerous standardization spectra were of course taken prior to the sample spectra to note possible deleterious effects on the sample spectra, e.g. solvent sample versus solvent reference (baseline correction), high vacuum grease (used with the Schlenk apparatus) dissolved in the solvent (in which case the peaks were of negligible intensity even at high concentration and appeared only in the charge transfer region), $AlEt_3$, $ZnEt_2$ and ethylene in the solvents (no peaks were found due to ethylene or other possible decomposition products in the $AlEt_3$ and $ZnEt_2$ spectra). Peaks appearing in the charge transfer region and of fairly low intensity were assumed not to have detrimental effects on the quality of the sample spectra. Confirmation of the values of the extinction coefficients obtained in the sample spectra was obtained by taking two or more spectra with the samples prepared at different times. Extreme care had to be taken to use the driest and most freshly prepared solvents possible to avoid the introduction of air, moisture and impurities through the apparatus used. In the case of TVA solutions, many attempts at sample loading ended in failure due to oxidation.

One experimental peculiarity observed while taking the spectra is worth mentioning. A suppression of the baseline, below the 0 absorbance value, was observed in the U.V. region exactly in the range of absorption of the solvent, apparently indicating that in this region the reference (pure solvent) absorbs more strongly than the sample. Preliminary baseline verification (pure solvent vs. pure solvent) showed nothing amiss. The phenomenon was also observed with other instruments, and even when the purest solvents were used. A reversal of the sample and reference beam positions showed that the pure solvent was absorbing much more intensely than the solution (sample). The explanation arrived at is that the absorption bands of the solvent in the U.V. region are so intense that coordination of even a small part of the solvent, as occurs in the solutions used, removes just enough from the absorbing solvent population in the solution so that there is an excess of absorbing material in the reference which give rise to the reverse absorption observed. Since however this occured only in the U.V. region, and all bands of interest to us were in the ligand field region, values of extinction coefficients were not affected.

Discussion

Only transitions observed in the ligand field (LF) region of the spectrum are of course of interest. The electronic transitions to be observed in an octahedral or near-octahedral field for V (Laporte-forbidden and thus likely to be of very low intensity) are the following [81].

V(II): 3 transitions - $^4A_{2g}$ to $^4T_{2g}$ (highest λ), $^4T_{1g}$(F) and $^4T_{1g}$(P) (lowest λ)

V(III): 2 transitions - $^3T_{1g} \rightarrow {}^3T_{2g}$ (at higher λ) and $\rightarrow {}^3T_{1g}$(lower λ)

V(IV): 3 bands - $^2B_2 \rightarrow {}^2E(I)$ (at highest λ), $^2B_1$ and $^2A_1$ (lowest λ).

V(V): Charge transfer transitions only.

Table V-A gives some results obtained by earlier workers on V(IV) and V(V) spectra, along with assignments and extinction coefficients where available (extinctions molar, ε). Tables V-B and V-C do the same for V(III) and V(II). Table V-D gives the results of this study in summarized form together with some other results for comparison. ε values (based on moles of V, usually as V(III) initially introduced) and the tentative assignments are included. The feature to be noted in tables V-A to V-C is the considerable shift of the bands in the various solvent media. It must be also noted that the region below ca. 400 nm was characterized by, in all cases, charge transfer (presumed) bands of extremely high intensity that were quite similar in appearance regardless of solvent used or oxidation state of V. Some representative spectra are given in Fig. V-1 to V-7 appended to this section.

The spectra of the various reaction mixtures and of the TVA solutions reveal something about the identity of the species present in solution. In all cases, an extremely intense band is observed at ca. 487 nm, almost insensitive to change in solvent or reactants used. The solutions in all solvents are of an intense violet; exposure to air causes decrease in intensity and ultimate loss of this coloration with concurrent decrease in intensity and ultimate disappearance of the 487 nm band, so it is this band that is responsible for the coloration. A band near 600 nm is also observed in all cases, more or less corresponding to the second V(II) transition ($^4A_{2g} \rightarrow {}^4T_{1g}(F)$). The first transition is most probably swallowed up by the intense 487 nm band (exp.,

TABLE V-A

SPECTRAL PROPERTIES OF V(IV) AND V(V)

(N.B.: Probable assignments are given only for the first set of data; for other sets use the symbols for comparison).

Compound	Bands (nm) (ε in $1mole^{-1}cm^{-1}$, where given).
V(IV) in 5.6 M H_3PO_4 [82]	833 ($^3B_2 \rightarrow {}^2E(I)$) (A) 746 ($^2B_2 \rightarrow {}^2B_1$) (B) 675 ($^2B_2 \rightarrow {}^2A_1$) (C)
V(V) in 5.6 M H_3PO_4 [82]	244 (charge transfer)
V(IV) in: 0.5 M, 5 M H_2SO_4, 0.5 M, 5 M HCl and 0.5 M $HClO_4$ [83]	750-770 (ε 15.0 in $HClO_4$) (B)
V(IV): $(Et_2NH_2)_2VOCl_4$ and $MeNH_2)_5$-$V_2O_2Cl_4$ in MeCN solution.	720 (ε 54) (B) 415 (ε 15) (C)
V(V): (py)$HVOCl_4$ [84]	621 (ε 210) (B) 465 (ε 2000) (C) (N.B.: The existence of these transitions, apparently of d-d character, was not explained by the authors)
V(IV): VO^{2+} in ascorbic acid medium	714 (B)

TABLE V-B

SPECTRAL PROPERTIES OF V(III)

Compound	Bands (nm) (ϵ in $lmole^{-1}cm^{-1}$ where given)
V(III) in 5.6 M H_3PO_4 [82]	660 ($^3T_{1g} \rightarrow {}^3T_{2g}$) (A)*
	430 ($^3T_{1g} \rightarrow {}^3T_{1g}$)* (B)
	(*Assignments given only once; for other data please compare using the symbols)
V(III) in 0.5 M H_2SO_4 [83]	605 (A)
	400 (B)
V(III) in 0.5 M $HClO_4$ [83]	590 (ϵ 6.0) (A)
	400 (B)

TABLE V-C

SPECTRAL PROPERTIES OF V(II)

Compound	Bands (nm) (ε in $lmole^{-1}cm^{-1}$, where given)
(N.B.: Assignments are given only once. For other data please compare using the symbols)	
V(II) in 5.6 M H_3PO_4 [82]	877 ($^4A_{2g} \longrightarrow {}^4T_{2g}$) (A) 585 ($^4A_{2g} \longrightarrow {}^4T_{1g}$ (F)) (B) 391 ($^4A_{2g} \longrightarrow {}^4T_{1g}$(P)) (C)
V(II) in: 0.5, 5 M H_2SO_4, 0.5, 5 M HCl and 0.5 M $HClO_4$ [83]	565 (ε 4.5) (B)
$VCl_2:4H_2O$ (Diffuse reflectance spectrum [86])	1010, 585 & 401 (A,B,C)
$VCl_2:2H_2O$ (Diffuse reflectance spectrum [86])	1125, 689 & 427 (A,B,C)
$VSO_4:6H_2O$ (Diffuse reflectance spectrum [87])	840, 562 & 357 (A,B,C)
$(Li,K)_4(VCl_6)$ (melt, 400°C, [88])	1389 (ε 811) (A) 833 (ε12.4) (B) 525 (ε 17.5) (C)
$(NH_4)_2V(H_2O)_6(SO_4)_2$ (aqueous solution)	810, 541 & 358 (A,B,C)

TABLE V-D

SUMMARY OF U.V.-VIS. SPECTRAL RESULTS (of this work)

(N.B.: Asterisked portions are from previous tables, for comparison)

(Tentative assignments are in brackets)

$V(III)/H_2O$ (*)	VCl_3/THF	VCl_3/CH_3CN
(885, weak forbidden)		
660 ($^3T_{2g}$)	758 (ε 30)	695 (ε 31)
(560, weak, forbidden)		
430 ($\rightarrow$ $^3T_{1g}$)	503 (ε 30)	470 (ε 28)

$V(II)/H_2O$ (*)	VCl_2/THF (*)	VCl_2/CH_3CN (*)
877 ($\rightarrow$ $^4T_{1g}$)	994	685
585 ($\rightarrow$ $^4T_{1g}$ (F))	643	495
391 ($\rightarrow$ $^4T_{1g}$(P))	404	unobservable due to charge-transfer bands

VCl_3-$ZnCl_2$/THF reaction mixture

745 (ε ca. 50.0) (probably V(III))

340 (charge transfer)

TABLE V-D, cont.

(Note abbreviations: r.m.= reaction mixture, pr.= probably)

TVA r.m. (in THF)	TVA/THF	TVA, oxidized, in THF
598 (ε 66) (pr. V(II))	766 (ε ca. 30) (obsvd. with excess V(III), is pr.V(III))	525
	605-598 (ε 149)	
487* (ε 240) (pr. VOV^{4+})	487* (ε 631) (pr. VOV^{4+})	406 (pr. V(II))

(* this peak probably overshadows the second (ca. 404 nm) peak of V(II) in these spectra)

$ZnEt_2/VCl_3$/THF r.m.	TVA/DMF	TVA/CH_3CN
600 (ε 72) (pr. V(II))	678 (ε 500) (pr. V(II))	680 (ε 70) (pr. V(II))
483* (ε 390) (pr. VOV^{4+})	482*(ε ca. 4,000) (pr. VOV^{4+})	487 (ε ca. 600) (pr. VOV^{4+})

(* probably overshadows second (ca. 404 nm) V(II) peak)

for instance, at 404 nm in THF solvent [59]). The third transition (expected near 900 nm in THF, for instance) is out of the range of the measurements. The V(II) band near 600 nm has a fairly low intensity (ca. 60-70 except in the anomalous case of the DMF solution) and shifts with the solvent of coordination; both properties correspond with earlier observations (see tables V-A to V-C).

The band near 487 nm is probably due to some variety of a charge transfer transition within the VOV^{4+} entity. The factors that point to this are the fact that the band is observed on dissolving the crystals of TVA (of known structure - having the VOV^{4+} entity) in various solvents, and the fact that the band shifts almost negligibly with solvent of coordination and involves high transition probability (implying high intensity). This latter observation indicates that it is not a d-d transition.

The observed ε's of this intense band are low (ca. 600) and are at variance with what the eye seems to tell us from previous experience with intensely colored solutions (e.g. permanganates). One may account for this, and for the extremely high (and seemingly normal) observed intensity and ε in DMF by proposing that the actual concentration of the VOV^{4+} species in any of these solutions (including the reaction mixtures) is very small at the very large dilutions at which the spectra must be taken, due to disproportionation into VO^{2+} and V^{2+}. Such disproportionation is to be expected considering that VOV^{4+} is presumed to be formed from V^{2+} and VO^{2+} (see Prior Art section). One may assume that on dissolution of the TVA crystals disproportionation occurs and this is enhanced on dilution of the solution formed. It occurs to a lesser extent in solvents of high coordinative capability (e.g. DMF in which the TVA solutions were observed to be extremely stable). The degree of disproportionation is very large, so that VOV^{4+} exists in solution with much larger concentrations of V(II) and V(IV) (VO^{2+}) and perhaps also of V(III) (V^{3+}).

The spectrum of the VOV^{4+} species in aqueous solution has been recorded before. Gandeboeuf and Souchay ([69]) recorded an intense absorption at ca. 430 nm. They used a solution 0.02 M in V^{3+} in a medium containing $NaClO_4$ and $HClO_4$, and varied the pH of the solution by addition of base (NaOH) or acid, defining the acidity by the parameter $n = x + [H^+]/c$, where c is the molar concentration of V^{3+} and x is the number of equivalents of base added. The band at ca. 430 nm was first observed at n= ca. 0.1, had a maximum at n= ca. 0.85 (ε = 400.0 based on moles of V added) and, as the solution was made still more basic, again dropped in intensity. On the basis of polarographic and other evidence, the authors postulated the existence of the species $V_2(OH)_3^{3+}$ (probably a better formulation is $V_2(OH)_2^{4+}$, i.e. $VOV(H_2O)^{4+}$), but as briefly mentioned in the Prior Art section earlier, they wrongly assigned the band at ca. 430 nm to VOH^{2+}, crediting instead a less intense band at ca. 330 nm to $V_2(OH)_3^{3+}$. The same ca. 430 nm band with approximately the same intensity was also observed in sulfate ion media as well as in acetate ion media (with however a much lower intensity, ca. 70 at n= 2.0). In the latter medium, the existence of the ion $[V_2(CH_3COO)_3(OH)_2]^+$ (also formulable as $[VOV(CH_3COO)_3H_2O]$) was postulated.

In a later study, also in acid media (where incidentally the rate of oxidation of V^{2+} to V^{3+} by oxygen has been shown to be the slowest [67] and where thus any intermediate or metastable species such as VOV^{4+} is likely to have the greatest opportunity to form), Newton and Baker [65a,65b] also recorded a band at ca. 425 nm (with ε based on moles of V of 6.4) which they definitively ascribed to the VOV^{4+} species, whose existence they convincingly demonstrated.

A detailed discussion of the structure of the VOV^{4+} entity is presented in the discussion section on the TVA structure (see later). Briefly, however, if one assumes sp hybridization for the bridging oxygen in the VOV^{4+} "ion", one finds a nonbonding p orbital on the

oxygen holding a lone pair of electrons (4 electrons are donated to the two Vs). The band observed in the VOV^{4+} solutions then could be due to a transition of one of these electrons to the e_g orbitals of the V, evidently a possibility of greater likelihood than the reverse transition of one of the 3 d_π V electrons to the σ^* orbital centered on the O in terms of energy match. The latter type of transition could conceivably be mediatory in an exchange of the type $V^{III}\text{-}O\text{-}V^{III} \longrightarrow V^{II}\text{-}O\text{-}V^{IV}$ but this is highly unlikely. In a study of NH_3RuOVL^{n-4} (L= EDTA, n= 4; L= HEDTA, n= 3; L= EDDA, n= 2) - a $Ru^{II}\text{-}O\text{-}V^{IV}$ bridged compound - Kristine and Shepherd [91] ascribed a band near 605 nm (ϵ 3,100) to the transition $Ru_{(d_{xy})}{}^{B}{}_{2} \longrightarrow$ "Ligand" $(VO^{2+}]\ \pi^*(E)$, but did not consider the existence of nonbonding electrons of π symmetry on the O.

In the representative spectra appended to this section (Figs. V-1 to V-7), of particular note are the intense bands near 487 nm (in Figs. V-3 to V-7) and the similarity of the spectra in the charge-transfer region (in Figs. V-1 and V-2).

It is difficult to determine where precisely the oxygen required to oxidize V(II) to VO^{2+} (producing VOV^{4+} subsequently) comes from. Oxygen penetration due to leaks in spite of the extreme precautions taken is hopefully not the cause, especially since the concentrations required to effect the extent of oxidation observed will be large. Abstraction of oxygen from THF, if the cause, would be expected to produce decomposition products which were however not looked for. Another possibility for oxygen entry is through the OH-butylated toluene added as a preservative to the THF (concentration 0.025%, see appendix A) by the manufacturer. It must be remembered however that the same phenomenon was observed in CH_3CN solvent. Kress et al. [92] state that in Ziegler-Natta systems involving tungsten halides, an oxo ligand appears on the W (which seems to make it more active) possibly through impurities or "adventitous oxygen" (a scape-

goat phrase used by many workers). Hensson et al. [93], Mocella et al. [94a], Basset et al. [94b] and Burwell and Brenner [95] also reported similar observations due to inexplicable oxygen entry.

One final point is very important to note. It must be remembered that a VOV entity was isolated only in one case. In all other cases of the present study, the crystalline product contained only V(II) (cf. thus VEZN and $V(THF)_4ZnCl_4$ ("TVEZ"));

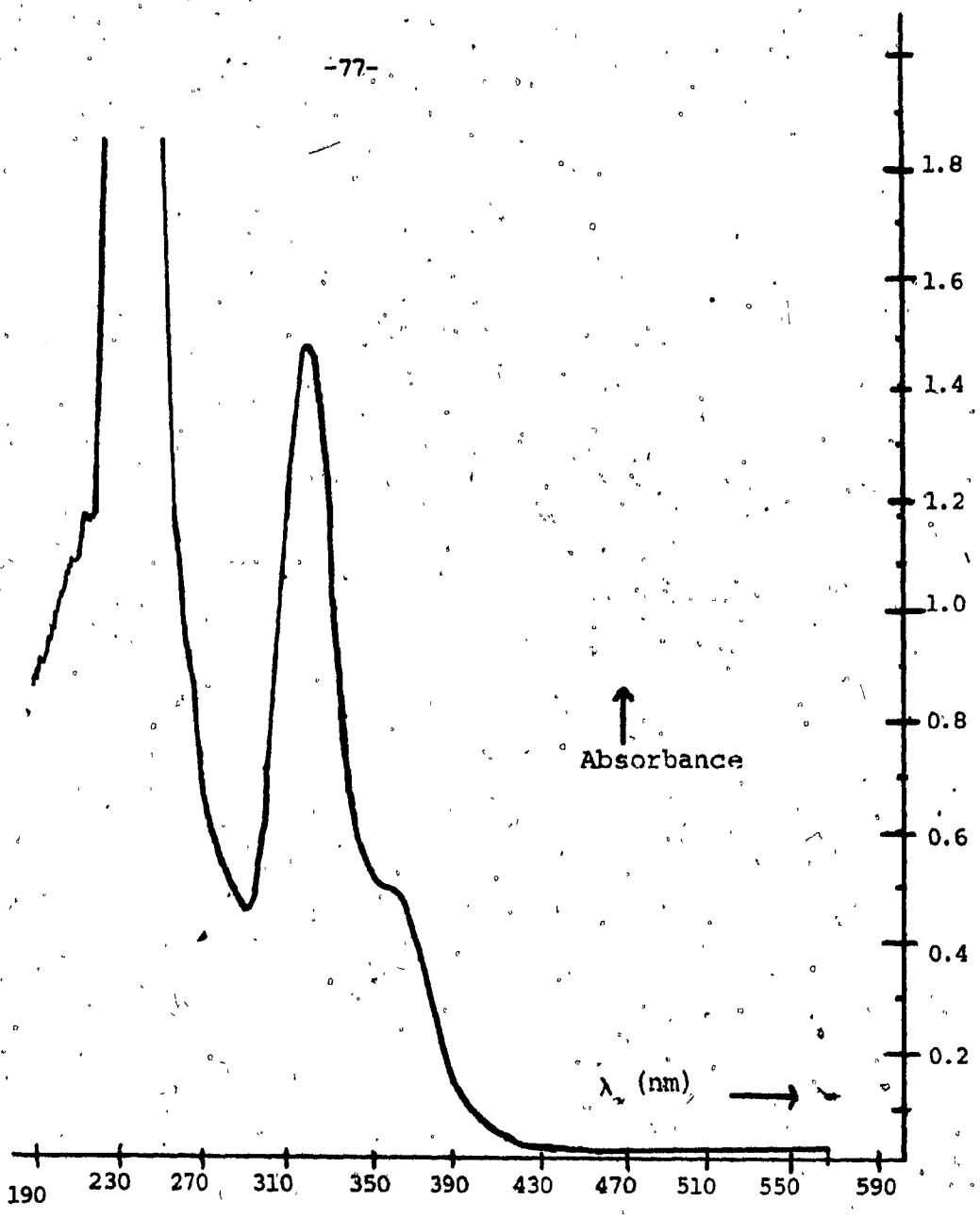

Fig. V-1

U.V.-Vis. spectrum of VCl_3 in CH_3CN, concn. 4 X 10^{-4} M

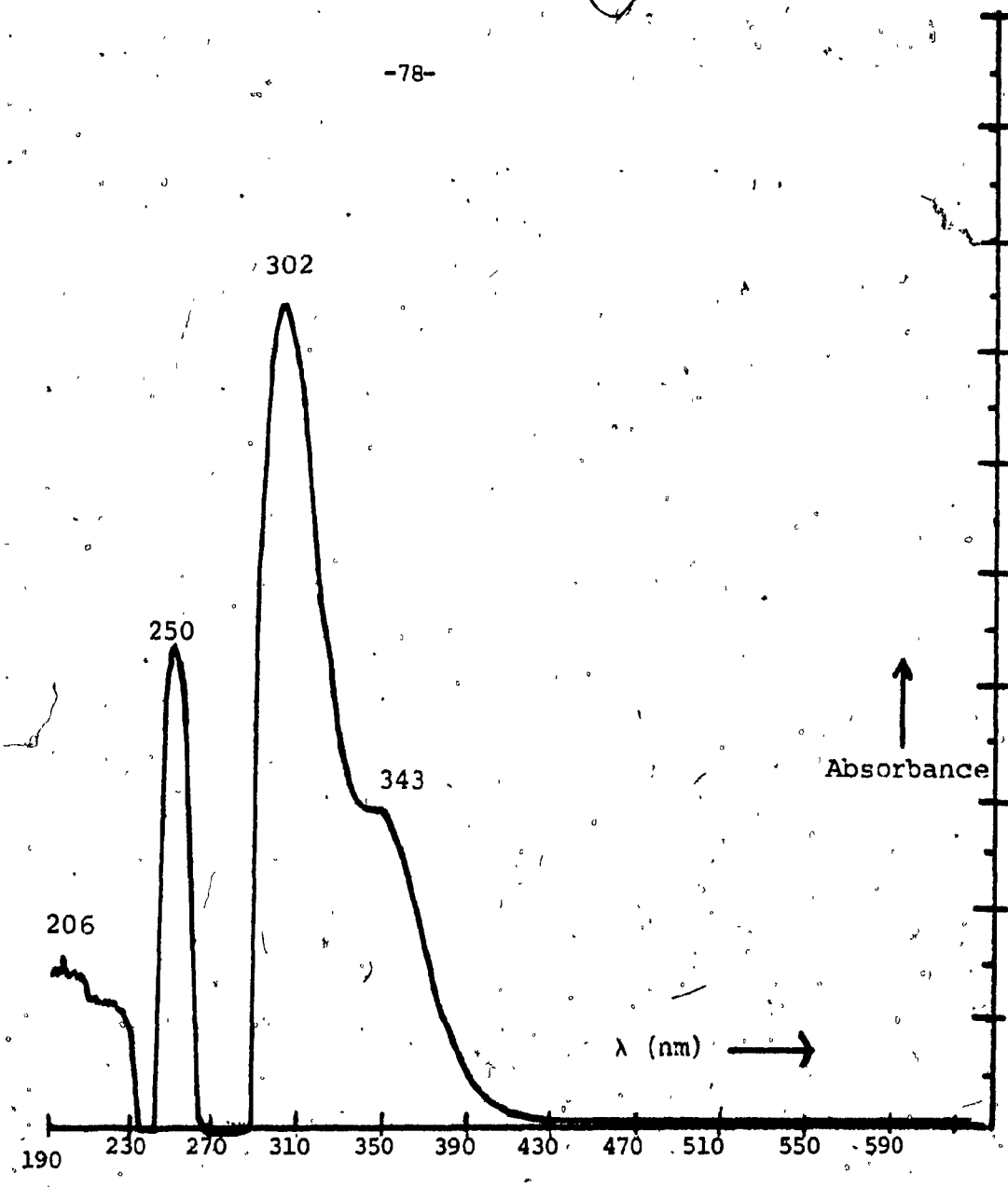

Fig. V-2

U.V.-Vis. spectrum of VCl_3 in THF, concn. 5×10^{-4} M.

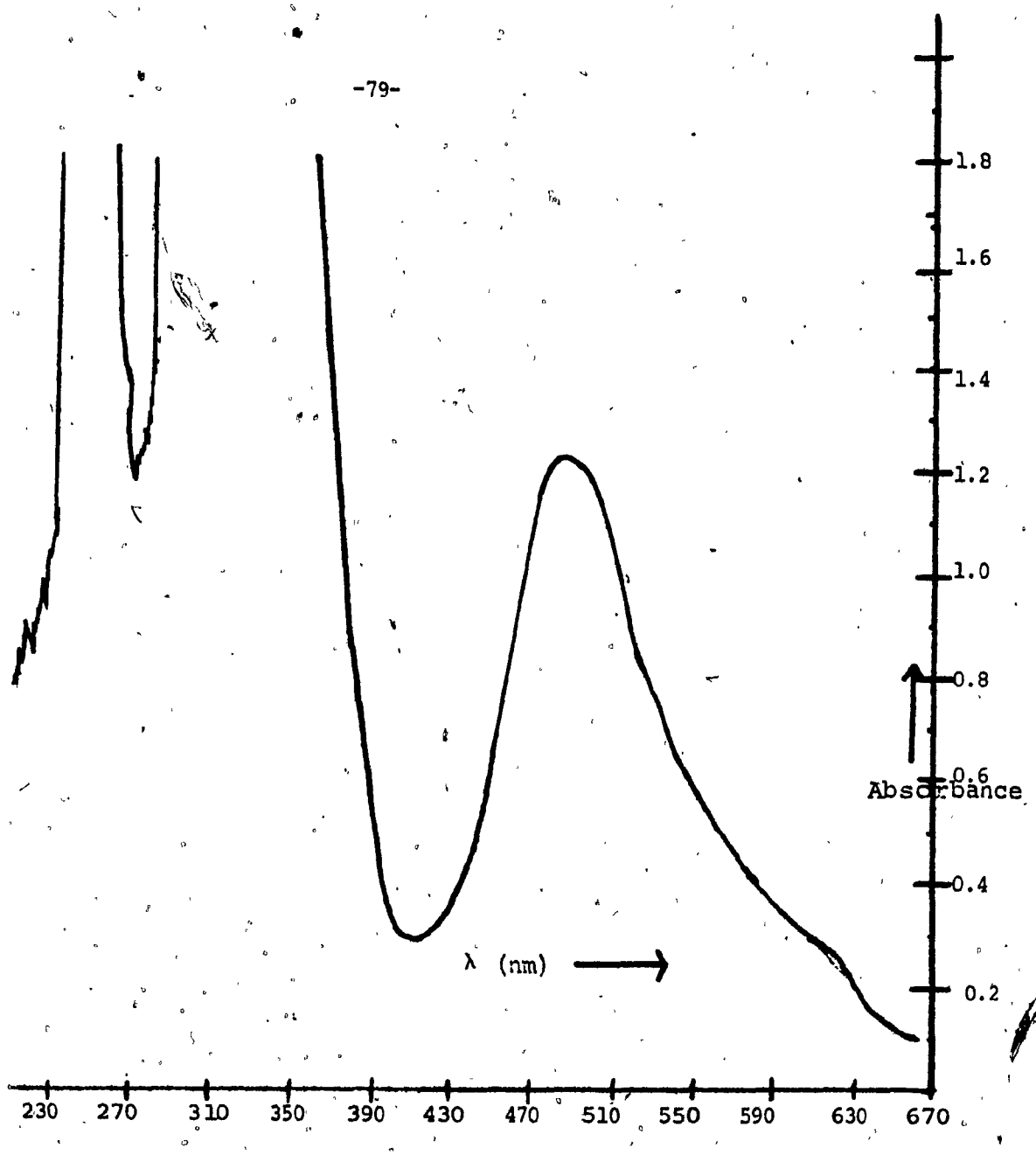

Fig. V-3

U.V.-Vis. spectrum of mixture from reaction of VCl_3 with $AlEt_3$ in THF; concn. 5 X 10^{-3} M in vanadium.
Note band near 487 nm.

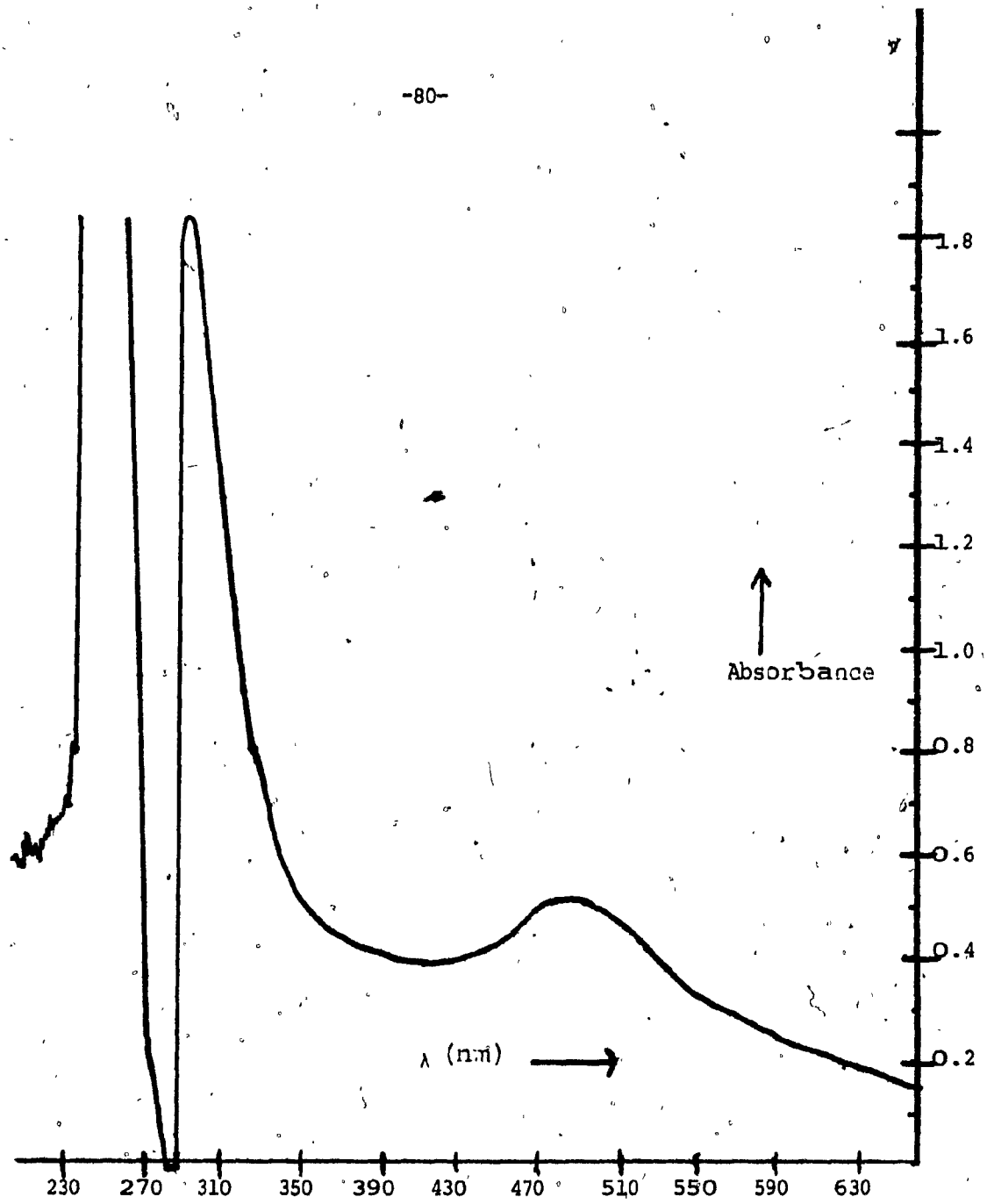

Fig. V-4

U.V.-Vis. spectrum of mixture from reaction of VCl_3 and $ZnEt_2$ in THF; concn. 1.33 X 10^{-3} M in vanadium. Note band near 487 nm.

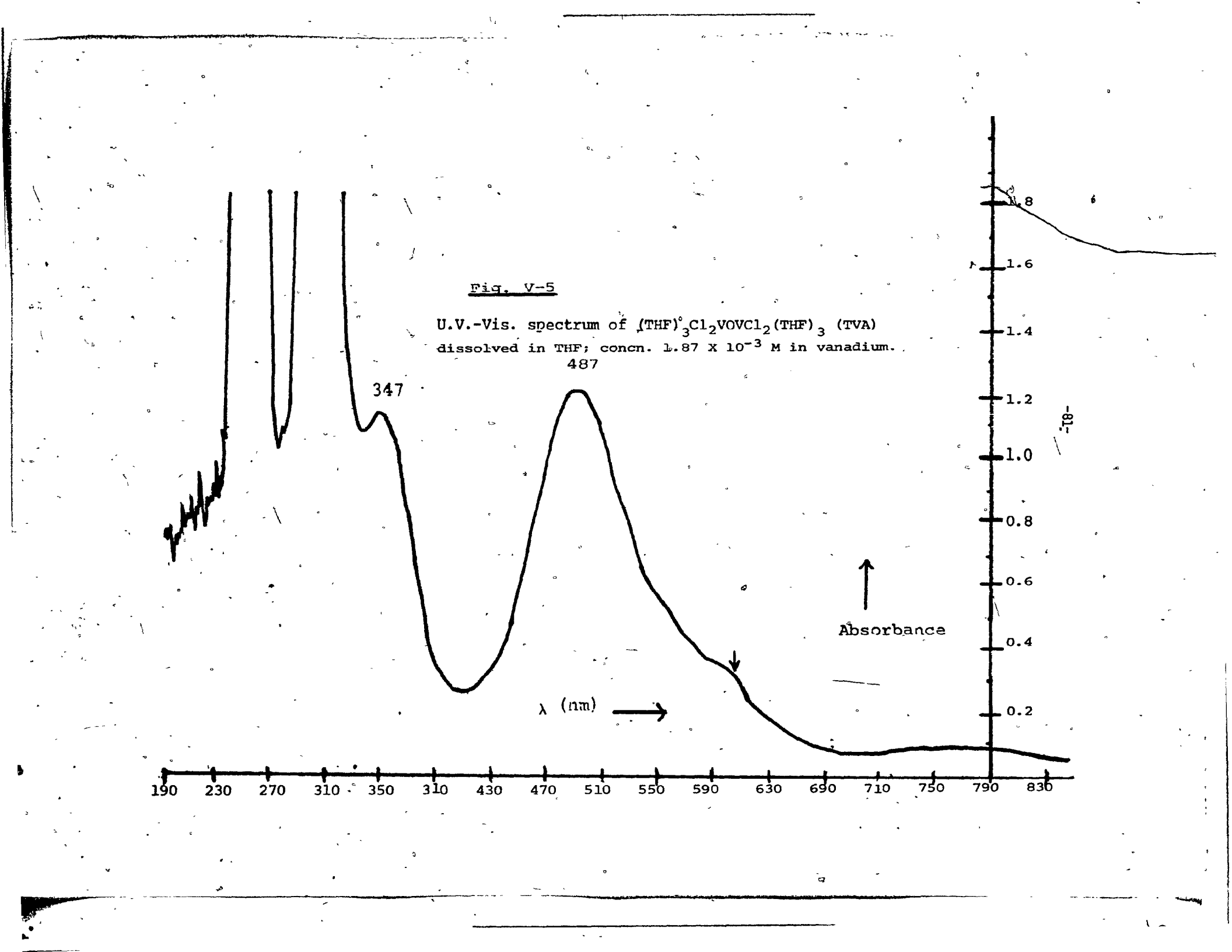

Fig. V-5

U.V.-Vis. spectrum of $(THF)_3Cl_2VOVCl_2(THF)_3$ (TVA) dissolved in THF; concn. 1.87 X 10^{-3} M in vanadium.

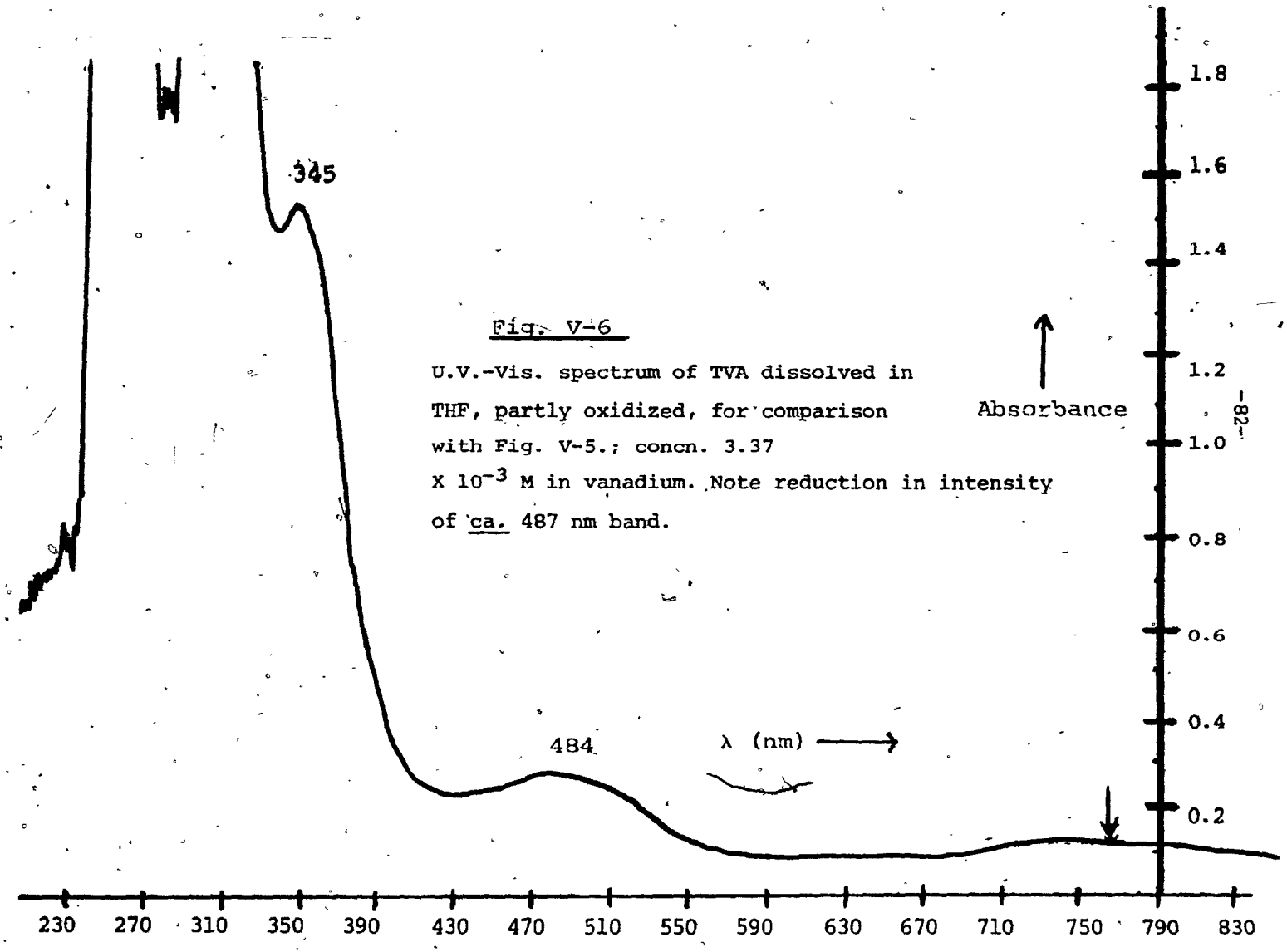

Fig. V-6

U.V.-Vis. spectrum of TVA dissolved in THF, partly oxidized, for comparison with Fig. V-5.; concn. 3.37 X 10^{-3} M in vanadium. Note reduction in intensity of ca. 487 nm band.

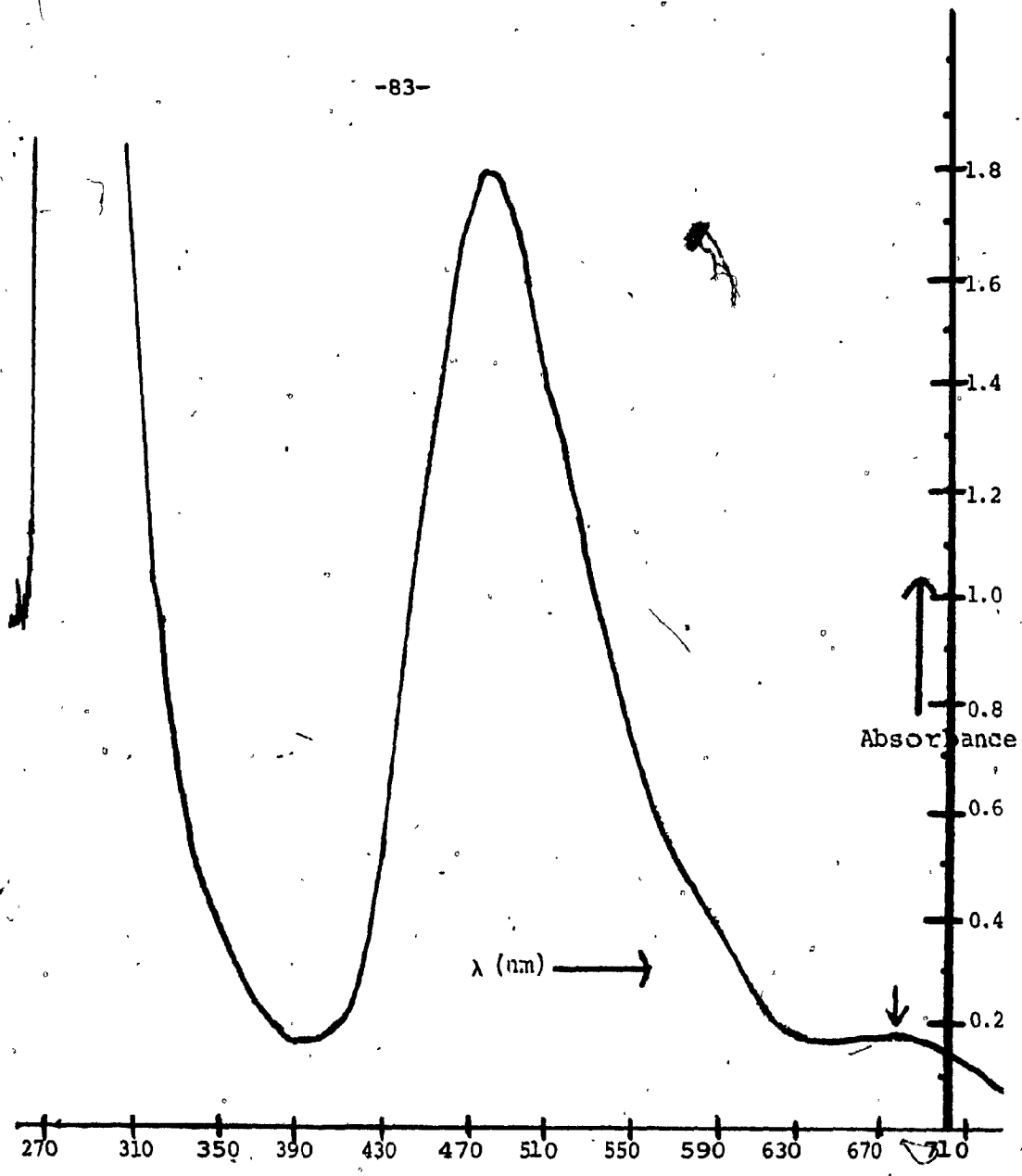

Fig. V-7

U.V.-Vis. spectrum of TVA dissolved in DMF; concn. 3.24 X 10^{-4} M in vanadium, showing intense ca. 487 nm band due to VOV^{4+} (presumed), particularly strong in this solvent.

SECTION VI

INFRARED SPECTRAL RESULTS

Experimental

IR spectra of the solid crystalline compounds were measured as nujol mulls on a Perkin-Elmer IR 599 spectrometer (double beam). The samples were ground finely in nujol in the dry box and placed between two AgCl windows (Wilks "minicell"). The cutoff frequency (0% transmittance) of the windows was ca. 250 cm^{-1} (ca. 40% at 400 cm^{-1}, ca. 20% T at 350 cm^{-1}, ca. 10% T at 330 cm^{-1}). Thus in the region 330-400 cm^{-1} only the strongest bands would be visible. The cutoff for VCl_3:3THF was ca. 400 cm^{-1}. Although no referece was used for the spectra (nothing placed in the reference beam) the nujol bands were found to cause very little distortion of the sample spectra. Nujol was found ipso facto to protect the samples from the effects of oxidation. Nevertheless, to ascertain the effects and extent of oxidation, all samples were exposed to the air after their spectra had been taken (for a period of appr. 3 hrs) and their spectra retaken. For the samples exposed thus, in all cases strong bands due to H_2O were found to appear and solvent bands became weaker and in some cases disappeared; this was seen to indicate, in sequence of occurence, decomposition, loss of solvent and hygroscopicity of product.

Discussion

The spectra are summarized in tabular form in table VI-A, beginning with the spectrum of the coordinating solvent in each case and including tentative assignments [96a-99b].

In the case of the acetronitrile-coordinated compounds, the feature most worth noting, is the slight increase in the C≡N stretching frequency and the very large increase in the C-C≡N bending, indicating shortening and strengthening and/or bending in the C-C≡N bonds. These

TABLE VI-A

SUMMARY OF IR SPECTRAL RESULTS

(Abbreviations: ν_{as} = asym. stretch, ν_s = sym. stretch, δ = bend, r = rock, v. = very, s. = strong, w = weak, m. = medium, br. = broad, sh. = sharp, cmbn. = combination; assignments also given where possible; all figures in cm^{-1})

$VCl_3(CH_3CN)_3$	CH_3CN (neat)
	3160 m-s
2920 v.s. (also nujol)	3000 m-s $\nu_{as}(CH)$
2830 v.s. (nujol)	2955 m.-s. $\nu_s(CH)$
2295 s.-v.s. cmbn.	2290 s. cmbn.
2265 s.-v.s.	2245 s; $\nu(C\equiv N)$
2230 s.-v.s. cmbn.	
1472 v.s. (nujol)	1455 v.s. $\nu_{as}(CH_3)$
1430 v.s. (nujol)	1372 v.s. $\nu_s(CH_3)$
1155 m., br.	
1030 m.-s.	1035 v.s. $\nu(CH_3)$
940 s.	
915 w.	915 v.s. $\nu(CH_3-CN)$
815 w.	
718 s. (nujol)	742 v.s. $r(CH_2)$ (?)
415 v.s.	373 v.s. C-C≡N bend

N.B.: V-Cl bands are probably below 400 cm^{-1}

TABLE VI-A, SUMMARY OF IR SPECTRAL RESULTS, cont.

VEZN

2920-2830 br., s.	(for assignments compare with
2720 m.	previous tables for
2310 s.	$VCl_3(CH_3CN)_3$ & CH_3CN (neat))
2280 s.	
2245 s.	
1450 br., s.	
1370 br., s.	
1300 w.	
1155 m.w., br.	
1030 m.	
970 w.	
940 w,	
915 w.	
880 w.	
715 s.	
415 v.s.	

TABLE VI-A, SUMMARY OF IR SPECTRAL RESULTS, cont.

$VCl_3(THF)_3$ (cutoff 400 cm^{-1})	THF (neat)
2980-2850 s., br. (nujol)	2977 v.s., br. $\nu_{as}(CH_3)$
	2850 v.s., br. $\nu_s(CH_3)$
2680 w.	2680 (cmbn.)
	1960 m., br. ν(cmbn.)
1475 s. (nujol)	
1435 s. (nujol)	1450 s. $\nu(CH_3)$
1415 m.	
1395 m.-w.	
1370 m.w.	1360 m.w. $\nu(CH_2)$
1310 m.-w.	1330 w. $\nu(CH_2)$
1255 m.-w.	1285 w. $\nu(CH_2)$
1180 m.	1140 w. ν_{as}(ring)
1080 s.	
1040 s.	1065 s. ν_{as}(ring) OR ν_{as}(C-O-C)
1015 sh., s.	1030 w. $r(CH_2)$
1010 v.s.	
950 m.w.	
920 m.-s.	905 m.-s. ν_s(ring) OR ν_s(C-O-C)
835 v.s.	
715 s. (nujol)	
675 m.s.	650 s. $r(CH_2)$ (?)
570 w.	

TABLE VI-A, SUMMARY OF IR SPECTRAL RESULTS, cont.

$V(THF)_4ZnCl_4$ ("TVEZ")

(For assignments, compare with previous tables of THF-compds.)

2980-2830 s., br.

2720 w.
1455 s.
1372 s., sh.
1362 s. sh.
1340 w.
1310 w.
1295 w.
1255 w.
1245 w.
1175 w.
1070 m.
1035 m.-s.
1015 s.
955 w.
925 w., sh.
915 s., m.
855 s.
717 m.
675 m.
665 sh., w.
600 w., sh.
560 w.
460 w.
362 s.

TABLE VI-A. SUMMARY OF IR SPECTRAL RESULTS, cont.

TVA	VCl_2:2THF
(For assignments, see previous tables on THF (neat) and VCl_3:3THF)	
2980-2830 br., s.	2980-2830 br., s.
	2720 m.w.
	2560 w.
	1740 m.w.
1455 v.s., br.	1460 s., br.
1372 v.s.	1372 s:, sh.
1360 m.w.	1362 s., sh.
1340 w.	1340 w.
1300 w.	1300 w.
1255 m.w.	1250 w.
1165 w.	1165 w.
	1145 w.
1070 m.	1070 w.
1035 m.	1030 m.-w.
1010 v.s.	990 m.
	960 w.
910 m.s.	920 m.w.
	880 m.w.
860 s.	825 s.
795 w.	765 w.
720 m.	717 s.
675 m.w.	670 m.w.
420 w.	
365 s.	380 s.

changes for coordinated acetonitrile (in comparison to the free ligand) have been noted before ([14], [100]). A detailed discussion is presented later in the section on discussion of the VEZN crystal structure.

The strong C-C≡N bending frequency increases from 373 cm^{-1} in the free ligand to 415 cm^{-1} in both $VCl_3:3CH_3CN$ and VEZN. This compares with 404 cm^{-1} recorded by Einstein et al., [100] in $VO(NO_3)_3CH_3C^{14}N$. Increases to near 400 cm^{-1} have been noted by other workers also [102, 103].

The two frequencies ascribed to the C≡N stretch increase slightly, from 2290 and 2245 cm^{-1} in the free ligand to 2295 and 2265 cm^{-1} in $VCl_3:3CH_3CN$, and markedly, to 2310 and 2280 cm^{-1} in VEZN, which is V(II), apparently indicating that the C≡N bond shortening is more pronounced in the case of V(II)-$NCCH_3$ than in the case of V(III)-$NCCH_3$. The above figures may be compared with 2294 and 2285 cm^{-1} registered for $VO(NO_3)_3CH_3C^{14}N$ by Einstein et al. [100]. The VEZN values agree almost exactly with those of Seifert and Auel [14] for $VCl_2:4CH_3CN$ (2310 and 2285 cm^{-1}), and thus confirm that these are values for CH_3CN coordinated to V(II). It is interesting to note that the CH_3-CN stretching frequency did not change position in the coordinated acetronitrile. The important V-N bands were not observed due to the high cutoff frequency. For the V-N stretch, Issigoni et al. [38] give values of 312, 292 and 276 cm^{-1} for $VCl_2(imidazole)_6$, $VCl_2(pyrazole)_4$ and $VCl_2(py)_4$ respectively. Einstein et al. [100] believe that the band near 400 cm^{-1} (at 415 cm^{-1} for VEZN, i.e. the C-C≡N bend) may also be due to ν(V-N) and they cite isotope shifts due to ^{15}N as evidence, but from the evidence of the present work, especially the crystal structure, this seems unlikely.

Brunette et al. [104] ascribed bands at 211, 230 and 238 cm^{-1} to ν(V-N) in $VO(MeCN)_5^{2+}$ in their study of $[VO(MeCN)_5(SbCl_2)MeCN]$,

whereas in a similar compound, Khamar et al. [105] observe a V-N stretch of 286 cm^{-1}.

Very little is discernable from the IR spectra of the THF-coordinated compounds since for the most part they appear to be identical to that of the free ligand. The band near 370 cm^{-1} is of note. It appears at 365 cm^{-1} in TVA, nearly identically at 362 cm^{-1} for $V(THF)_4ZnCl_4$ and at a somewhat higher 380 cm^{-1} for the presumably polymeric VCl_2:2THF. It may conceivably be due to either the V-O-(bridge) stretch or the V-O(THF) stretch, the assignment to the latter being based on the location of the ν(V-N) frequencies for "very long bonds" [100, 103] (the V-O(THF) bonds were observed to be exceptionally long in TVA, see TVA crystal structure section; the band was not observed for VCl_3:3THF due to the cutoff point for that particular spectrum being at 400 cm^{-1}). It may be mentioned here that the vanadyl (V=O) stretch is usually observed in the region 960 to 1025 cm^{-1} as a strong band [106,107].

In the coordinated THF, the $\nu_{C-O-C(as)}$ (asymmetric stretch) is observed to decrease from 1065 cm^{-1} (free ligand) to 1040 cm^{-1} in VCl_3:3THF, to 1035 cm^{-1} in TVA and to 1030 cm^{-1} in VCl_2:2THF. This is to be expected due to the loss of electron density from the O on coordination, and it is in accord with results found earlier by Seifert and Auel [59] (1018 cm^{-1} for VCl_2:2THF) and Kern [108]. The $\nu_{C-O-C(s)}$ (symmetric stretch) bands were not clearly identified.

The V-Cl stretching bands were below the cutoff frequency for the spectra. For V(II)-Cl they have been observed as of considerable strength at 314 and 310 cm^{-1} for V(β-picoline)$_4Cl_2$ and V(γ-picoline)$_4Cl_2$ respectively [32,109,110] and at 312 and 311 cm^{-1} for VCl_2(pyrazole)$_4$ and $VCl_2(py)_4$ [38]. For V(III)-Cl a shift to 330 cm^{-1} is noticed [111].

Schwendt et al. [112] have recorded far-IR spectra for $Zn_2V_2O_7$ and $Mg_2V_2O_7$ (which contain V-O-V bridges as in TVA) and have

observed that the difference between the symmetric and asymmetric types of vibrations assignable to the bridge bonds are related to the V-O-V angle (which is not necessarily linear always, as contrasted to the linear TVA).

Some representative spectra are given in Fig. VI-1 and VI-2 appended to this section. The portion of the spectrum that appears to be a "fingerprint" of THF coordinated to non-polymeric octahedral V (observed in VCl_3:3THF, $V(THF)_4ZnCl_4$ and TVA but not in the presumably polymeric VCl_2:2THF) in Fig. VI-2 is worth noting. Fig. VI-1 shows the change in the sharp C-C≡N bending vibration from CH_3CN to VEZN.

Fig.VI-1: Infrared spectra, top, of $V(NCCH_3)_6ZnCl_4$ (VEZN) as nujol mull, bottom of CH_3CN neat only. Note especially the shift in the sharp C-C≡N bending frequency near 400 cm^{-1}.

Fig. VI-2 (overleaf):

Comparative infrared spectra of the compounds having THF as solvent of coordination. From top to bottom: THF neat; $V(THF)_4ZnCl_4$ ("TVEZ") (nujol mull); $(THF)_3Cl_2$-$VOVCl_2(THF)_3$ (TVA) (nujol mull); note fingerprint for TVEZ and TVA (1100 to 800 cm^{-1}) and qualitative difference in spectra of $VCl_2(THF)_2$, presumably due to polymeric character.

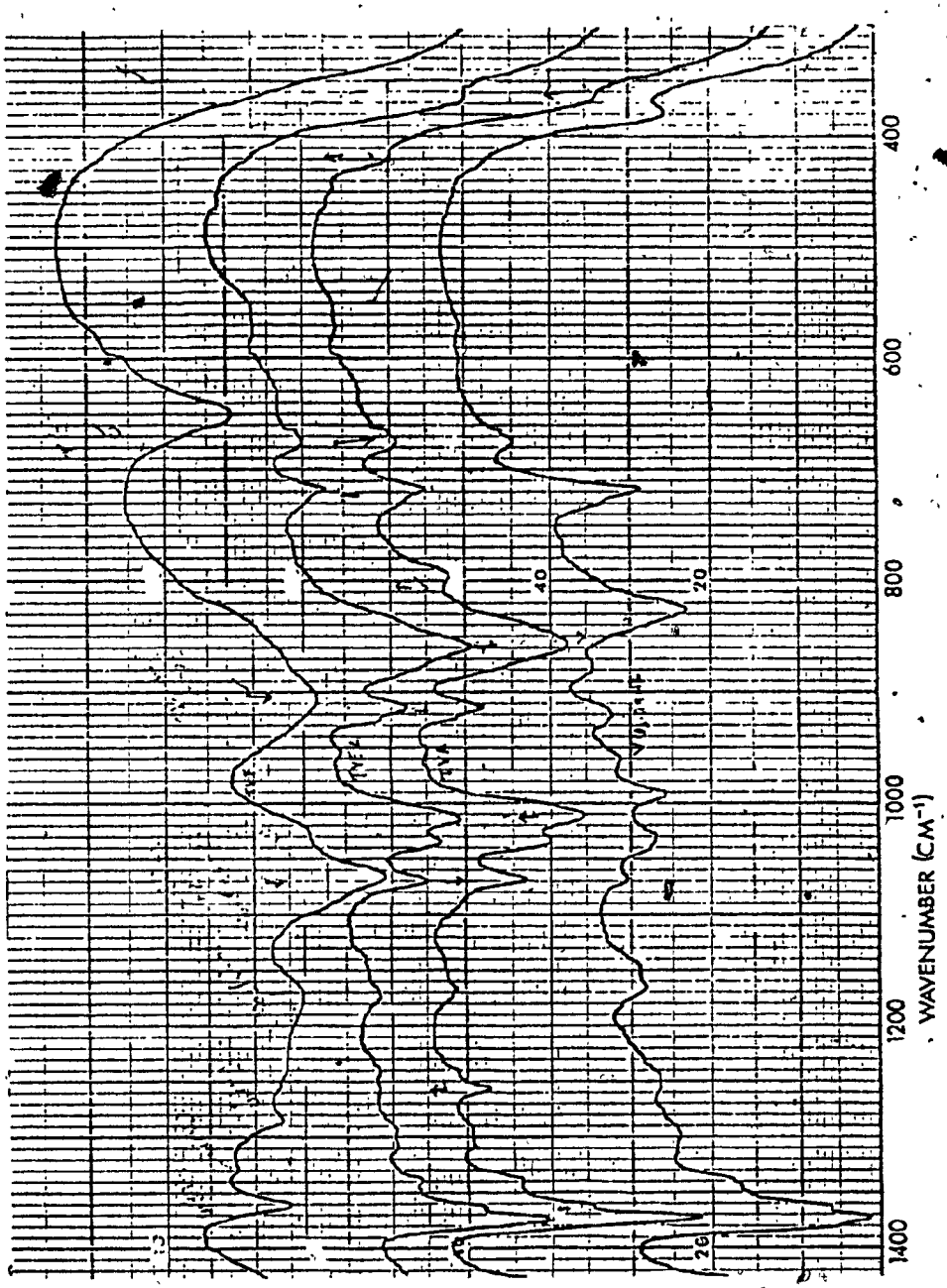

Fig. VI-2

SECTION VII

GAS-CHROMATOGRAPHIC ANALYSES

Experimental

Gas-chromatographic analyses were conducted on a computer-controlled, fully automated Perkin-Elmer Model Sigma 2 Gas Chromatograph with a stainless steel column (1/4" X 6') packed with "Chromosorb 102".

The analyses were conducted with the object of searching for ethylene, ethane and butane as gaseous products of the reactions of $ZnEt_2$ and $AlEt_3$ with VCl_3 in THF solvent. These products were assumed to be retained in part in solution by the solvent. A search for alkyl halides or H_2 was not attempted. The analysis was hampered by the surprising lack of data in the literature on separations of this kind, involving gases dissolved in an organic solvent. In order to ascertain the optimum conditions for an efficient separation of the three gases in THF, column parameters were varied with standard solutions prepared by bubbling ethane, ethylene and butane through THF. The peaks were identified by comparison with peaks of the pure gases. It was found that at higher temperatures (ca. 150°C) an efficient separation of butane from the other two gases was obtainable but the ethane and ethylene appeared together as one broad peak, whereas at lower temperatures (ca. 75°C) the gases were resolved well but butane and the solvent took an inordinately long time to emerge from the column. The chromatograph was accordingly temperature-programmed so that after the first two peaks of ethane and ethylene had been resolved at ca. 75°C, the column temperature was increased to a final value of 200°C to quicken the exit of butane and the THF solvent. It must be mentioned that the column material chosen was not the best for the purpose - activated charcoal, for instance, would perhaps have been better - but this was due to time constraints. In addition, mass spectral analysis of the gases as they emerged from the column, which would have been more informative, was also not attempted.

Fig. VII-1 illustrates schematically the procedure for collection of an unknown sample. The sample was preserved, after collection, in a bath of liq. N_2 until just before use. After a trial with the unknown samples, standard samples of the pure gases (ethylene, ethane and butane) were injected for confirmation of the peaks. Two blank samples were also collected by the same procedure as the unknown samples (according to the scheme of Fig. VII-1) but with only $ZnEt_2$ and $AlEt_3$ in the THF solution (and at three times the concentrations used in the actual reactions) in place of the samples of reaction mixtures. These blank spectra were taken to seek assurance that the ethane, ethylene and butane peaks detected in the unknowns were not due to gases evolved from decomposition of the metal alkyls (U.V.-Vis. spectra of these "blank" samples also showed no such gases dissolved).

In Figs. VII-2 and VII-4 are shown representative chromatograms for the Zn and Al samples respectively; the Zn chromatogram has inset the corresponding peaks for the pure gases. Figs. VII-3 and VII-5 show the corresponding "blank" chromatograms.

Table VII-A shows the quantitative composition of each chromatogram. The three 3 µl sample injections of the pure gases were used as standards. To obtain the estimated peak magnitudes in µl shown in the third column, ("RPA/RPA standard") the area of the unknown gas peak was divided by the area of the standards given in part A of the table and multiplied by 3 µl. For example, the magnitude of the butane peak in the Zn sample is (21.7/20.9) X 3 µl. Note that the solvent THF peaks had relative areas of more than 700 and appeared near 20.0 minutes retention time.

In some of the spectra several smaller peaks were obtained at locations that seemed to indicate the presence of higher, even-numbered hydrocarbons. A search for these was not attempted. Some samples,

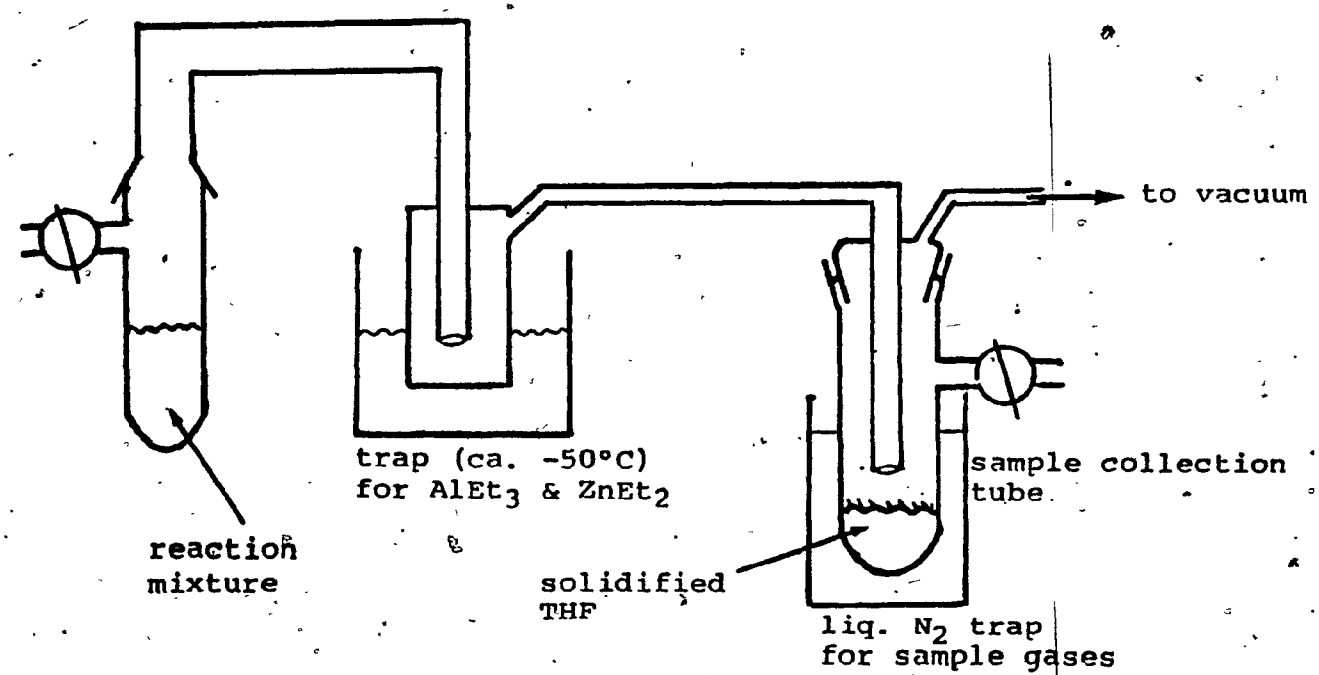

Fig. VII-1 Schematic diagram of procedure for collection of gas chromatographic samples

Figs. VII-2 through VII-5 (pages following):

Gas-chromatographic analyses of reaction mixtures for the gases ethane, ethylene and butane. All chromatograms shown are representative. Parameters for all are:

Injection port temperature: 175°C

Oven temperature: initial, 70°C; after 6 minutes, increased at 30°/minute to final of 200°C at ca. 30 minutes.

Column: Chromosorb (see text)

Carrier N_2 flow rate: 25 ml/minute

Sample size: 3 microliters

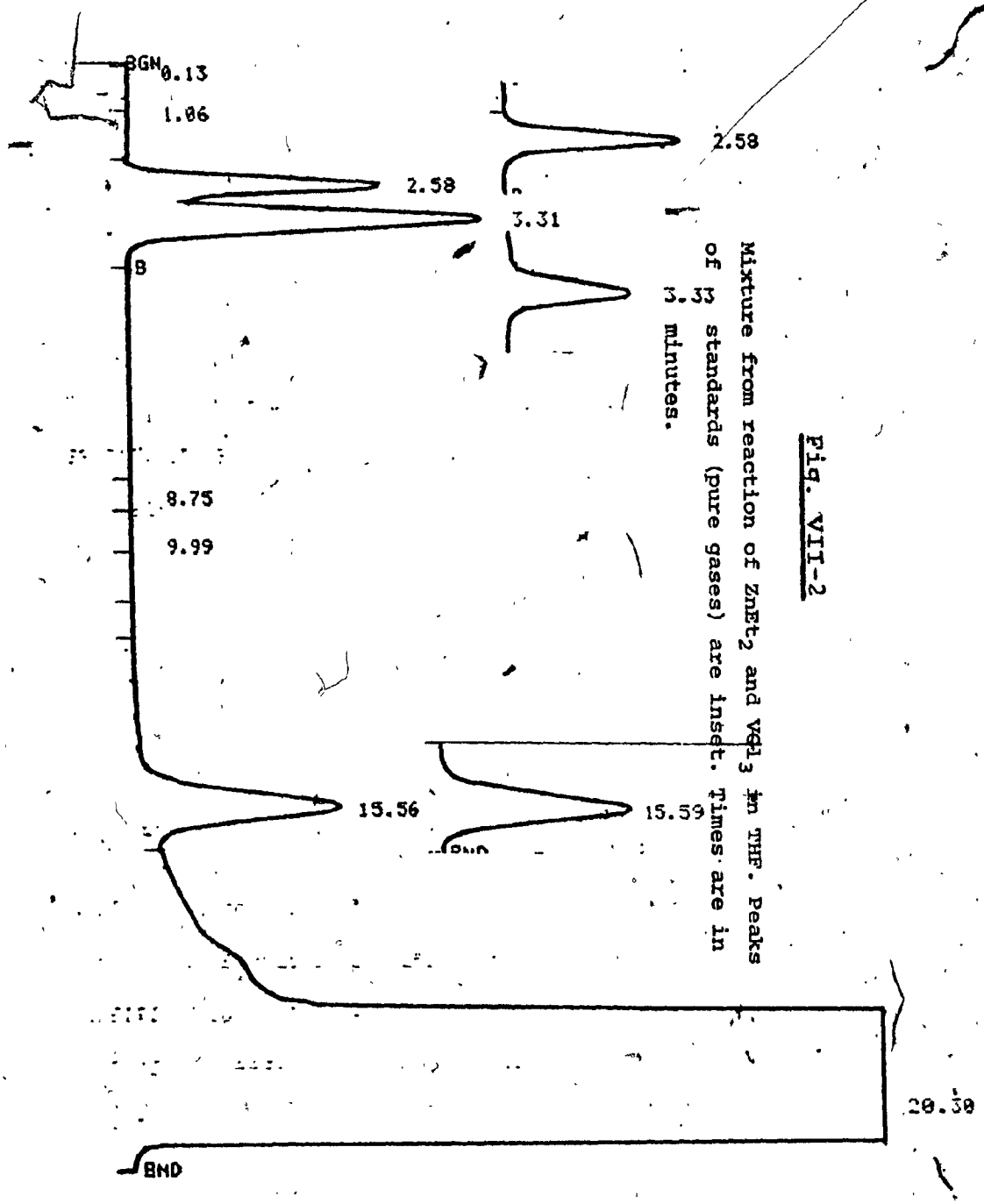

Fig. VII-2

Mixture from reaction of $ZnEt_2$ and VCl_3 in THF. Peaks of standards (pure gases) are inset. Times are in minutes.

INST 1 / METH 2 FILE 62

RUN 5 REACTION MIXTURE2 ZINC 3 : 31.4 5 / 8 / 80

Fig. VII-3

Blank corresponding to Fig. VII-2.

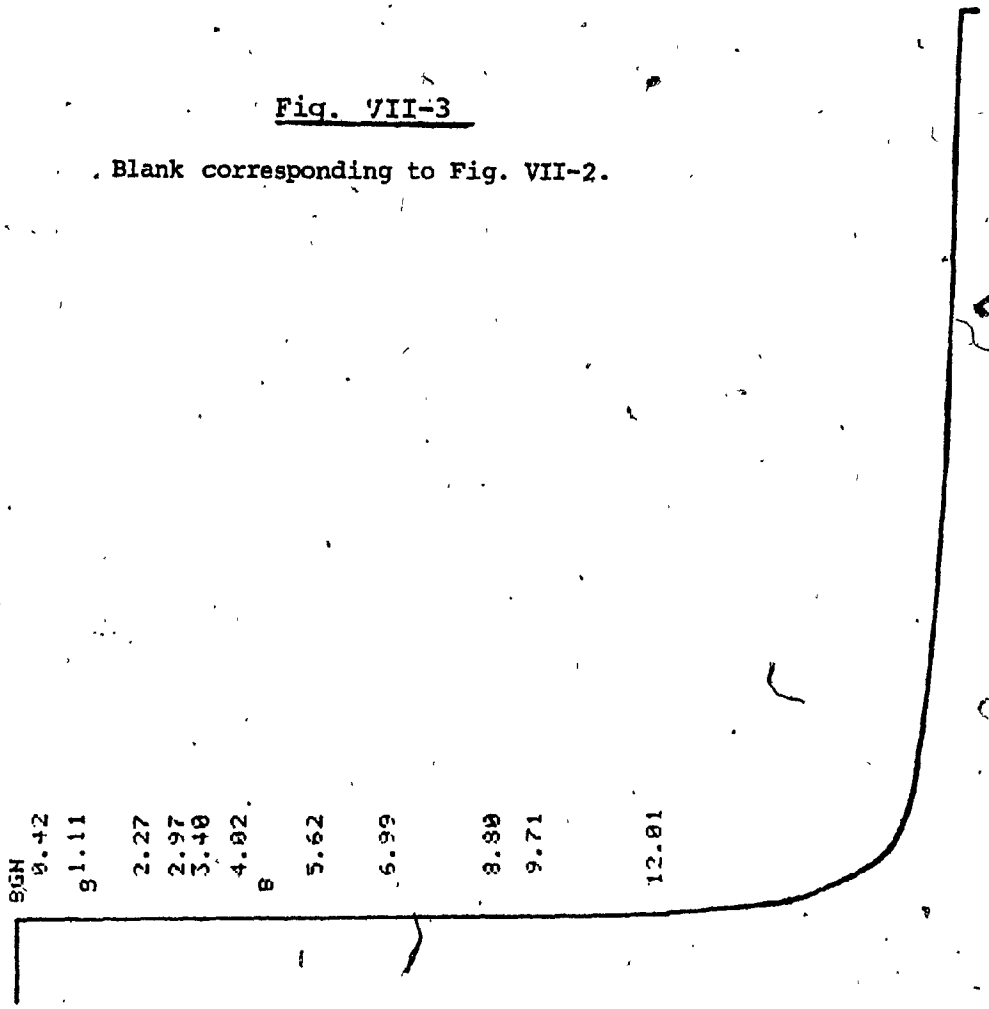

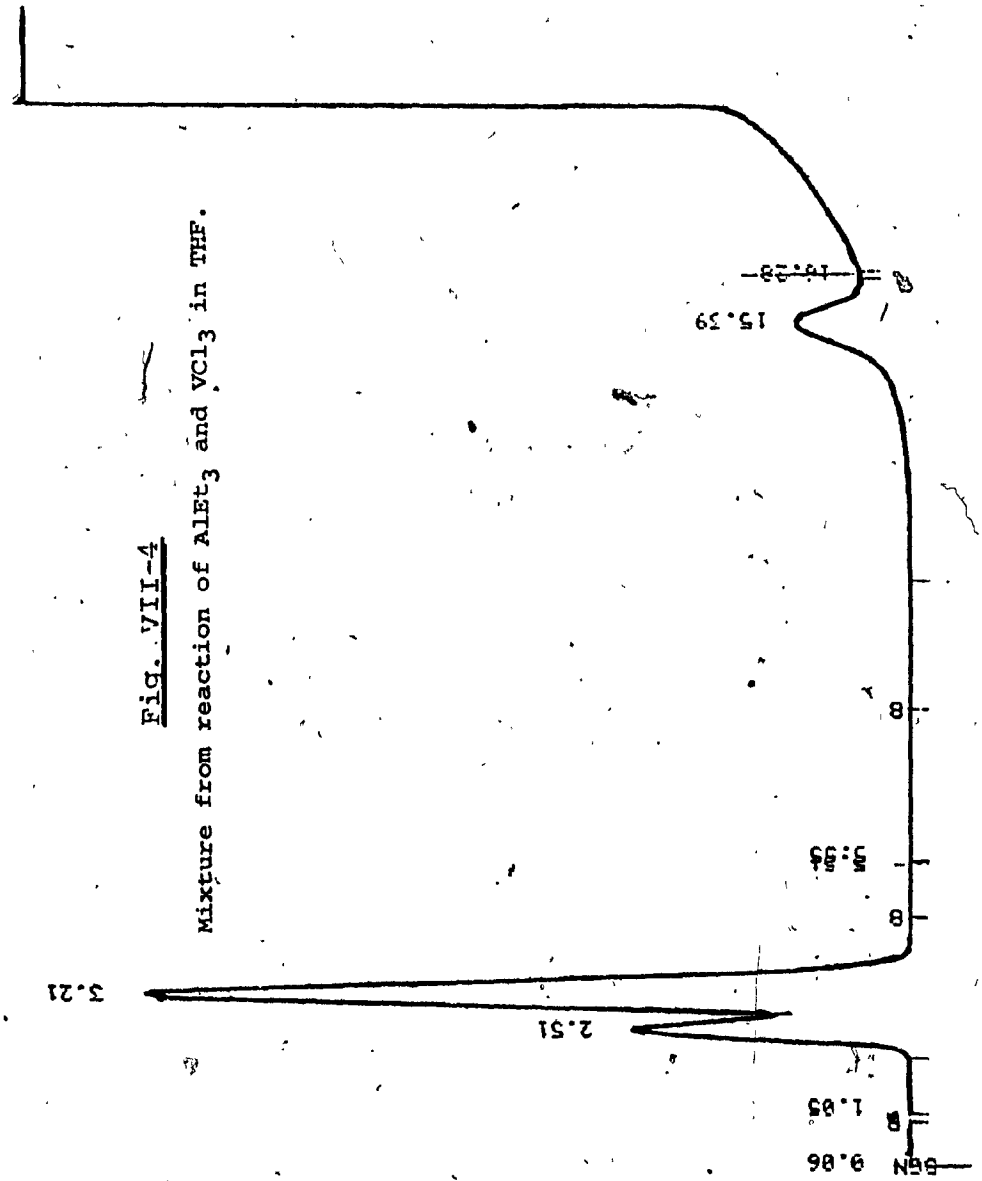

Fig. VII-4

Mixture from reaction of $AlEt_3$ and VCl_3 in THF.

Fig. VII-5

Blank corresponding to Fig. VII-4.

TABLE VII-A

SUMMARY OF GAS-CHROMATOGRAPHIC ANALYSES

Reactions of VCl_3 with $ZnEt_2$ and $AlEt_3$ in THF solvent

A: STANDARDS

Substance	Relative Peak Area
Butane, 3 μ l	20.9
Ethane, 3 μ l	10.0
Ethylene, 3 μ l	11.0, 11.2 (2 trials, av. 11.1)

B: VCl_3 + $ZnEt_2$ sample, 3 μ l

Substance	RPA	Ratio, RPA/RPA^{standard}, ="magnitude" of peak	%age composition, =(Column 3/TOTAL) X 100
Butane	21.7	1.04	19.6
Ethane	28.4	2.84	53.5
Ethylene	15.9	1.43	
	TOTAL =	5.31	

C: VCl_3 + $AlEt_3$ sample, 3 μ l

Substance	RPA	Ratio, RPA/RPA^{standard}	%age composition
Butane	8.8	0.42	5.6
Ethane	56.3	5.63	74.9
Ethylene	16.3	1.47	19.5
	TOTAL=	7.52	

after keeping for several (5-6) days, showed an absence of the ethylene peak, a smaller ethane peak and the appearance of a large peak after that of the solvent, possibly indicating dimerization of or oligomerization of the ethylene. This was also not further pursued.

Discussion

A summary of prior work on the analysis of gases obtained as products in the reactions similar to those conducted in this work has been given in an earlier section (see Prior Art), which may be reviewed at this point. Briefly, a large excess of ethane over ethylene and butane - much greater than would be expected according to the stoichiometry of 1,1, 1,n, dinuclear or β-eliminations - was observed. Observation of H-abstraction from solvent and the fact that the presence of hydride on the Al increased the ethane/ethylene excess 40-fold [2] lead one to believe that the ethane excess was caused by premature elimination of ethyl groups from the Al by various processes of H-abstraction, including free-radical abstraction and abstraction from metal hydride products of β-elimination. Presumably, thus, the reduction of the TM halide being used occured not through alkylation and subsequent elimination of the alkyls, but by abstraction of halide from the TM by a reduced Al, viz.

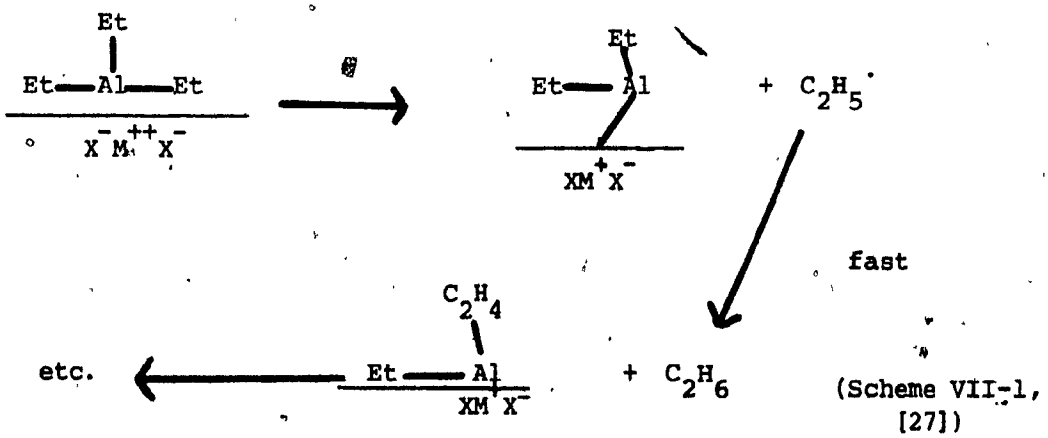

(Scheme VII-1, [27])

The above-cited reactions were conducted at high temperature (ca. 100°C). There is however no reason to assume that these reactions do not at least partially contribute to the overall scheme of things at low temperature. On the basis of various kinetic studies [113,27 and references cited therein) as well as on the basis of the results of the present study, we may however conclude that reactions involving preliminary alkylation of the TM atom through exchange do contribute substantially at low temperature. Thus, K.-H. Thiele et al. have observed in a very extensive study [114] that alkylation of TM halides is more successful at low temperature and with less polar metal alkyls, e.g. those of Zn and Hg - in preference to those of Al, which of course is famous for its Lewis acid properties. In later work, Thiele and coworkers isolated products such as $C_2H_5VCl_2$ (reaction of VCl_4 and $Zn(C_2H_5)_2$ in n-pentane at -10°C). Alkylation of the TM at low temperature would thus be expected to proceed more towards completion in the case of diethyl zinc than in the case of triethyl aluminum, and more ethane would be produced in the case of the $AlEt_3$, where premature elimination of ethyl groups (due to various processes of H-abstraction described earlier - including free radical-abstraction and abstraction from TM hydrides formed during β-elimination) from the Al itself would predominate over alkylation and subsequent elimination from the TM. This is precisely what has been observed in the present work, cf.:

1) In the case of the reaction of $AlEt_3$ with VCl_3 in THF (where TVA was produced) only one chloro group was eliminated on the V, whereas with $ZnEt_2$ all chloro groups were removed (thus the formulae $V(THF)_4ZnCl_4$ and $V(NCCH_3)_6ZnCl_4$, both products obtained from $ZnEt_2$);

2) ca. 75% ethane was evolved with $AlEt_3$ whereas only ca. 54% was evolved with $ZnEt_2$; in addition, the quantity of ethylene (which may also be produced to a small extent by β-elimination from the metal (i.e. Al or Zn) alkyl but is more likely to arise from β-elimination from the TM (i.e. V) [114]) was slightly increased in the case of $ZnEt_2$, and the quantity of butane was drastically in-

creased (from ca. 5% to ca. 20%). Butane assuredly proceeds mainly through dinuclear elimination from the TM. The corresponding process on the Al or Zn atom is thought to be highly unlikely [115,116,117].

SECTION VIII

CRYSTAL AND MOLECULAR STRUCTURE OF VEZN, $V(NCCH_3)_6\ ZnCl_4$

A: Structure Solution

Crystal Mounting

The crystal mounting was conducted with the help of a microscope (Bausch & Lomb, Stereo Zoom, 0.7 3 X plus 2 X objective) in a glove bag in which an inert atmosphere was maintained by purging with a constant stream of dry N_2. A batch of dried crystals was poured out onto a microscope slide and a suitable crystal, rhomboid in appearance and of approx. dimensions 0.3 X 0.2 X 0.2 mm was selected and was lifted with the help of a needle (to which it clung due to static electricity) and transfered into the opening of a standard crystallographic capillary of 0.3 mm internal diameter (borosilicate, supplier Cambridge Instruments, Montreal). It was inserted to a suitable position in the capillary by pushing with a glass fiber. The opening of the capillary was sealed with a septum cap and it was removed from the glove bag. The capillary was evacuated by means of a needle connected to a vacuum line pierced through the septum cap and sealed thus under vacuum with a small flame. The sealed capillary was afixed to a pinhead and attached to the goniometer head.

Structure Solution

Weissenberg photographs along an axis assigned as the b axis were taken. Precession photographs of the a*b* and b*c* regions along with the 0-level Weissenberg indicated no symmetry elements except for the usual Friedel relations hkl and $\bar{h}\bar{k}\bar{l}$ and the triclinic space group was tentatively assigned. Centrosymmetric character was an assumption which was proved correct by the successful solution of the structure. The twelve reflections centered for least-squares calculation of the orientation matrix were the (030), (740), (040), (0$\bar{3}$5), 5$\bar{4}$0) and (006) and their Friedel-related analogs. The axes selected on the Weissenberg happened to correspond to an F-centered cell, and besides being unconventional, this proved complicating.

After the intensity data were collected, therefore, indices of the reflections had to be transformed thus:

$$h_{new} = \frac{h-k}{2} \qquad k_{new} = k \qquad l_{new} = \frac{l+k}{2}$$

(Scheme VIII-1)

to obtain a primitive cell, and the cell parameters were recalculated for the new cell. They are given in table VIII-A.

A Patterson map was plotted. On the basis of the equivalent positions for the space group, the following interatomic vector peaks were to be expected [$(x_1y_1z_1)$= coordinates of V, $(x_2y_2z_2)$= coordinates of Zn):

V ⟷ V	$\pm 2x_1$	$\pm 2y_1$	$\pm 2z_1$
Zn ⟷ Zn	$\pm 2x_2$	$\pm 2y_2$	$\pm 2z_2$
Zn ⟷ V	$\pm (x_2 \mp x_1)$	$\pm (y_2 \mp y_1)$	$\pm (z_2 \mp z_1)$

(Scheme VIII-2)

Addition of the third most intense peak on the Patterson map (Intensity I= 306 (all intensities relative), approx. position (0.45, 0.06, 0.645)) to the most intense peak (I=454, (0.180, 0.540, 0.820)) yielded a position related to a peak of I= 186, which was taken as a Zn⟷Zn vector peak, the I= 454 peak being assigned as a multiple V⟷V vector. This yielded the initial positions (0.082, -0.2338, 0.616) for Zn and (0.27, 0.31, -0.25) for V. A structure factor calculation with these coordinates and initial isotropic thermal parameters ("B") set at 3.0 and unrefined yielded an R-factor of 0.83, which on least-squares (LS) refinement came

TABLE VIII-A

VEZN CELL PARAMETERS

Space group: $P\bar{1}$; Equivalent positions:

x,y,z; -x,-y,-z

Lattice constants: (standard deviations to one significant figure, in parentheses)

a = 11.832(5) Å	α = 62.17(1)°
b = 12.592(5) Å	β = 119.90(1)°
c = 11.801(5) Å	γ = 117.78(1)°

down to 0.516, indicating that the positions were at least partially correct. A difference Fourier (DF) was then plotted, and from this - on the basis of the electron-density-difference distributions - it was diagnosed that the positions of Zn and V ought to be reversed. With these positions the R-factor came out as 0.454 (unweighted) on LS refinement. The positions of 3 chlorine atoms were also determined from the DF map, and when inserted into the LS routine they yielded an R-factor of 0.431 (unweighted). Another DF map was then plotted and this yielded the positions of the fourth chlorine and 2 nitrogens, which on insertion into the LS routine gave an R-factor of 0.296. The structure solution was pursued in this manner. Another DF map was plotted using the new refined positional parameters and from this the positions of the remaining (4) nitrogen atoms and of six of the 12 carbon atoms (which were assumed to be present from the elemental analysis) were obtained, these yielding an R-factor of 0.236 when inserted into the LS routine. The remaining 6 carbons were observed when another DF map was plotted, and with these inserted into the LS refinement routine an R-factor of 0.174 was obtained. The scale factor (1.0 initially) had been unrefined so far and refinement of this brought the R-factor to 0.113 (unweighted). A DF map at this stage showed that there was a lot of vague and diffuse electron density in a particular, large region of the unit cell otherwise conspicuously empty. The best possible accouning for this electron density was accomplished by inserting one N and 3 carbon atoms in the approximate geometry of a pyramid, but the extremely high isotropic thermal parameters for these atoms obtianed on refinement (B near 25.0) showed that the assignment was not really tenable. It was decided that this electron density was very probably due to a lot of differing, clathrated impurities (the space in question was a large "hole" in the unit cell). Accordingly it was decided to omit the anomalous atoms from the final structure. The final reliability indices obtained for the structure, along with some other data

are given in table VIII-B. A list of the final positional coordinates with estimated standard deviations is given in Appendix B.

Final thermal parameters are given in Appendix C.

TABLE VIII-B

$V(NCCH_3)_6ZnCl_4$: FINAL REFINEMENT PARAMETERS

Without anomalous atoms (24 atoms only)

R= 8.67% (unweighted)
R= 13.2% (weighted)

With anomalous atoms (28 atoms total)

R= 6.9% (unweighted)
R= 8.6% (weighted)

Total number of reflections used (I more than $3\sigma(I)$)

2,018

Goodness of fit parameter

4.270

Initial (Wilson plot) scale factor

0.595 (for space group $P\bar{1}$)

Final (refined) scale factor

1.272 (for space group $P\bar{1}$)

SECTION VIII

CRYSTAL AND MOLECULAR STRUCTURE OF VEZN

B: Discussion

The structure of VEZN, $V(NCCH_3)_6ZnCl_4$, is illustrated as its ORTEP diagram in Figs VIII-1A and VIII-1B. A simplified diagram for interpretation is given in Figs. VIII-1C and VIII-1D. Table VIII-C and table VIII-D give the distances and angles. There are two units of the molecule per unit cell. This packing arrangement is shown in Fig. VIII-1E.

The molecule consists essentially of two ions: a hexakis (acetonitrile) V(II) species with a formal charge of +2, in which the V is octahedrally coordinated (or nearly so, assumed d^2sp^3 hybridization with 3 d electrons in the nonbonding d_{xy}, d_{yz} and d_{xz} orbitals) and a tetrachlorozincate species, with a formal charge of -2, in which the Zn has (nearly) tetrahedral coordination.

The feature of this molecule first worth noting is that in the packing of the two ions in the lattice a very large void exists between them, a void in which impurities can be trapped during the process of crystallization. During the course of this crystal structure solution, electron density maps showed the presence of species in this void which could not be classified according to atomic type (as noted in the previous section) and it is thought that these were the clathrated impurities briefly referred to earlier, not necessarily identical in every unit cell. The best fit to the structure was obtained with one N and 3 C atoms, having extremely large thermal vibration parameters.

As noted earlier, the omission of these species did not produce a marked decrease in the reliability of the structure (R-factor 6.9% (weighted) for all atoms vs. 8.6% without anomalous atoms). It is the effect on the geometry of the final crystal structure solution that one must trouble about most however, either in terms of actual distortion, from ideal geometry, of the ions due to effects (repulsions, attractions, etc.) of the clathrated species, or in terms of

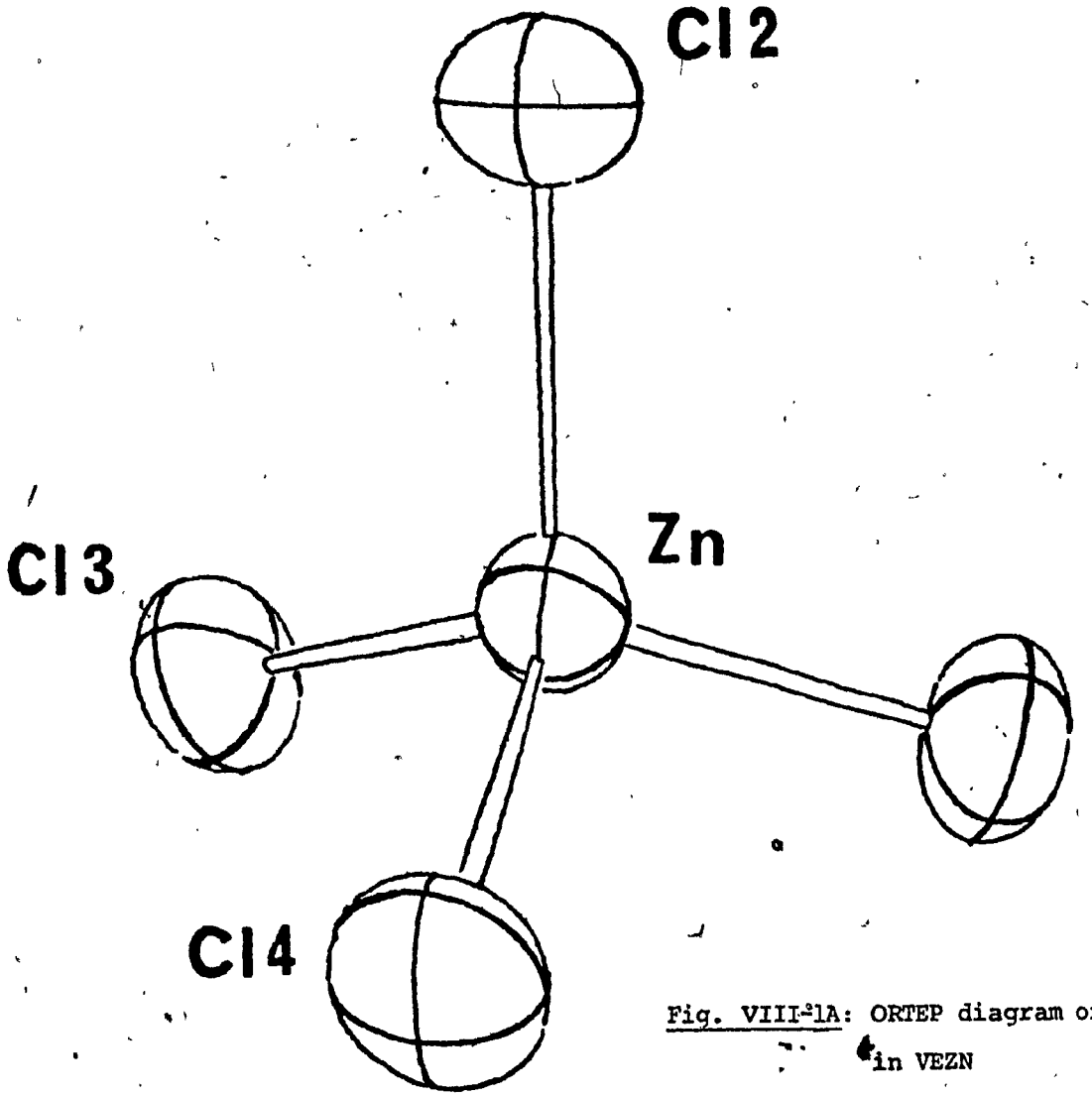

Fig. VIII-1A: ORTEP diagram of $ZnCl_4^{2-}$ in VEZN

$ZnCl_4^{2-}$

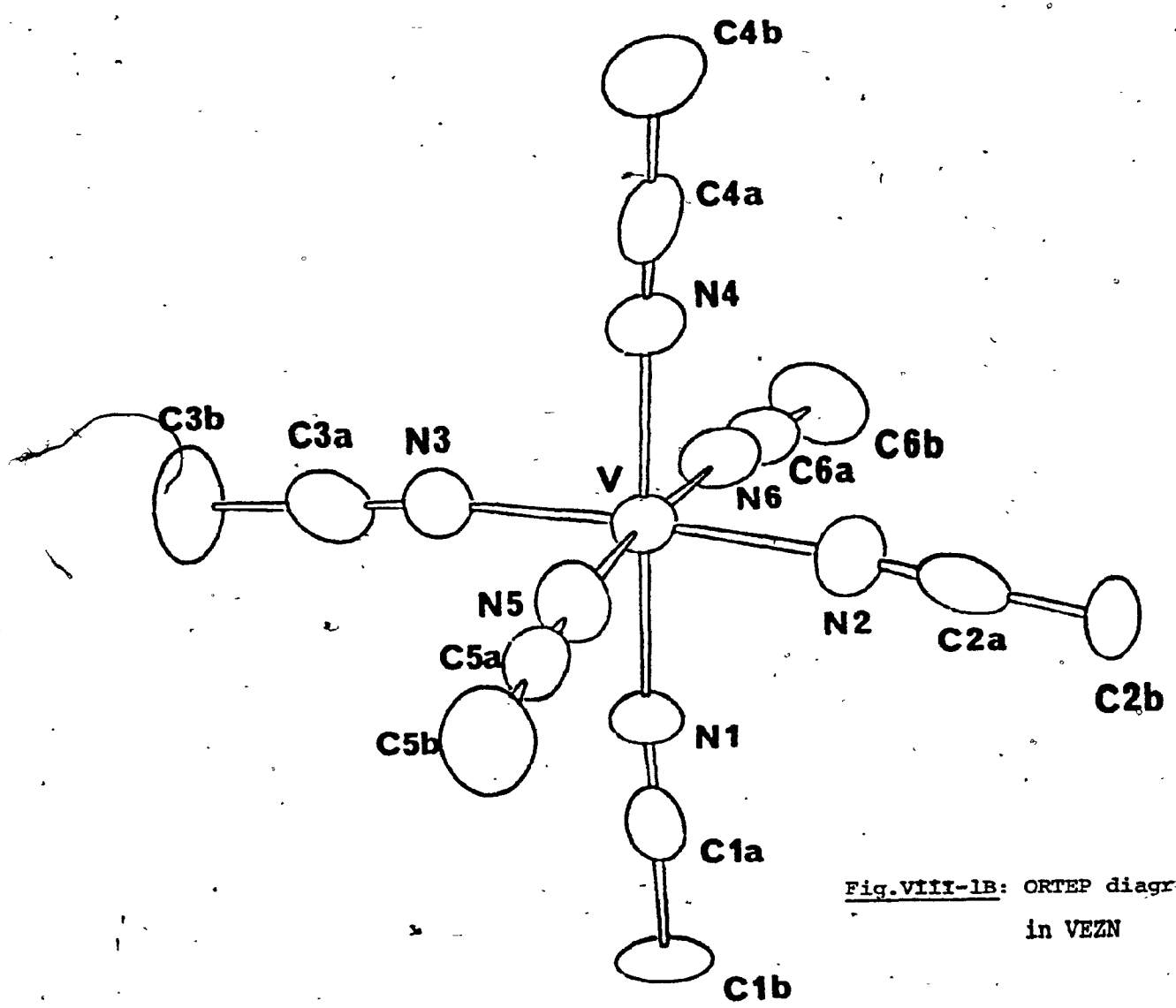

$V(NCCH_3)_6^{2+}$

Fig.VIII-1B: ORTEP diagram of $V(NCCH_3)_6$ in VEZN

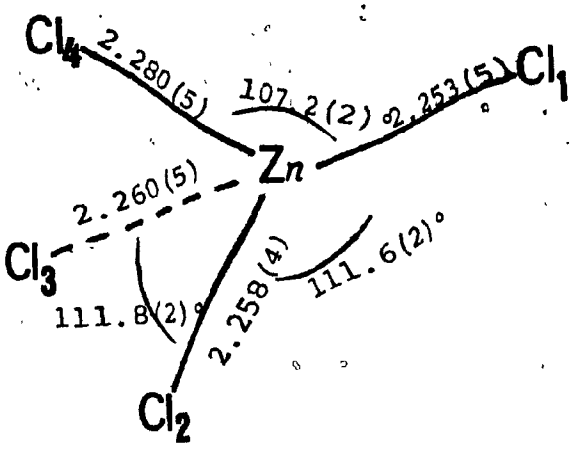

(All distances in Å)

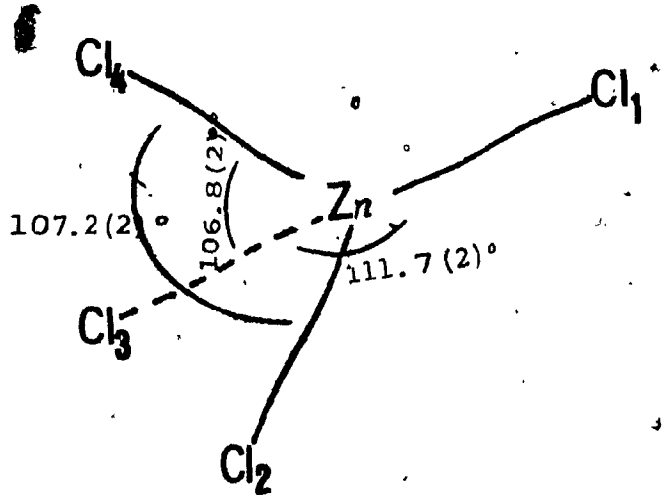

Fig. VIII-1C: $ZnCl_4^{2-}$ geometry in VEZN

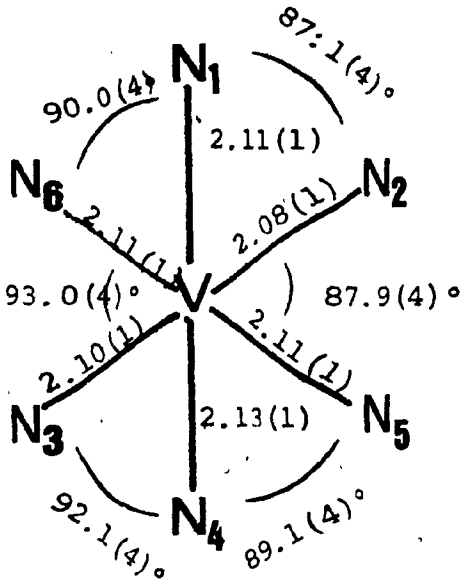

(All distances are in Å)

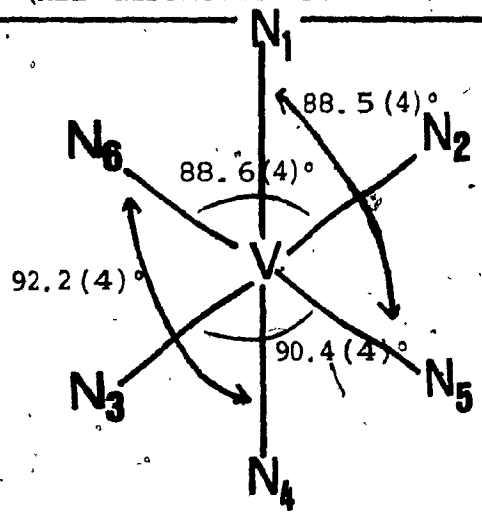

Fig. VIII-1D: $V(NCCH_3)_6^{2+}$ geometry in VEZN

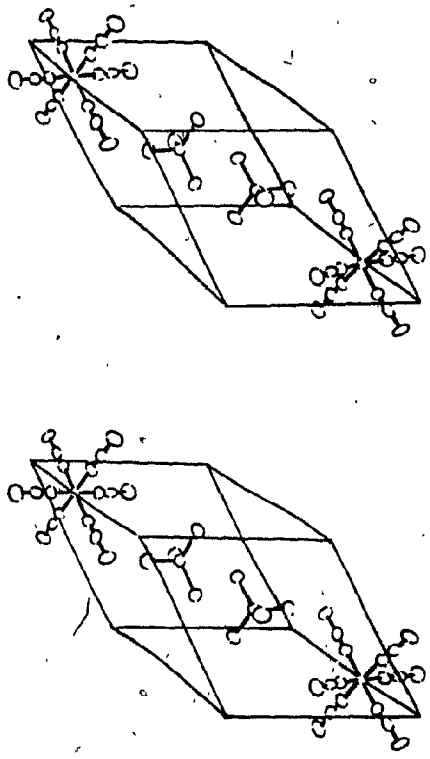

Fig. VIII-1E: Packing diagram for VEZN (stereo view).

RELEVANT BOND DISTANCES, WITH STANDARD DEVIATIONS, FOR VEZN

(Distances in Å; standard deviations rounded off to one significant digit)

$Zn-Cl_1$	2.253(5)
$Zn-Cl_2$	2.258(4)
$Zn-Cl_3$	2.260(5)
$Zn-Cl_4$	2.280(5)
$V-N_1$	2.11(1)
$V-N_2$	2.08(1)
$V-N_3$	2.11(1)
$V-N_4$	2.14(1)
$V-N_5$	2.11(1)
$V-N_6$	2.12(1)

N_1-C_{1a}	1.14(2)	$C_{1a}-C_{1b}$	1.50(2)
N_2-C_{2a}	1.17(2)	$C_{2a}-C_{2b}$	1.47(2)
N_3-C_{3a}	1.13(2)	$C_{3a}-C_{3b}$	1.50(2)
N_4-C_{4a}	1.12(2)	$C_{4a}-C_{4b}$	1.49(2)
N_5-C_{5a}	1.16(2)	$C_{5a}-C_{5b}$	1.46(2)
N_6-C_{6a}	1.13(2)	$C_{6a}-C_{6b}$	1.46(2)

RELEVANT BOND ANGLES, WITH STANDARD DEVIATIONS, FOR VEZN

(Angles in degrees; standard deviations rounded off to most significant digit)

Cl_1-Zn-Cl_2	111.6(2)	N_1-V-N_2	87.1(4)
Cl_1-Zn-Cl_3	111.8(2)	N_1-V-N_3	90.0(4)
Cl_1-Zn-Cl_4	107.2(2)	N_1-V-N_4	176.8(4)
Cl_2-Zn-Cl_3	111.8(2)	N_1-V-N_5	88.5(4)
Cl_2-Zn-Cl_4	107.3(2)	N_1-V-N_6	90.0(4)
Cl_3-Zn-Cl_4	106.9(2)		
N_2-V-N_3	176.7(5)	N_3-V-N_4	92.1(4)
N_2-V-N_4	90.7(4)	N_3-V-N_5	90.4(4)
N_2-V-N_5	88.0(5)	N_3-V-N_6	93.0(4)
N_2-V-N_6	88.6(4)	N_4-V-N_5	89.1(4)
N_5-V-N_6	176.3(4)	N_4-V-N_6	92.2(4)
V-N_1-C_{1a}	173(1)	N_1-C_{1a}-C_{1b}	178(1)
V-N_2-C_{2a}	172(1)	N_2-C_{2a}-C_{2b}	177(2)
V-N_3-C_{3a}	173(1)	N_3-C_{3a}-C_{3b}	176(2)
V-N_4-C_{4a}	174(1)	N_4-C_{4a}-C_{4b}	179(2)
V-N_5-C_{5a}	173(1)	N_5-C_{5a}-C_{5b}	179(1)
V-N_6-C_{6a}	174(1)	N_6-C_{6a}-C_{6b}	177(1)

the effect on the reliability index (R) of the crystal structure solution and consequently on the geometry calculated. The conclusion one can come to is that within the limits of reliability of the structure solution, the bond angles did not conform to a perfect or even near-perfect octahedron for V, though the bond distances showed much less variation (see table VIII-C).

In the tetrachlorozincate moiety, the angles vary from 106.8° to 111.8°, the nominal tetrahedral value being 109°28'. The average Zn-Cl distances, 2.26 Å, agree exactly with those found in the $ZnCl_4^{2-}$ ion in Na_2ZnCl_4 (2.26 Å [119]). In this latter molecule, there is almost no distortion from the tetrahedral, however. The Zn-Cl distances are known to have shorter values, however. The Zn-Cl distances are 2.206, 2.204 and 2.207 Å in $4(ac\text{-}py)_2ZnCl_2$, $ZnCl_2$ and $4(CN\text{-}py)_2ZnCl_2$ respectively [120, 122]. In $C_4H_{10}N_2S_2ZnCl_2$, the Zn-Cl distance is 2.252 Å [123]. The value of 2.26 Å for Zn-Cl in VEZN may be compared with the values for the sum of the covalent radii for Zn + Cl (2.19 Å) and the sum of the Bragg-Slater radii (2.35 Å)**.

The Zn atom is assumed to be sp^3 hybridized, a state that is quite commonly observed for Zn complexes [125, 126].

Turning to the other ion, a slight angular distortion from octahedral geometry is noticeable even within the limits of the crystal structure solution's reliability. The angles at a (weighted) R-indiex of 6.9% vary from 87.1° to 93.0° (see table VIII-C). The fairly constant and consistent V-N distances (2.11 Å average) may be compared with the sum, for V and N, of the Bragg-Slater radii, 2.0 Å.

** The values for atomic radii given by Bragg and Slater [124] take into account charge distortions and have been found more appropriate for use by the author than the conventional covalent or ionic radii.

Substantial $d_{\pi} \rightarrow \pi^*$ (ligand) interaction may be expected to shorten the V-N bond. This distance does compare favorably with that in (2,2 bipy)FO_2V(V) (2.131 Å) [127] and with that in the hexahydrate of the barium salt of VO(EDTA) [128] (2.18 Å) where V is V(IV); all this seems to show that the oxidation state of V does not affect the V-N distance much. In acetonitrile coordinated to V(V) ($VO[NO_3]_3:CH_3CN$), Einstein et al. [100] observed a V-N distance of 2.24 Å, which they consider as long when viewed comparatively with the metal-bond distances in $Cu_2Cl_2(CH_3CN)_2$, $Cu_3Cl_6(CH_3CN)_2$ [129] and $ReOBr_4(CH_3CN)$ [130] (1.96, 1.97 and 2.31 Å respectively). Brauer and Kruger [131] believe that when unsaturated N atoms are trans, across V, to oxo atoms, the V-N distance is lengthened; thus the values of Einstein et al. [100] cited above and the values of 2.05 Å to 2.13 Å obtained by Mathew et al. [132].

Brauer and Kruger [131] obtained a value of 2.189 Å for V-N in their solution of $V(py)_4Cl_2$, which is similar in many respects to V(II) - V(II) coordinated to N in a ligand capable of acting as a π-acceptor. The shorter V-N distance in VEZN may be attributed to the stronger M→L backbonding expected in a cyano ligand. These authors calculate a "covalent octahedral radius" for V(II) of 1.48 Å, which with the accepted N covalent radius (0.75 Å) gives a sum of 2.23 Å for V(II)-N.

One feature of note in this molecule, as for TVA (see later), is that the V does not conform to the conventional 16 and 18 electron rules [1] for TM atoms (see General Introduction section). The V atom has only 15 electrons assignable to it.

SECTION VIII

CRYSTAL AND MOLECULAR STRUCTURE OF VEZN

C: The acetonitrile enigma

A simplified representation of the coordinated CH_3CN is given in Fig. VIII-1F. The bond parameters obtained agree extremely well with those obtained by other workers for coordinated acetonitrile [130, 133-135]. Thus Einstein et al. [100] obtained 1.17 Å for the N≡C distance in coordinated acetonitrile compared with the average of 1.14 Å for VEZN and the normal uncoordinated 1.16 to 1.17 Å for VEZN, and a distance of 1.46 Å for the NC-CH_3 single bond, to be compared with the average 1.48 Å for VEZN and 1.53 Å for a normal C-C single bond [132].

The primary feature of the structure of the coordinated ligand is the deviation from linearity (very slight for ∠ NCC = 177.6° av., and noticeable for ∠ VNC = 173.4° av.). The CCN stretch in the IR spectrum is also shifted considerably to higher frequency, indicating either a shortening of the CN bond, or nonlinearity in C-C-N, or both. In most earlier work where these phenomena have been noticed [14, 100 and references therein, 101,132,134,135], a clear explanation has not been afforded as to why they occur. For the NCC bond, crystal packing forces or lattice distortions could well account for the small change observed, but for the V-N-C bond a more rigorous explanation is required. SCF-MO calculations show [165,166] that N (as well as C) is sp hybridized in the CN entity. The sp lone pair can be treated as essentially nonbonding and the energy levels are ordered such that the two π-orbitals are the HOMOs and the nonbonding lone pair is next in energy. The bonding picture is thus the following: "nonbonding" σ-symmetry lone pair donated to V(II) atom (the V-N bond); some π-electron density back donated from V π-symmetry orbitals to the CN π* orbitals. Both these interactions would be expected to decrease the strength of the C-N bond, contrary to what is observed.

To account for the observations, then, one must either assume that

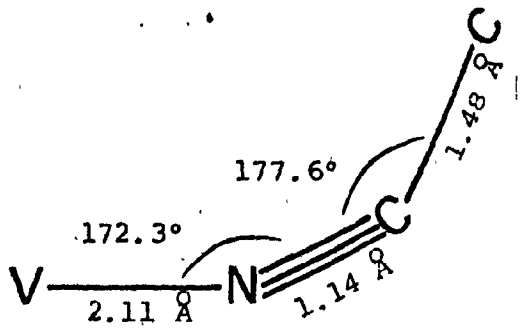

Fig. VIII-1F: Geometry of coordinated acetonitrile in VEZN. All values are averages. Note that the "normal" C-N triple bond distance is 1.17 Å and the normal C-C single bond distance 1.48-1.52 Å (reference 132).

the σ(sp) lone pair somehow acquires antibonding character, or that the π* orbitals have a negative net energy (which they do not have in the free ligands as indicated by SCF-MO calculations (references cited above)). The former possibility seems to be excluded especially in view of the fact that the C-N bond shortening is much more pronounced in the case of CH_3CN coordinated to V(II) than in CH_3CN coordinated to V(II), as discussed in an earlier section (see IR section): a V(III)-N -bond would be expected to be stronger and shorter than a V(II)-N σ-bond. The latter possibility - that the π* orbitals have a net negative energy - is supported by observations on many CN-ligand-containing molecules, such as TCNQ [136b] where this phenomenon has been observed; the presence of a cation, V(II), would especially enhance such effects since its presence, in the MO treatment, would mean a perturbation that would lower all energy levels by a certain amount. Even this possibility may still not account completely for the bond distortions. What is however clear is that some perturbation occurs due to the presence of the V(II) near the ligand and especially due to V→N backbonding, which causes a re-ordering of the CN-group orbital energies.

The distortion of acetylenes, for instance, from linearity on photochemical excitation of π-electrons [136a] or even sometimes during normal coordination [136b] may also be mentioned in the context of the above discussion.

Einstein et al. [100] observed an N-C-C angle of 178.1° in coordinated acetonitrile, very close to our own average value of 177.6°

In reference to the above discussion, it has been suggested that a Molecular Orbital perturbation treatment of the matter be carried out [136c], using the known results of various perturbations on the MO structure of the simpler HCN molecule as a basis.

SECTION IX

CRYSTAL AND MOLECULAR STRUCTURE OF TVA, $(THF)_3Cl_2VOVCl_2(THF)_3$

A: Structure solution

Crystal Mounting

An initial mounting was attempted with a batch of ether-washed crystals in the glove bag, but the crystals decomposed to a slimy mass almost instantaneously on exposure to the atmosphere in the glove bag. An attempt was then made to mount the crystals in the dry box, with the microscope mounted outside the dry box on its glass face and the crystals manipulated within for selection. A few crystals obtined thus, sealed under vacuum (as described for VEZN) showed only powder diffraction patterns and in good cases patterns due to a number of crystals. These crystals had the property of crumbling under the touch of the needle; all this pointed to a breakdown of the crystal lattice due to loss of solvent (see earlier sections, [118]). An attempt was then made to mount a crystal along with some introduced mother liquor. One crystal so mounted behaved fairly well and served for the purpose of space group determination (through the photographs) but subsequent mountings in this fashion again yielded defective crystals. The crystal mounted for the space group determination was however very tiny and shifted position constantly in the capillary, a problem that was found difficult for the photographs and insurmountable on the diffractometer. A final mounting procedure was then attempted in which the crystals, covered by a little mother liquor, were inserted into a jar of nujol (nujol has very high viscosity making O_2 diffusion difficult). Nujol was also introduced into the capillary in such a way as to completely cover the inserted crystal; and it (the nujol) appeared to adhere well enough to the crystal during the short trip from jar to capillary to protect the crystal well. The crystal and nujol in the capillary were then sealed under vacuum. The final crystal mounted in this fashion had the approx. dimensions 0.2 X 0.1 X 0.1 mm.

Structure Solution

Weissenberg photographs were taken along an axis assigned as the b axis (an assignment that proved correct and useful for the space group that was determined, C2/c). Precession photographs of the a*b* and b*c* regions showed, along with the 0-level Weissenberg, systematic absences corresponding to C-face centering (all reflections h + k odd absent). A 2-fold axis being present, space group assignment was a question of chosing between the centrosymmetric C2/c (more likely) and the acentric Cc, since a c-glide was also diagnosed. The space group C2/c was assumed and the successful solution of the structure with this assumption as well as a later analysis according to the method of Howell, Philips and Rogers [137,138] proved this to be correct.

Intensity data collection was conducted, in a similar manner to that for VEZN, with a preliminary centering of the reflections $(0\ 0\ \bar{1}\bar{0})$, (10 0 0) and (0 6 0). Additionally, for each of these reflections, a preliminary scan - with both the ω and the θ-2θ techniques - was conducted to ensure that there was no duplicity in the peaks, in view of the previous experience with cracked crystals. The 16 reflections comprising (10 0 0), (0 6 0), $(\bar{1}\ 3\ 8)$, $(\bar{1}\ \bar{3}\ 8)$, (7 3 0), $(7\ \bar{3}\ 0)$, (0 4 6), $(0\ \bar{4}\ 6)$ and their Friedel-related counterparts were centered and their anglular parameters used to calculate the orientation matrix. Data collection was then started. Final cell parameters obtained are given in Table IX-A.

As the first step in structure solution, a Patterson map was plotted. On the basis of the equivalent positions for the space group, the peaks to be expected for the V↔V interatomic vectors were (multiplicities given in brackets; V position is

TABLE IX-A

FINAL CELL PARAMETERS FOR TVA

Space group: C2/c

Equivalent positions:

-x,y,1/2 - z ; x,-y,1/2 + z

and centrosymmetric counterparts

Lattice constants: (standard deviations to one significant digit in parentheses)

a = 19.181(5) Å	α = 90.00(1)°
b = 9.200(5) Å	β = 103.09(1)°
c = 18.935(5) Å	γ = 90.00(1)°

(x,y,z)):

0, 0, 0 [X 4]	$\pm$ 2x, 0, 1/2 $\pm$ 2z [X 2]
$\pm$ 2x, $\pm$ 2y, $\pm$ 2z [X 1]	
$\pm$ 2x, $\pm$2y, $\pm$ 2z [X 1]	0, $\pm$ 2y, 1/2 [X 2]

(Scheme IX-1)

The most intense peak (I[relative intensity] = 1,387, at the position (0, 0, 0.5) was taken as representing the (0, 2y, 1/2) vector from the set in Scheme IX-1, giving a value of y for vanadium of 0.0. The next most intense peak, of I= 1,082 (appearing at (0.167, 0.0, 0.167)) was taken as representing either of ($\pm$2x, 0, 1/2 $\pm$2z), giving rough values for the position of V of (x,y,z) = (0.0835, 0.0, -0.1665) for the first case. An analysis similar to that of Scheme IX-1 was prepared for the V Cl vectors, taking (x_1,y_1,z_1) as the position of the V and (x_2,y_2,z_2) as the position of the Cl. Substituting the position of V determined above, (0.0835, 0.0, -0.1665), in one of the V↔Cl vectors, $(x_1-x_2, y_1-y_2, z_1-z_2)$, gave the positional values for one of the chlorines, (x_2,y_2,z_2), of (0.0205, -0.167, -0.6165). Substituting these values in the expression for another V↔Cl vector, $(x_1+x_2, y_1+y_2, z_1+z_2)$, in order to attempt to locate this on the map gave the positional values for this vector of (0.104, 0.167, 0.217), which corresponded to a peak of I= 623, confirming that the evaluation had been correct to this point.

An arbitrary scale factor was introduced at the beginning of the refinement and this refined to a final value of 4.085. A Wilson plot, though conducted later (and thus out of turn), gave a scale factor of 4.192.

Using the position of V only determined from the Patterson (above), a multiple least-squares (LS) refinement yielded an R-factor of 0.683 (0.523 weighted). A Fourier electron density map was then plotted with phasing on the basis of this V position. This map confirmed the position found for one of the chlorines from the Patterson (see above) and revealed the positions of an additional Cl and an O atom. On insertion into the LS refinement routine these gave an R-factor of 42.7% (48% weighted). A Difference Fourier was then plotted yielding the positions of additional atoms, and the structure pursued in this manner until the positions of all atoms were determined. The limits of refinement with isotropic thermal parameters gave an R-factor of 11.93% (12.71% weighted) and final refinement with anisotropic thermal parameters gave values for the R-factor of 9.73% (4.79% weighted).

It should be noted that the selection of a larger crystal would probably have yielded a far better value for the R-factor; a determination of the geometry of the structure as refined here however showed it to be quite satisfactory. Final refinement parameters are given in table IX-B. Appendices D and E give final positional coordinates and final thermal parameters with estimatated standard deviations.

TABLE IX-B

FINAL REFINEMENT PARAMETERS FOR TVA. $(THF)_3Cl_2VOVCl_2(THF)_3$

Total N° of reflections used in refinement (I more than 3σ(I))

937 (out of total of 1,518 reflections)

Details of final refinement

168 variables; block diagonal method

Refined scale factor: 4.085 Initial (Wilson plot) scale factor: 4.192

Final R-factor

9.73% unweighted 4.79% weighted

Goodness of fit parameter

4.4175

SECTION IX

CRYSTAL AND MOLECULAR STRUCTURE OF TVA

B: Discussion

The structure of the molecule $(THF)_3Cl_2V^{III}OV^{III}Cl_2(THF)_3$ as its ORTEP diagram is illustrated in Fig. IX-1. Fig. IX-2 gives a simplified diagram for interpretation. Tables IX-C and IX-D give the important bond distances and angles with standard deviations. Table IX-C also gives some relevant nonbonded contacts. There are four molecular units in each unit cell. This is shown in Fig. IX-3, which gives the packing diagram for the structure.

The molecule consists basically of an oxygen-bridged dimer. The V atoms are octahedrally coordinated - each to the three oxygens of the three THFs, two chlorines and the bridging oxygen. The V atoms are in a formal oxidation state of 3. The chlorines are trans to each other, across V and perpendicular to the main V-O-V axis. One THF molecule is along this axis (hereinafter referred to as the "main-axial THF") and the remaining two sites are occupied by the two other THF molecules.

The trans positions of the chlorines are to be expected because of the nature of this ligand, and past experience has shown that chlorines will almost always be trans [14, 131]. A look at the structure as represented in Fig. IX-1 immediately reveals as a primary feature a staggered character of the ligands on the two opposite Vs with respect to each other: each chlorine pair and each trans-THF pair on one of the Vs is staggered relative to its counterpart on the other V if one looks down the V-O-V axis. This situation is to be expected due to steric factors. A comparison with the structure of $V(py)_4Cl_2$ [131] is interesting in this respect: the four pyridines in this molecule, arranged as two pairs of trans-axial ligands, are non-planar and perpendicular - i.e. staggered. Additionally, the planes of the axially opposite (i.e. trans) pyridines are perpendicular to each other; this is approximately observed for the two main-axial THF molecules. When TVA is in solution, rotation may of course be expected to occur along the V-O-V bond.

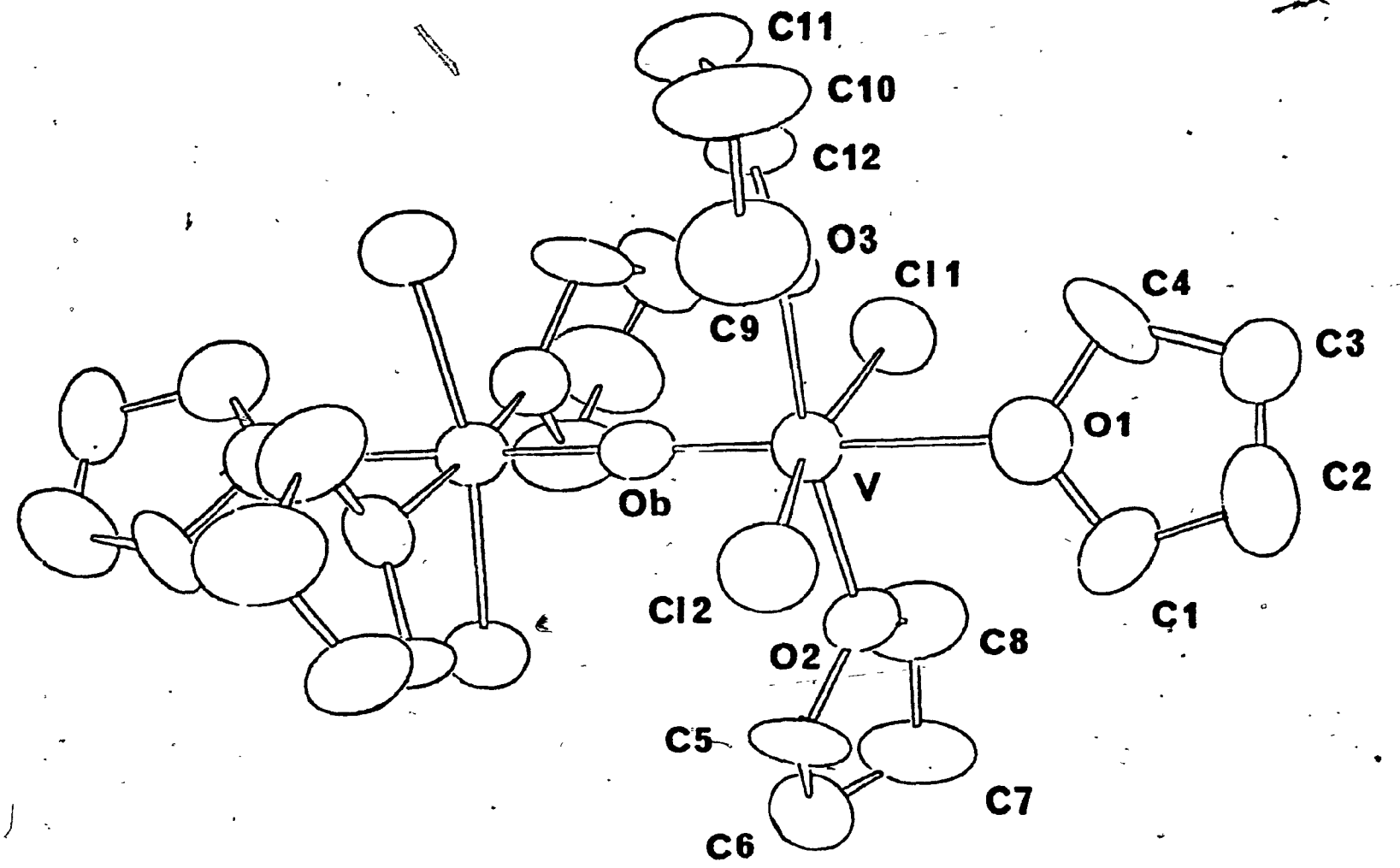

Fig. IX-1: ORTEP diagram for TVA

$(thf)_3(Cl)_2VOV(Cl)_2(thf)_3$

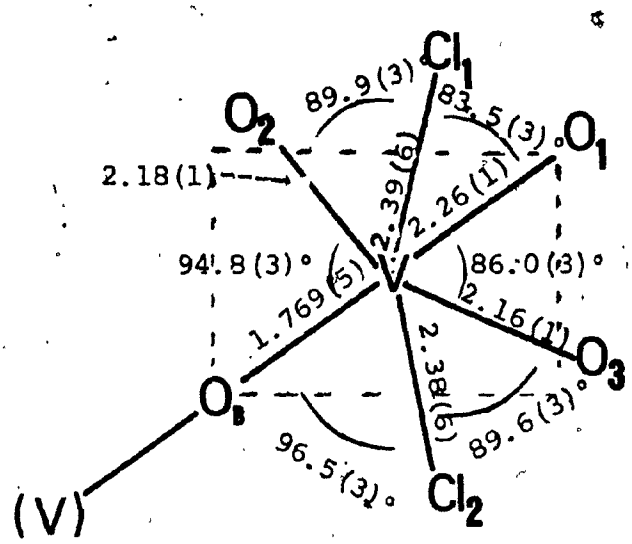

(All distances in Å)

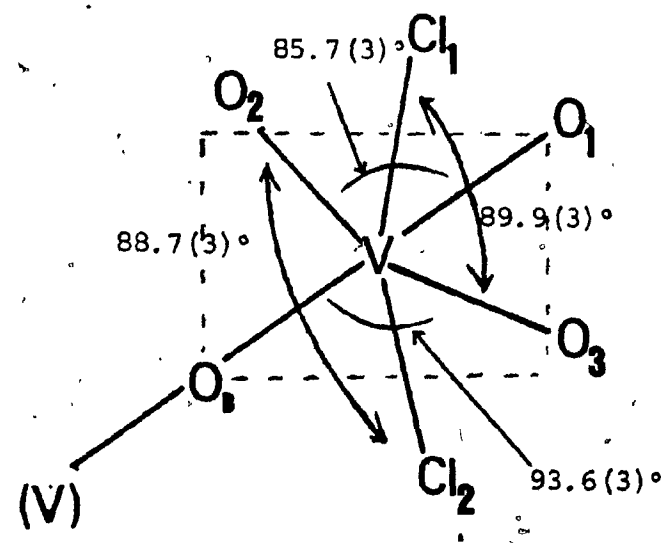

Fig. IX-2: TVA geometry

TABLE IX-C

RELEVANT BOND LENGTHS, WITH STANDARD DEVIATIONS, FOR TVA

(Figures in Ångstroms; standard deviations rounded off to one significant digit only)

A: Bonded Contacts

$V-Cl_1$	2.390(6)	$V-O_1$	2.26(1)
$V-Cl_2$	2.384(6)	$V-O_2$	2.18(1)
$V-O_B$	1.769(5)	$V-O_3$	2.16(1)
O_1-C_1	1.43(2)	O_2-C_5	1.48(2)
O_1-C_4	1.44(2)	O_2-C_8	1.47(2)
O_3-C_9	1.44(2)		
O_3-C_{12}	1.46(2)		
C_1-C_2	1.45(2)	C_5-C_6	1.51(2)
C_2-C_3	1.46(2)	C_6-C_7	1.46(2)
C_3-C_4	1.47(2)	C_7-C_8	1.49(2)

B: Nonbonded Contacts

O_B-O_2	2.866(2)	O_B-Cl_1**	3.124(2)	Cl_1-O_1**	3.069(2)
O_B-O_3	2.877(2)	O_B-Cl_2**	3.142(2)	Cl_2-O_1**	3.062(2)

(**Note that the sum of the van der Waals radii is 3.35 to 3.6 Å)

TABLE IX-D

RELEVANT BOND ANGLES FOR TVA, WITH STANDARD DEVIATIONS

(Angles in degrees; standard deviations rounded off to one significant digit)

Cl_1-V-Cl_2	167.0(2)	Cl_1-V-O_2	89.9(3)
Cl_1-V-O_B	96.5(4)	Cl_1-V-O_1	83.5(3)
Cl_1-V-O_3	89.9(3)	O_2-V-O_1	85.7(4)
O_2-V-Cl_2	88.7(3)	O_2-V-O_3	171.7(3)
O_2-V-O_B	94.9(5)	O_1-V-Cl_2	83.5(3)
O_1-V-O_3	86.0(4)	O_1-V-O_B	179.4(5)
Cl_2-V-O_3	89.6(4)	Cl_2-V-O_B	96.5(4)
		O_3-V-O_B	93.4(5)

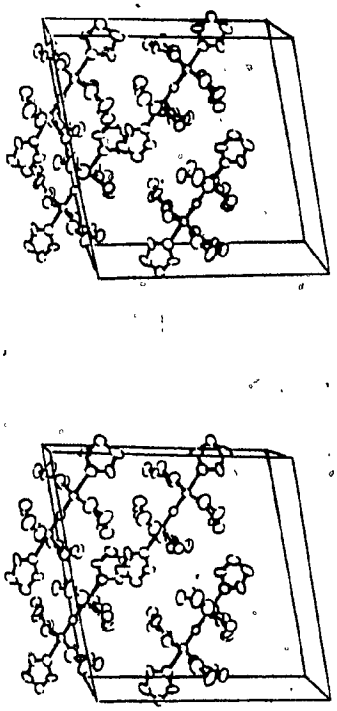

Fig. IX-3? Packing diagram for TVA (stereo view)

The nature of steric effects in the sort of molecule that TVA is will give rise to a slight distortion of an octahedral structure; this is apparent even with the bonding parameters obtained from the not altogether satisfactory refinement of the structure (Reliability Index of 9.74% or 4.79% unweighted). A look at the bond angles will reveal that the two chlorines appear to be bent slightly away from O_B, towards O_1 (see Figs. IX-1 and IX-2 and table IX-C). Similarly, on the plane perpendicular to this dichloro axis, the THFs corresponding to O_3 and O_2 are also bent away from O_B and towards O_1.

The V-Cl bond length (2.39 Å average) compares extremely favorably with the sum of the Bragg-Slater atomic radii for V and Cl, 1.35 Å (V) and 1.00 Å (Cl. A certain amount of L→M $p_\pi \rightarrow d_\pi$ (Cl→V) bonding would be expected but this should be markedly less than for V(IV) or V(V) because of the presence of 2 d-electrons in the d (T_{2g}) orbitals of V in TVA (V(IV) and V(V) have one and no d electrons in the T_{2g} orbitals respectively) but more than for V(II). One may therefore hypothesize that a bond length somewhat longer than that of V(IV)- and V(V)- Cl but shorter than that of V(II)-Cl would be expected. This hypothesis is proved correct by the following data: Brauer and Kruger [131] report a length of 2.46 Å for V(II)-Cl in $V(py)_4Cl_2$; Fieselman and Stucky [140] report a value of 2.39 Å for V(III)-Cl in $(Cp)_2VCl$, a value identical to that in TVA. Drake et al. [141] measured a V(III)-Cl bond length (in $VCl_3[N(CH_3)_3]_2$) of 2.205 Å. For V(IV)-Cl and V(V)-Cl, in molecules with no bulky ligands, values of 2.03 Å and 2.12 Å (for $VCl_{4(g)}$ and $VCl_{3(g)}$ respectively) are reported [142]. In $V(IV)OCl_2[N(CH_3)_3]_2$ [143] a value of 2.03 Å is reported, and in $V^{IV}OCl_2[OC[N(CH_3)_3]_2]$ the V-Cl bond length is 2.340 Å [144]. In the case of V(V)-Cl, typical bond lengths are 2.21 Å for $VOCl_3{:}NCCH_3$ [145] and 2.166 Å in VCl_5 [146]. For the most part these bond lengths are consistent with our hypothesis, showing decreasing character in the V-Cl bond length from V(II) to V(V), if one keeps steric effects of bulky ligands in mind.

The V-O bond length for the main-axial THF appears to be somewhat longer (2.26 Å), within the limits (again!) of the reliability of this structure refinement, than that for the other trans-axial THFs (2.17 Å) average). This is to be expected as a result of the slight distortion in the molecule described earlier - where chlorines and THFs are bent towards this main-axial THF. The $V-O_B$ bond is quite short 1.77 Å. A comparison of the V-O(THF) bond lengths with V-O single bond lengths in other molecules containing O-ligands coordinated to V reveals that the former are extraordinarily long: typical values for V-O(ligand) single bond lengths are near 1.95 Å, the sum of the Bragg-Slater atomic radii for V (1.35 Å) and O (0.6 Å). Thus for V-O(acac) in $VO(acac)_2$, the length is 1.97 Å [147]; for V-O(ligand) in oxoisopropoxo bis(8-OH quinolinato) V^V it is 1.902 Å. In $V^VO(NO_3)_3CH_3CN$, it is 1.92 Å for monodentate NO_3^- and 2.04 Å for bidentate NO_3^- [149]. No doubt the data quoted above all involve either a V(IV) or V(V) atom associated with a V=O bond, but similar results have been obtained for molecules without V=O bonds as well [151 and references therein]. Only in the molecule:

(THF)(2,6 dimethoxy phenyl)$_2$-V≡V-(2,6 dimethoxyphenyl)$_2$(THF)

(Scheme IX-1 [150])

do we find a V-O(2,6 DMP) bond length of 2.138 Å, close to that in TVA.

Brown and Wu [151] have calculated empirical parameters, derived from a very large number of observations, on the basis of which bond lengths or bond valences can be calculated for metal-oxygen bonds if either one of them is known. They give the relation

$$s = [R/R_1]^{-N} \qquad \text{(Eq. IX-2)}$$

where s is the bond valence or bond order, R the bond length and

R_1 and N are empirical parameters unique to the valence state of the metal atom. For V(III) these are 1.762 and 5.2 respectively; for the usual ca. 1.95 Å bond length observed for the V-O(ligand) single bonds, this relation gives a bond order of ca. 0.6. Substituting the av. bond length for the $V-O_{THF}$ bonds in TVA, one obtains bond orders of 0.98; doing the same for the $V-O_B$ bond one obtains a bond order of 0.98. The $V-O_B$ bond is thus almost a single bond according to Brown and Wu's equation, whereas the $V-O_{THF}$ bonds have very low order, in accordance with the low coordinative capability of THF (due to absence of π-acceptor ability and low $p_\pi \longrightarrow d_\pi$ donative capability). The almost prodiguous ability of TVA to lose THF from the lattice (see earlier sections) may be viewed in this context. Cotton and Mullen [150, cited above] also reported this phenomenon for the THF in their molecule (Scheme IX-1 above).

For comparison with the $V-O_B$ bond length one may mention here that the normal V=O bond length for V in valence states (III) to (V) is 1.52 Å to 1.65 Å [-47,152-154] and does not vary much with the oxidation state of V as such.

A V^{III}-O single bond length for octahedral coordination varying from 1.76 to 2.10 Å (1.98 Å) av.) is usually accepted [155].

In contrast to the V-O(ligand) bonds quoted above, the bond lengths of V atoms linked with bridging O-atoms resemble more closely the $V-O_B$ bond length observed in TVA (1.76 Å). Thus in $NaV_2^{iv}O_4F$, in which the V is 5-coordinate and the two V atoms share 2 oxygens on a square plane, the length is 1.85 Å [156], while for a similarly structured molecule, $Li_2V_2O_5$, it varies from 1.74 Å to 1.98 Å [157]. For V(V)-O in VO_4 tetrahedra, Tilmans and Baur [158] report values near 1.696 Å (in $Na_{12}(OH)(H_2O)_{48}-(VO_4)_4$) whereas for the molecule alpha-$[Zn_3(V^VO_4)_2]$, Gopal and Calvo [159] give a value of 1.79 Å, very close to our own; in both the latter cases, the O-atoms

are bridged in different ways between three cations. A bond length as long as 2.49 Å for V-O has been cited in molecules where vanadyl units are linked by two basally shared oxygen atoms in chains [160]. In CaV_3O_7, where $V(IV)O_5$ pyramids share edges, a V-O(bridge) av. bond length of 1.96 Å is reported [161]. In another structure involving a V-O-V bridge, that of $NH_4[O(VO(O_2/2)_2]$ (sic.) [162], a length for V(V)-O(bridge) of 2.01 Å is reported, but this structure represents a very strained molecule in which a peroxo group also acts as a bridging ligand.

The absence of any M→L $d_n \rightarrow \pi^*$ backbonding may also explain in part the extreme sensitivity of the TVA molecule. Very limited $p_n \longrightarrow d_n$ (Cl→V) bonding may be said to occur, making the V-Cl bonds somewhat shorter and stronger than others in the molecule excepting the V-O-V bridge bonds. In the case of the V-O(THF) bonds, which may be said to be simple "coordinate covalent" single bonds (to use classical phraseology), i.e. with no backbonding, the relatively low bond order explains the very great tendency of the THFs to leave the molecule, as noted earlier. The O(bridge) along the almost exactly single V-O bonds may be said to be sp hybridized with two electron pairs donated to the Vs and one lone pair in either of the two nonbonding orbitals (the choice being arbitrary); the lone pair causes repulsion of the trans-axial (terminal) THF, though this bending may also be said to occur due to a need to compensate for the shorter $V-O_B$ bond (as compared to the $V-O_{(main\ axial\ THF)}$ bond) which brings the chlorines and O_B closer together. A list of relevant nonbonded contacts is given in table IX-C. It is to be noted that the $Cl_{1,2}-O_B$ and the $Cl_{1,2}-O_1$ distances come within the van der Waals sphere of interaction, lending support to the view that repulsion between the Cls and the O_B lone pair causes the Cls to bend away; these distances also indicate that the chlorines are closer to O_1 than to O_B, as noted earlier.

The V(III) atoms are of course d^2sp^3 hybridized with two electrons

in the nonbonding d (T_{2g}) orbitals. The V-O_B-V axis can be taken to be essentially linear.

According to the conclusions arrived at in the above discussion, regarding the bond distances and probable bond orders, it is safe to say that there is virtually no $p_n \longrightarrow d_n$ (L → M) interaction for the THF oxygens (bond order less than ca. 0.35) and very little if any for the O_B (bond order ca. 1.0). Very limited interaction of this kind may be assumed for the chlorines, as noted earlier. L→M electron donation is in any case quite abhorrent to the d^2 system that is V(III) (and even more so for the d^3 V(II)), which as it is suffers from a large accumulation of charge.

The values of the bond lengths and angles on the THF molecules are in substantial agreement with those generally found in coordinated THF molecules [150a,b]. Electron donation by the O-atom should cause an increase in the C-O bond distance and perhaps a slight increase in the C-C bond lengths also. Where the degree of electron donation is the smallest (for the O_1 main-axial (i.e. terminal) THF, which has the longest V-O bond), the increase should be the least. This is observed for the C-O bond length here, within the limits of reliability for the structure refinement, (1.435 Å av. compared to a normal C-O bond length for a single bond of 1.44 Å). The vibration of the carbons in the CH_2 units, as represented by their thermal ellipsoids, is also as expected, greatest perpendicular to the plane of the THF molecule.

One feature of note for TVA, as in the case of VEZN, is that it does not conform to the usual 16 and 18 electron states observed for TM compounds. To each V may be assigned only 14 electrons.

SECTION X

CONCLUSIONS

Any conclusions other than those of a very tentative nature are difficult to draw from just the results of this work, without a much more extensive study being first conducted, and it is precisely for this reason that a section on scope for further work has been thought necessary.

The work seems to indicate that alkylation of the TM chloride in reactions of this type is accomplished to a greater extent with less polar alkyls such as those of Zn than with polar alkyls such as those of Al. The compositions of the two products whose crystal structures were determined and the composition of the gases evolved in the reaction are evidence for this. The gas analyses also appear to indicate that in the case of Al, much premature loss of ethyl groups takes place - by various processes of H-abstraction - from the Al itself, while it is initially coordinated through a bridge (halogen for instance) to the TM (according to the mechanism illustrated earlier, Scheme VII-1). This probably accounts for the lower alkylating capability of the Al alkyls. This mechanism, requiring a higher activation energy, is the one predominant at higher temperatures [27]. The second mechanism by which the reactions can be said to proceed is the more conventional one, requiring a smaller activation energy and more favorable at low temperature, where alkylation of the TM (vanadium) occurs and alkyl groups are subsequently eliminated from this TM and not from the main-group metal.

The role of the solvent** seems clear when we consider that in this work no V-alkyl bonds were isolated, whereas in similar work, for example that of Thiele et al. [16] in n-pentane solvent (a non-coordinating

---

** Note that the solid adducts of VCl_3 and the solvents have the compositions $VCl_3:3CH_3CN$ and $VCl_3:3THF$ and it is quite likely that these formulations reflect the state of coordination in solution also.

solvent for all intents and purposes) compounds such as $C_2H_5VCl_2$ (from $ZnEt_2$ and VCl_4) were isolated. Thus for instance in the case of VEZN, what appears to be happening is that after alkylation, a net process that is the equivalent of the elimination of only one alkyl group (leading to the reduction of V to V(II)) occurs and at this stage of reduction of V, the solvent (the strongly coordinating CH_3CN) intervenes by displacing ligands (C_2H_5) present on the V, leading to a $V(NCCH_3)_6$ entity with a formal exitation state of (II) for the V. A substantial amount of the butane produced could perhaps be accounted for by this process (see General Introduction for detailed discussion of mechanisms involved in such processes). A general scheme can thus be formulated:

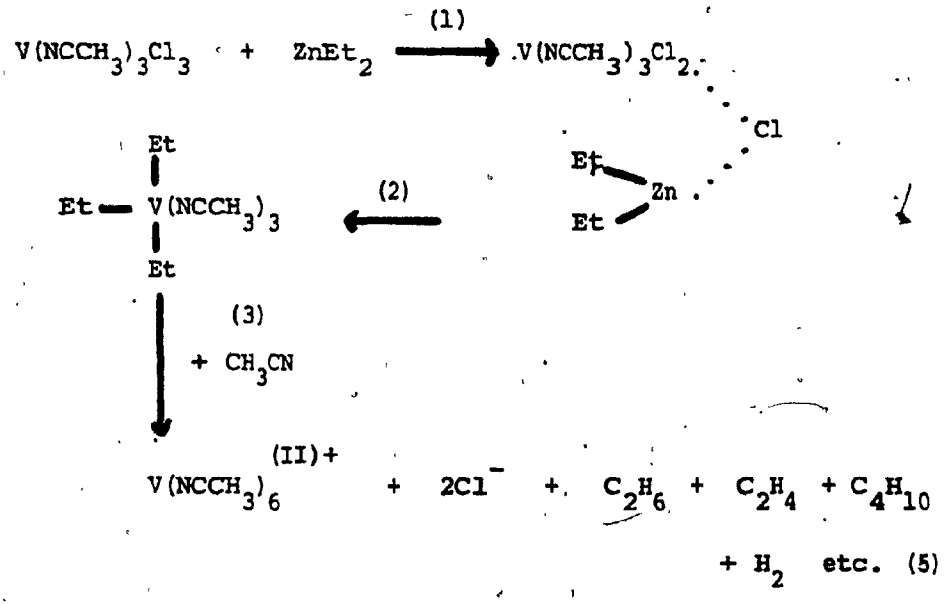

(Scheme X-1)

The products (5) originate from (3) through the various mechanisms described earlier.

In Thiele's work [16] a V-C_2H_5 bond was isolated presumably because of the weak coordinative (and thus displacement) capability of n-pentane.

This led to a coordinatively unsaturated V in the product, $C_2H_5VCl_2$, probably attached to $ZnCl_2$ in some way. It is precisely these three factors - a V-alkyl bond, coordinative unsaturation and attachment to $ZnCl_2$ (exerting an orienting effect) that would presumably give the molecule catalytic activity with respect to Ziegler-Natta polymerization, incidentally; (it would thus be very interesting indeed to obtain crystal structures and catalytic activity test results for Thiele's compounds, but that is another matter).

In the case of the Al (TVA) reaction, probably only one alkyl group is attached to the V at any time. Elimination, (according to the various mechanisms described earlier, but mainly dinuclear or β-elimination), of this alkylgroup with concurrent reduction of V(III) to V(II) followed or simultaneous with occupation of the vacant site thus created by a solvent (THF) molecule leads to the presumed intermediate, $VCl_2(THF)_4$*† in solution, which on oxidation gives a VO^{2+} species, this subsequently reacting with more $VCl_2(THF)_4$ to give the observed $Cl_2(THF)_3VOV(THF)_3Cl_2$. The general scheme that can be formulated is thus:

$$V(THF)_3Cl_3 + AlEt_3 \longrightarrow V(THF)_3Cl_2 \cdot\cdot\cdot Cl\text{–}AlEt_2 \quad (1)$$

[C_2H_6 from premature elimination]

$$V(THF)_3Cl_2Et \xrightarrow{(+\ THF)} V(THF)_4Cl_2 \quad (2)$$

$$+ C_2H_6 + C_2H_4 + C_4H_{10}, \text{ etc.} \quad (3)$$

(Scheme X-2)

** Note that the product of the reaction VCl_3 + $ZnEt_2$ in THF conformed to the formulation $V(THF)_4Cl_2{:}ZnCl_2$ ("TVEZ").

The products (3) originate from (2), as for VEZN, from the various processes described earlier. (2) may be oxidized in part to $VO^{2+}Cl_2(THF)_3$ (4), which then reacts with more (2) to give the observed $(THF)_3Cl_2VOVCl_2(THF)_3$ ("TVA").

Some other results of this work are also notable. An intense visible absorption band probably due to intramolecular charge-transfer within the VOV^{4+} entity was observed. It was postulated that when the VOV^{4+} entity (e.g. from TVA) is dissolved in a solvent, disproportionation occurs to VO^{2+} and V^{2+} to a considerable extent. IR and crystal structure data confirmed that while coordinated to V, acetonitrile distorts visibly from linearity and the C-N bond shortens. Above all, it was shown that V(II) can have an extensive coordination chemistry in organic solvents, and a source of V(II) (being TVA, giving VO^{2+} + V(II) in solution)** in just about any solvent of good coordinative capability and moderate polarity was produced.

** The existence of this equilibrium was not proved conclusively but the evidence overwhelmingly points to it.

SECTION XI

SCOPE FOR FURTHER WORK

As a beginning, of course, one could determine the crystal structures of $V(THF)_4ZnCl_4$ and VCl_2:2THF to see if they conform to our predictions (a tetrachlorozincate for the former and a polymeric chloro-bridged structure for the latter). A more extensive analysis of the gases evolved in the reactions including a search for alkyl chlorides and hydrogen with the additional auxiliary use of mass spectrometry is required. More sets of data on the composition of the gases evolved are required to confirm the predictions regarding mechanisms of reaction made in this thesis. It would also be interesting to note the composition of the gases when $ZnMe_2$ and $AlMe_3$ as well as the propyls and isopropyls are used in place of the ethyls.

A study in more varied solvents - including non-coordinating ones like heptane to see if any V-alkyl bonds can be isolated - is called for. The study may be extended with the use of Ti and Cr halides to see if their behavior is the same (and if the fundamental postulate of this thesis with regard to reaction mechanism holds in general) and to attempt to isolate reduced crystalline compounds of these metals also.

With the use of TVA, so extensively soluble (giving VO^{2+} and V(II)), as well as the reaction mixtures, which also are presumed to contain large concentrations of V(II), the coordinative capability of various ligands to V(II) can be studied. At this writing, this is being attemped [79] for the ligand:

(see overleaf)

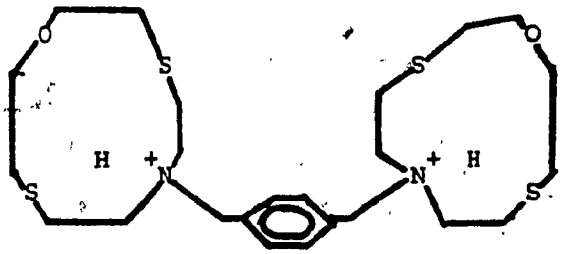

[⌒ = $-CH_2-CH_2-$]

(Scheme XI-1)

Finally, the homogeneous and heterogeneous catalytic activities of TVA in Ziegler-Natta polymerization need to be studied, if for nothing more than just confirmation and clearing up a big question mark. Preliminary results (experiments conducted by the author in June 1980) indicate that in n-hexane the crystals of TVA are able to act as catalysts for the polymerization of 1,3 butadiene to the atactic polymer, and ethylene to the isotactic polymer, but these results are extremely tentative and surely need confirmation. A compound such as TVA - with no alkyl group attached and not coordinatively unsaturated (though admittedly the THF ligands are almost too easily displaced) and quite likely no orienting effect (though again the V-O-V bridge may possibly exert such an effect as evidenced by the repulsion of the two chlorines by the O lone pair in the structure) - would be expected to show no catalytic activity. Such activity of the reacting systems studied but with noncoordinating solvents substituted in place of CH_3CN and THF could also be studied, though indeed the patents issued on Ziegler-Natta systems using $AlEt_3$ and VCl_3, $ZnEt_2$ and VCl_3, and even the likes of $AlEt_3$-VCl_3:3THF and $Al(alkyl)_3$-$VOCl_3$:THF [163] are almost too many to count [164].

Finally, an extensive quantum mechanical perturbation calculation on the effect of coordination on the CH_3CN ligand needs to be done to ascertain if the antibonding π-orbitals do indeed, as predicted in this work, show unconventional ordering of their energy levels.

APPENDIX A

LIST OF CHEMICALS AND SUPPLIERS

A: SOLVENTS

Acetonitrile: "Certified grade", Fisher Scientific Company (Fairlawn, New Jersey).

CH_2Cl_2, CH_2ClCH_2Cl, "Certified grade" Fisher Scientific Company.

Diethyl ether, dimethyl formamide (DMF): "ACS Reagent Grade", Anachemia Chemicals Ltd., Montreal, Quebec.

Tetrahydrofuran (THF): "Certified grade", Fisher Scientific Company; Contains 0.025% butylated OH-toluene as preservative.

B: REAGENTS

VCl_3: "Reagent grade", Alfa Division of Ventron, Inc., Danvers, Massachussetts

$AlEt_3$: "95%", Alfa Division of Ventron, Inc.

$ZnCl_2$, EtI, EtBr, benzene: Certified grade, Fisher Scientific Company.

Zn dust, Na metal: Local suppliers.

Cu oxalate: Prepared, for an earlier synthesis, by V. Kumar using conventional methods described in the literature.

P_2O_5: "98%", "Reagent grade", Anachemia Chemicals Limited, Montreal, Quebec.

APPENDIX A, cont.

C: GASES

Ethane, ethylene, butane, 1,3 butadiene: "99.0%"", "Reagent grade", Matheson of Canada, Ltd., Montreal, Quebec

N_2, Argon, H_2: "99.997%", "High Purity", Linde (Union Carbide) K Grade, local supplier.

D: MISCELLANEOUS:

Nujol: "Certified grade", Fisher Scientific Company.

High-vacuum grease (silicone base): Dow Corning Corp., St. Louis, Mo.

APPENDIX B

FINAL POSITIONS FOR VEZN ATOMS

(Estimated standard deviations, rounded to one significant digit, in parentheses)

Atom	X	Y	Z
Zn	0.2658(1)	0.2878(1)	0.7340(2)
V	0.9108(2)	0.2826(2)	0.0893(2)
Cl_1	0.2418(4)	0.2346(4)	0.5712(4)
Cl_2	0.0644(3)	0.2351(4)	0.7583(4)
Cl_3	0.4294(3)	0.2358(3)	0.9360(4)
Cl_4	0.3373(4)	0.5127(3)	0.6624(4)
N_1	0.7329(9)	0.1144(9)	0.1367(9)
N_2	0.8602(9)	0.115(1)	-0.018(1)
N_3	0.9562(9)	0.3428(8)	0.2054(9)
N_4	1.0942(8)	0.3434(9)	0.0446(9)
N_5	1.0188(9)	0.1132(9)	0.2663(9)
N_6	0.7953(8)	0.3427(8)	-0.0937(9)
C_{1a}	0.640(1)	0.040(1)	0.164(1)
C_{1b}	0.516(1)	-0.054(1)	0.198(1)
C_{2a}	0.837(1)	0.039(1)	-0.063(1)
C_{2b}	0.803(1)	-0.054(1)	-0.126(1)
C_{3a}	0.976(1)	0.390(1)	0.277(1)
C_{3b}	0.999(2)	0.459(1)	0.365(2)
C_{4a}	1.193(1)	0.391(1)	0.026(1)
C_{4b}	1.326(1)	0.456(2)	0.004(2)
C_{5a}	1.066(1)	0.038(1)	0.363(1)
C_{5b}	1.126(1)	-0.054(1)	0.485(1)
C_{6a}	0.724(1)	0.391(1)	-0.192(1)
C_{6b}	0.637(1)	0.457(1)	-0.322(1)

APPENDIX C

FINAL ANISOTROPIC THERMAL PARAMETERS FOR VEZN, WITH ESTIMATED STANDARD DEVIATIONS (X 10,000)

Atom	U_{11}	U_{22}	U_{33}	U_{12}	U_{13}	U_{23}
Zn	536(107)	453(101)	516(107)	85(75)	213(082)	-142(077)
V	430(123)	429(127)	423(126)	70(96)	161(100)	-149(099)
Cl_1	911(284)	804(272)	618(243)	217(217)	296(214)	-310(210)
Cl_2	631(239)	718(258)	870(286)	114(194)	374(213)	-224(214)
Cl_3	622(234)	796(271)	596(239)	208(201)	082(190)	-184(203)
Cl_4	985(303)	463(229)	940(306)	085(203)	410(249)	-160(212)
N_1	496(601)	506(650)	529(661)	-041(490)	260(515)	-177(529)
N_2	566(700)	520(714)	628(764)	153(566)	217(566)	-256(605)
N_3	643(685)	560(697)	499(638)	173(552)	187(541)	-202(550)
N_4	431(597)	520(671)	592(680)	-045(497)	222(528	-219(553)
N_5	566(622)	653(702)	423(643)	220(550)	132(529)	-156(547)
N_6	493(603)	357(574)	493(665)	117(483)	181(522)	-019(489)
C_{1a}	669(382)	570(813)	356(715)	184(693)	171(648)	-165(621)
C_{1b}	492(882)	570(813)	356(715)	184(693)	171(648)	-165(621)
C_{2a}	383(772)	656(966)	436(804)	173(711)	238(647)	042(711)
C_{2b}	995(1127)	655(941)	784(1014)	070(809)	434(876)	-483(830)
C_{3a}	754(915)	642(872)	540(858)	422(731)	299(728)	011(697)
C_{3b}	1362(1410)	976(1261)	835(1121)	627(1092)	183(1010)	-525(1008)
C_{4a}	645(895)	691(945)	591(955)	134(739)	077(757)	-446(799)
C_{4b}	517(954)	1104(1323)	1362(1474)	-171(866)	533(978)	-667(1145)
C_{5a}	490(772)	541(876)	562(863)	007(640)	253(679)	-315(707)
C_{5b}	909(1104)	821(1105)	383(830)	471(915)	-64(759)	-60(780)
C_{6a}	461(765)	486(800)	643(892)	73(637)	274(691)	-150(689)
C_{6b}	891(1126)	1033(1276)	539(955)	570(1108)	187(842)	140(862)

APPENDIX D

FINAL POSITIONAL PARAMETERS FOR TVA

(Estimated standard deviations, rounded to one significant digit, in parentheses)

Atom	X	Y	Z
V	0.0716(1)	-0.0146(4)	0.3275(1)
Cl_1	0.0191(2)	0.1538(5)	0.3965(2)
Cl_2	0.3540(2)	0.3186(5)	0.2180(2)
O_B	0.0000*	-0.015(2)	0.2500*
	(*special position)		
O_1	0.3376(5)	0.484(1)	0.0731(5)
O_2	0.1287(5)	0.163(1)	0.2899(5)
O_3	0.4718(5)	0.307(1)	0.1220(4)
C_1	0.2345(7)	0.027(2)	0.4290(8)
C_2	0.2741(8)	-0.008(3)	0.0035(9)
C_3	0.2222(8)	0.011(3)	0.0482(8)
C_4	0.1543(8)	0.052(2)	-0.0012(7)
C_5	0.1576(8)	0.149(2)	0.2243(8)
C_6	0.1596(8)	0.305(2)	0.1978(8)
C_7	0.1616(9)	0.394(2)	0.262(1)
C_8	0.1177(8)	0.317(2)	0.3060(9)
C_9	0.4521(9)	0.157(2)	0.1289(9)
C_{10}	0.4970(9)	0.079(2)	0.0865(9)
C_{11}	0.4381(8)	0.168(2)	0.412(8)
C_{12}	0.4609(7)	0.322(2)	0.4014(7)

APPENDIX E

FINAL ANISOTROPIC THERMAL PARAMETERS FOR TVA

(Estimated standard deviations, rounded to one significant digit, in parentheses)

Atom	U_{11}	U_{22}	U_{33}	U_{12}	U_{13}	U_{23}
V	0.059(2)	0.048(2)	0.052(2)	0.003(2)	0.010(1)	-0.006(3)
Cl_1	0.087(4)	0.059(4)	0.068(3)	0.005(3)	0.025(3)	0.009(3)
Cl_2	0.086(4)	0.064(4)	0.089(4)	-0.089(4)	0.030(3)	0.013(4)
O_B	0.061(9)	0.019(9)	0.057(9)	0.0*	0.022(8)	0.0*
			(*special position)			
O_1	0.083(8)	0.076(9)	0.069(8)	0.001(9)	0.013(6)	0.020(9)
O_2	0.058(8)	0.056(9)	0.066(8)	-0.015(7)	0.019(6)	-0.005(8)
O_3	0.067(8)	0.058(9)	0.044(7)	0.006(7)	0.015(7)	-0.012(7)
C_1	0.04(1)	0.14(2)	0.09(2)	-0.01(2)	0.005(9)	-0.01(2)
C_2	0.09(2)	0.11(2)	0.07(1)	-0.01(2)	-0.02(1)	-0.01(2)
C_3	0.09(1)	0.14(2)	0.07(1)	0.05(2)	-0.01(1)	0.02(2)
C_4	0.12(2)	0.13(2)	0.03(1)	-0.01(1)	0.02(1)	-0.02(1)
C_5	0.10(2)	0.05(1)	0.07(1)	-0.01(1)	0.07(1)	-0.01(1)
C_6	0.11(2)	0.07(2)	0.06(1)	-0.03(1)	0.03(1)	0.003(12)
C_7	0.16(2)	0.10(2)	0.12(2)	-0.04(2)	0.08(2)	0.02(2)
C_9	0.13(2)	0.02(1)	0.14(2)	-0.03(1)	0.05(1)	-0.02(1)
C_{10}	0.13(2)	0.09(2)	0.18(2)	0.05(2)	0.09(2)	-0.05(2)
C_{11}	0.07(1)	0.04(1)	0.12(1)	0.002(12)	0.05(1)	0.02(1)
C_{12}	0.05(1)	0.06(1)	0.07(1)	0.007(10)	0.036(9)	0.004(11)

ACKNOWLEDGEMENTS

The author wished to thank Dr. P.H. Bird, without whom this work would not have been possible, for his inestimable guidance during the course of the work.

Thanks are also due to Mr. P. Aysola for help with the gas-chromatographic analyses.

REFERENCES

1. C.A. Tolman, Chem. Soc. Rev. (1972) 1. 337

2. H. Funk, G. Mohaupt and A. Paul, Z. anorg. allgem. Chem., (1959) 302 199

3. E. Kurras, Monatsber. deutsch. akad. Wiss., Berlin, (1960) 2 109

4. F. Mani, Inorg. Nucl, Chem, Lett. (1976) 12 271-5

5. G. Trageseser and H.H. Eysel, Inorg. Chem., (1977) 16(3) 713

6. W. Hieber, J. Peterhans and E. Winter, Chem. Ber. (1961) 94 2572

7. N.L. Babenko, A.I. Busev & M.Sh. Blokh, Zhur. neorg. Khim., (1973) 18, 2108; ibid. 2088

8. M.F. Grigoreva, V.I. Pankrateva, I.A. Tserkovnitskaya, Zhur. neorg. Khim., (1975) 20 667

9. P.S. Braterman & R.J. Cross, Chem. Soc. Revs., (1973) 2 271

10. J.H. Swinehart, Inorg. Chem., (1965) 4(7) 1069

11. F.A. Cotton, & G. Wilkinson, "Advanced Inorganic Chemistry", John Wiley, 1966. Section on V(II), p. 817

12. H.-J. Seifert & B. Gerstenberg, Z. anorg. allgem. Chem., (1962) 315 56

13. J. Chatt & L.A. Duncanson, J. Chem. Soc. (1953) 2939

14. H.-J. Seifert & T. Auel, J. Inorg. Nucl. Chem., (1968) 30 2081

15. C. Eden & H. Felchenfeld, Tetrahedron, (1962) 18 233

16. K. Jacob, S. Wagner, W. Schumann & K.-H. Thiele, Z. anorg. allgem. Chem., (1976), 427 75

17.a. J. Chatt & B.L. Shaw, J. Chem. Soc. (1959) 705

17.b. ibid., (1960) 1718

18. P.S. Braterman & R.J. Cross, J. Chem. Soc. Dalton. Trans,, (1972) 657

19. G.E. Coates & C. Perkin, J. Chem. Soc. (1963) 421

20. F.S. Dyachovsky & N.E. Krush, Zhur. obschei. Khim., (1971) 41 1779

21. G. Fachinetti, J. Chem. Soc. Chem. Comm. (1972) 654

22. W. Mowat, J. Chem. Soc. Dalton Trans., (1972) 533

23. W. Mowat & G. Wilkinson, J. Organome. Chem., (1971) 28 C34

24. G. M. Whitesides, E. R. Stedronsky, C.P. Casey & J. San Filippo, Jr., J. Am. Chem. Soc., (1970) 92 1426

25. H. Gilman & R.G. Jones, J. Org. Chem., (1945) 10 505

26. W. M. Saltman, W.E. Gibbs & J. Lal, J. Am. Chem. Soc., (1958) 80 5615

27. M.I. Prince & K. Weiss, J. Organomet. Chem., (1964) 2 166

28. L. E. Manzer, Inorg. Chem, (1978) 17(6) 1552

29. T.A. Cooper, J. Am. Chem. Soc. (1973) 95:13 4158

30. G.A. Razuvajew, Dokl. Akad. Nauk. SSSR, (1967) 172 1337

31. L. S. Zborovskaya, T.N. Aizenshtadt, A.N. Artemov & A.S. Emelyanova, Trudy Khim. i Khim. Tekhnol., (1974) 4 29

32. G. Henrici-Olive & S. Olive, Angew. Chem. Int. Ed. Engl. (1967) 6 790

33. G.A. Razuvajew, Dokl. Akad. Nauk. SSSR, (1973) 208 876

34. E. Koehler, K. Jacob & K.-H. Thiele, Z. anorg. allgem. Chem.,(1976) 421 129

35. W. Mowat, A. Shortland, G. Yagupsky, N.J. Hill, M. Yagypsky & Gl Wilkinson, J. Chem. Soc. Dalton Trans., (1972) 533

36. M.M. Khamar, L.F. Larkworthy, K.C. Patel, D.J. Philips & G. Beech, Austr. J. Chem., (1974) 27 41

37. L.F. Larkworthy, K.C.Patel & D.J. Philips, Chem. Comm., (1968) 1667

38. M. Issiqoni, N. Katsaros, E. Uvachnou-Astra & E. Olympios, Inorg. Chim. Acta, (1974) 9 131

39. A. Dei & F. Mani, Inorg. Chim. Acta,(1976) 19 L39

40. F.A. Cotton & G. Wilkinson, "Advanced Inorganic Chemistry", John Wiley & Sons, 1966, p. 395

41. K. Ziegler, E. Holzkamp, H. Breil & H. Martin, Angew. Chem., (1955) 67 541

42. G. Natta, J. Polym. Scie., (1955) 16 143

43. G. Natta, Angew. Chem., (1956) 68 393

44. G. Natta, Chem. & Ind., (1957) 1520

45. G. Henrici-Olive & S. Olive, Angew. Chem. Int. Ed. Engl., (1967) 6 790

46. K.W. Egger, Trans. Faraday Soc., (1971) 67 2638

47. K. Ziegler in "Organomet. Chem.", ACS Monograph N° 147, Reinhold, New York, 1960, pp. 194-269

48. Patents are too numerous to quote, but see for instance Chem. Abstr. 53: P15,643b; 8647a; 52: P19107h; 54: P25978b; 55: P12939e; P10974; 20998f.

49. J. Obloj, Hanna Maciejewska, M. Uhniat, T. Zawada, M. Nowakowska, Vysokomolek. Soedin, (1965) 7(5) 939

50. L.A. Rishina, E.I. Vizen, F.S. Dyachokovskii, Europ. Polym. J., (1979) 15(1) 93

51. N. Kanoli, German patent 2,727,652

52. J. Supniewski, Rocz. Chem. (1927) 7 172

53. C.C. Vernon, J. Am. Chem. Soc., (1931) 53 3831

54. J. Meyer & W. Taube, Z. anorg. allgem. Chem., (1935) 222 167

55. W. Mowat, loc. cit. (ref. 35)

56. C.S. Cundy, B.M. Kingston & M.F. Lappert, Adv. Organomet. Chem., (1973) 11 253

57. J. Meyer, & M. Aulich, Z. anorg. allgem. Chem., (1930) 194 278

58. See also, for instance, E. Lupenko and A.I. Efimov, Fiz. Khim., (1973) 100

59. H.-J. Seifert & T. Auel, Z. anorg. allgem. Chem., (1968) 360 50

60. G.W.A. Fowles & R.A. Walton. J. Less Comm. Metals, (1965) 9, 457

61. A. Feltz, Z. anorg. allgem. Chem., (1967) 354 225

62. J.-J. Seifert & T. Sauertig, Z. anorg. allgem. Chem., 376 245

63. M.A. Porai-Koshitz & A.S. Antsishkina, Trudy Inst. Kryst. Nauk. SSSR, (1954) 10 117

64. P. Daporto, F. Mani & C. Mealli, Inorg. Chem., (1978) 17(5) ;323

65. T.W. Newton & F.B. Baker, Inorg. Chem., (1964) 3(4) 569; eusd., J. Phys. C-em., (1964), 68 2

66. N. Suton, Accts. Chem. Res., (1968) 1(8) 225

67. M. Ardon & R.A. Plane, J. Am. Chem. Soc., (1959) 81 3197

68. J.E. Earley & W.M. Riesen, Chemis. Analyst, (1966) 55(3) 76

69. J. Gandeboeuf & P. Souchay, J. Chim Phys., (1959) 56 358

70. L.A. Nikonova, N.I. Pershnikova, M.V. Bodenko, L.G. Liinyk, D.N. Sokolov, A.E. Shilov, Doklady Akad. Nauk. SSSR, (1974) 216 140

71. M.S. Kharasch & M. Kleiman, J. Am. Chem. Soc., (1943) 65 491

72. E.J. Gabe, ACA.C. Larsen, Yu Wang & F.L. Lee, Chem. Divn. of the National Research Council of Canada, Ottawa

73. "International Tables for X-Ray Crystallography", Ed. K. Lonsdale, Kynoch Press, Birmingham, England, 1962, pp. 202, 210

74. A.J.C. Wilson, Nature (1942) 150 152

75. A.L. Patterson, Z. Krist., (1935) A90 517

76. "X-Ray Structure Determination, A Practical Guide", G.H. Stout and L.H. Jensen, Macmillan, London, 1968, p. 270 ff. and references therein

77. after C. Prewitt

78. after A. Zalkin

79. after P.H. Bird

80.a. "Oak Ridge Thermal Ellipsoid Project", after Carrol K. Johnson, ORNL-3794, October 1970

80.b. see for instance J. Am. Chem. Soc., (1954) 79 2262

81. P.H. Bird, private communication

81.b. Abo El-Khair, B. Mostafa and S.M. Mokhtar, Indian J. Chem., 17A (April 1979), pp. 387-9

82. J.E. PSpressard, Spectrochim. Acta, (1972) 28A(10) 1925

83. E.L. Martin and K.E. Bentley, Anal. Chem., (1962) 34(3) 355

84. J.E. Drake, J.E. Vekris and J.S. Wood, J. Chem. Soc. (A)(1969) 345

85. E.E. Kriss, K.B. Yatsimirskii & G.T. Kurbatova, Zh. neorg. Khim., (1976) 21(8) 2075

86. L.F. Larkworthy, K.C. Patel & D.J. Philips, J. Chem. Soc. (A), (1970) 1095

87. L.F. Larkworthy, J.M. Murphy, K.C. Patel and D.J. Philips, J. Chem. Soc. (A), (1968) 2936

88. see for instance J. Phys. Chem., (1962) 66 57

89. C.K. Jorgensen, Acta Chem. Scand., (1951) 12 1537

90. L.E. Orgel, J. Chem. Phys., (1955) 23 1004

91. F.J. Kristine and R.E. Shepherd, Inorg. Chem., (1978) 17(11) 3145

92. J.R.M. Kress, J. Chem. Soc. Chem. Comm., (1980) 70 431

93. J.L. Hennson, C.R. Acad. Sci. Ser. C, (1961) 269 661

94.a. M.T. Mocella, R. Rovner and E.L. Muetterties, J. Am. Chem. Soc., (1976) 98 4689

94.b. J.M. Baaset, J. Catal., (1974) 34 152.

95. R.A. Burwell and A. N. Brenner, J. Mol. Catal., (1976) 1 77

96. Sadtler Standard Research Spectra, Sadtler Research Corp. Laboratories, Philadelphia, Penn.

97. A. Palm, E.R. Bissel, Spectrochim. Acta, (1960) 16 459

98. A.R. Katzritzky, "Physical Methods in Heterocyclic Chem.", Vol. 2, Academic Press

99.a. from "Interpreted Infra Red Spectra", Vol. III, Herman A. Szymanski, Plenum Press Data Division, New York, 1967

99.b. from "Infra Red Spectra & Charactersitic Frequencies, 700-300 cm^{-1}", E.F. Bentley, L.D. Smithson and A.L. Rozek, John Wiley, 1968

100. F.W.B. Einstein, E. Enwall, D.M. Morris and D. Sutton, Inorg. Chem., (1971) 10(4) 678

101. M.F. Ama El Sayed and R.K. Sheline, J. Inorg. Nucl. Chem., (1958) 6 187

102. C.C. Addison, J. Chem. Soc. (A), (1969) 2285

103. M.F. Farone and J.G. Graselli, Inorg. Chem., (1967), 6 1675

104. J.R. Brunette, C.R. hebd. Seances Acad. Ser. C., (1975) 281(5-8) 201

105. M.M. Khamar, L.F. Larkworthy, K.C. Patel, D.J. Philips and G. Beech, Austr. J. Chem., (1974) 27 41

106. F.A. Miller and L.R. Cousins, J. Chem. Phys., (1957) 26 329-31

107. C.G. Barrachlough, J. Lewis and R.S. Nyholm, J. Am. Chem. Soc., (1959) 3552

108. R.J. Kern, J. Inorg. Nucl. Chem., (1962) 24 1105

109. M.M. Khamar and L.F. Larkworthy, Chem. & Ind., (1972) 28 1297

111. R.A. Walton & B.T. Brisdon, Spectrochim. Acta (A), (1967) 23 2222

112. P. Schwendt and D. Joniakova, Chemicke Zvesti, (1975) 29(3) 381

113. see ref. [27] and references cited therein.

114. K.-H. Thiele, Pure & Applied Chem., (1972) 30 575

115. K. Ziegler in "Organometallic Chemistry", ACS Monograph N° 147, Ed. H. Zeiss, Reinhold, N.Y.C., 1960, pp. 194-269

116. K.W. Egger and A.T. Cocks, Trans. Faraday Soc., (1971) 67 2629

117. ibidem, (1971) 67 2638

118. numerous personal communications

119. C.J.J. van Loon and D. Visser, Acta Crystallogr., (B) (1977) 33 188

120. W.L. Steffer and G.J. Palenic, Acta Crystallogr. (B) (1976) 32 298

121. M.A. Porai-Koshits, Zh. Strukt. Khim., (1976) 17 1124

123. M. Rolies and C.J. de Ranter, Cryst. Strukt. Comm., (1977) 6 275

124. "Inorganic Chemistry", James Huheey, Harper & Row, 1978, p. 232

125. F.A. Cotton & G. Wilkinson, "Advanced Inorganic Chemistry", John Wiley & Son, 1966

126. "Inorganic Chemistry", Purcell & Kotz, W.B. Saunders Co., Philadelphia, Penn., 1977, pp. 586 ff.

127. A.J. Edwards, D.R. Slim, J.E. Guerchais and J. Sala-Pala, J. Chem. Soc. Dalton Trans., (1977) 984

128. J.M. Nesterova, Doklady Akad. Nauk. SSSR, (1977) 237 350

129. R.D. Willett and R.D. Rundle, J. Chem. Phys, (1964) 40 838

130. F.A. Cotton and S.J. Lippard, Inorg. Chem., (1966) 5 426

131. E. Brauer and C. Kruger, Cryst. Struct. Comm., (1973) 3 421

132. M. Mathew, A.J. Carthy and G.G. Palenic, J. Am. Chem. Soc., (1970) 92 3197

133. J.H. Enemark, B. Friedman and W.N. Lipsomb, Inorg. Chem., (1966), 5 2165

134. M. Webster and H.E. Blayden, J. Chem. Soc. (A), (1969) 2443

135. B. Duffin, Acta Crystallogr., (B) (1968) 396

136.a. Z. Hamlet, private communication
136.b. P. Coppens, private communication
136.c. J.M. McIver, H. King, private communications

137. E.R. Howells, D.C. Philips and D. Rogers, Acta Crystallogr., (1950) 3 210

138. see "International Tables for X-Ray Crystallography", Vol. III, and "X-Ray Crystallography, a Practical Guide", p. 209, (loc. cit.)

139. M. Niel, Mat. Res. Bull., (1976) 11 827

140. B.F. Pieselman and G.D. Stucky, J. Organometall. Chem., (1977) 137 43

141. J.E. Drake, J. Vekris and J.S. Wood, J. Chem. Soc. (A), (1968) 1000

142. see "International Tables for X-Ray Crystallography" (loc. cit.)Vol. III, pp. 257 ff.

143. W.N. Lipscomb and A.G. Whittaker, J. Am. Chem. Soc., (1945) 67 2109

144. J. Coetzer, Acta Crystallogr. (B) (1970) 26 872

145. J.C. Daran, Y. Jeannin, G. Constant and R. Morancho, Acta Crystallogr. (B) (1975) 31 1833

146. M.L. Ziegler, Z. Naturf. B. (1977) 32

147. R.P. Dodge, D. Templeton and A. Zalkin, J. Chem. Phys., (1961) 35 55-67

148. M. Schriv and Q. Fernandes, Chem. Comm., (1971) 63

149. numerous personal communications

150.a. F.A. Cotton and G. Mullen, J. Am. Chem. Soc., (1977) 99 7886

150.b. R.R. Rietz, N.M. Edelstein, H.W. Reuben, D.H. Templeton and A. Zalkin, Inorg. Chem., (1978) 17 658

151. I.D. Brown and K.K. Wu, Acta Crystallogr., (1976) (B) 32 1957

152. M. Pasquali, F. Marchetti, C. Floriani and S. Merlino, J. Chem. Soc. Dalton. Trans., (1977) 139-44

153. J. Borene, F. Casborn, Bull. Soc. franc. Mineral. Crist., (1971) 94 8

154. S. Jagner and N.J. Vannenberg, Acta Chem. Scand., (1973) 27 3482

155. see "International Tables for X-Ray Crystallography" (loc. cit.), Vol. III, pp. 257 ff.

156. A. Carfy, J. Galy, Bull. Soc. franc. Mineral. Crist., (1971) 94 24

157. D.N. Anderson and R.D. Willett, Acta Crystallogr. (B) (1971) 27 1476

158. E. Tilmans and W.H. Bauer, Acta Crystallogr., (B) 27 (1971) 2124

159. R. Gopal and C. Calvo, Can. J. Chem., (1971) 49 3056

160. W.B. Rice, W.R. Robinson and B.C. Tofield, Inorg. Chem., (1976) 15(2) 345

161. J.-C. Boulox and J. Galy, Acta Crystallogr., (B) (1973) 29 269

162. I+B. Svennson and R. Stomberg, Acta Chem. Scand., (1971) 25 898

163. A.G. Chesworth, R.N. Hazeldine and J.T. Tait, J. Polym. Sci., (1974) 12 1703

164. Innumerable patents have been issued on the subject; cf. for instance the U.S. patents of the years 1958-1965

165. "Molecular Wave Functions and Properties: Tabulated from SCF calculations in a Gaussian Basis Set", L.C. Snyder and H. Basek, John Wiley, 1972

166. "Tables of Linear Molecule Wave Functions", A.D. Mclean and D. Yoshimine, IBM Corp., 1967